EUROPEAN UNIVERSITY

Journal of Biomedical and Medical Sciences



2026, Volume 5, Number 12

ISSN 2667-9507

EDITOR-IN-CHIEF

Prof. **Maka Mantskava**, MD, PhD

CO-EDITORS

Prof. **Zaza Avaliani**, MD, PhD, Tbilisi, Georgia

Prof. **Natia Jojua**, PhD, Tbilisi, Georgia

Prof. **Victoria Lishnevska**, MD, PhD, Ghent, Belgium

Prof. **Jean Frederic Brun**, MD, PhD, Montpellier, France

Prof. **Marie Carlota Saldanha Lopes**, PhD, Lisbon, Portugal

Prof. **Nadia Antonova**, PhD, Sofia, Bulgaria

Prof. **Frederic Jung**, PhD, Brandenburg, Germany

PROJECT AUTHOR

Tamar Zarginava, European University, Tbilisi, Georgia

EDITORS (INTERNATIONAL AND NATIONAL ASSOCIATES)

USA

Samuel Bernal, Cedars-Sinai Medical Center, Medical Center

Nino Kharaishvili, Health System Resilience Practice at Jacobs

Germany

Mukhran Khundadze, Institute of Human Genetics, University Hospital Jena

Portugal

Ana Silva-Herdade, Institute of Biochemistry, University of Lisbon

France

Michel Mesnard, Research and Innovation Center, University of Bordeaux

Poland

Malgorzata Rogalinska, Department of Cytobiochemistry, Faculty of Biology and Environmental Protection, University of Lodz

India

Sunil Sharma, Indian Spinal Injuries Centre in New Delhi

Egypt

Ashraf Mohamed Ibrahim El Molla, Department of Anesthesiology, Cairo University

China

Silpak Biswas, Institute of Preventive Veterinary Medicine, College of Animal Sciences, Zhejiang University

Turkey

Ayhan Caliskan, Faculty of Medicine, Department of Medical Education, Ege University

Jordan

Mohammad Othman Nassar, Computer Information System Department, Amman Arab University

Georgia

Tinatin Gognadze, Faculty of Medicine, European University

Aleksandr Khelaia, Tsulukidze National Center of Urology

Natalia Maglakelidze, Aversi Clinic

Naomi Hoyle, Eliava Phage Therapy Centre

Shorena Tsiklauri, Depratment of Otorhinolaryngology, Aversi Clinic

Maia Zhamutashvili, Infectious Diseases, AIDS and Clinical Immunology Research Center

Nana Momtselidze, Department of Fundamental and Applied Researcher, Multidisciplinary Science High School

Giorgi Kuchava, Department of Rheology and Diagnostic Analytical Services, Ivane Beritashvili Experimental Center of Biomedicine

Shota Janjghava, Department of Andrology, National Institute of Endocrinology

Content

Letter from the Editor-in-Chief 6

Focus and Scope 7

Blood Rheology as an Indicator of Microcirculatory Changes in Experimental Preterm Labor 10
Karaman Pagava, Nana Momtselidze, Nino Mirianashvili, Fuyong Jiao

Extracellular Vesicles in Breast Cancer: Tumor Microenvironment Crosstalk, Organotropic Metastasis, Immune Evasion, and Therapeutic Resistance 18
Naman Chauhan, Irina Nakashidze

Clinical Outcomes Following Percutaneous Coronary Intervention, as Determined by Rheological Properties in Patients with Stable Ischemic Heart Disease..... 34
Spartak Lekveishvili, Vera Kapetivadze, Maka Mantskava

An Integrated Methodological Framework for Comparative Assessment of Coastal Seawater in the Black Sea Basin 48
Maka Mantskava, Giorgi Kuchava, Irina Imerlishvili, Gulnara Abashidze, Nino Mirianashvili, Nadia Antonova, Nana Momtselidze

Self-Inflicted Denial-of-Service in Digital Healthcare Systems: A Simulation Study of Retry Storms, Metastable Failure, and Mitigation Policies 57
Teimuraz Sturua

Machine Learning in Genomics, A Critical Review of Model Classes, Validation Practices, and Barriers to Translation..... 78
Ketevan Kartvelishvili, Giorgi Kuchava

Effects of Vitamin D on Erythrocyte Deformability in STZ-Induced Diabetes Mellitus..... 90
Nino Sakhanberidze, Manana Namoradze, Nino Charkviani, Maia Mantskava

Policy 102

DOI 10.51231/2667-9507-2026-005-12-6

Letter from the Editor-in-Chief

DEAR AUTHORS, REVIEW ERS, AND READERS,

Welcome to the second issue of 2026 of the JOURNAL OF BIOMEDICAL AND MEDICAL SCIENCES. As we continue our journey through this scientific year, we reflect on our shared achievements and set our sights on new frontiers in global medical research.

In this second issue of 2026, we present an exceptional collection of international studies that emphasize the power of multinational research consortia. The articles span a wide spectrum of biomedical disciplines, offering groundbreaking perspectives on environmental health, diagnostic analytics, personalized medicine, and preventive healthcare strategies. Our commitment to anti-plagiarism, copyright protection, and the highest standards of publishing ethics continues to define every step of our editorial workflow.

Science thrives when borders dissolve. Over the past years, our journal has grown into an international platform uniting researchers from across Europe, Asia, and beyond. This milestone would not have been reachable without the unwavering support of European University, which continues to position itself as a leading educational and scientific center in the region.

I express my heartfelt personal gratitude to Lasha Kandelakishvili and Dr. Tamar Zarginava, founders and key sponsors of our journal's scientific trajectory. Their long-term vision, leadership, and unwavering backing have built a foundation upon which high-level research can flourish and reach the global academic community.

On behalf of our entire editorial team, I invite you to explore this second issue of 2026. We hope these publications spark fruitful debates, trigger new research collaborations, and contribute meaningfully to the global advancement of human health.

Sincerely,

Prof. Maka Mantskava

Focus and Scope

We refer, peer-review and publish science articles about original study and clinical trial, theoretical reviews, preview and report of researcher project, preliminary data and the description of new and the newest hypothesis, essay in next directions.

- Epidemiology methods. Infection Diseases and Non-infection Diseases. Vaccinations
- Prevention of Epidemic. Prevention of Pandemic
- Multidisciplinary Approaches of Modern Science
- Polyprofile Medicine
- Biomedicine, Biorheology and Biotechnology
- Biochemistry and Biophysics in Fundamental and Applied Medicine. Micro – and Nanobiomechanics
- Innovative Methods. Bioinformatics. Biological Models. Mathematical Models
- Economic and Strategic Aspects of Biomedicine
- Blockchain and programming languages in Medicine. Digital Medicine. Chatbots
- The Role of Biomaterials in Biomedicine
- Theoretical, Clinical and Environmental Toxicology
- Radiology and Radiation Safety
- Nutritionology. Food, Biologically Active Substances, Medicines and Health. Enzyme
- Balneology, Wellness and SPA. Physical Education
- Beauty Industry
- Medical Physics. Medical chemistry
- Evidence Medicine. Medical and Biological Statistics
- Health Care and Policy
- Clustering in Biomedicine. Management systems in Biomedicine Areal. Strategic Communication in Biomedicine
- Ethics. Informed Consent. Doctor-Patient Relationship. Strategy and Using Instruments for Conflict Avoidance
- Grant application. Grant Management. Funding Science. Donors. Sponsors
- Mental Health. Defectology. ADD and ADHD

- Pharmacy and Pharmacology
- Reproductive Sciences and Sexual Medicine
- Cell Membranes, Structures and Function. Genome. Mechanisms of Aggregation and Deformation. Genome
- Blood, Blood Flow. Anatomy, Physiology and Pathophysiology of Blood Circulation
- Mechanisms of Thrombus and Stasis Formation
- Theoretical Hemodynamics and Hemorheology
- Clinical Hemorheology
- Rheology of Petroleum Products, Oils, Food and Construction Materials
- Neonatology. Pediatrics
- Gerontology and Geriatrics
- The Brain and its Functioning
  - ◊ Sleep-wakefulness Cycle
  - ◊ Pain and Analgesia
  - ◊ Behavioral and Cognitive Functions
  - ◊ Stress
  - ◊ Experimental and Clinical Neurology
  - ◊ Neurophysiology
  - ◊ Ultra – and Nanoarchitectonics
  - ◊ Alzheimer's Disease
  - ◊ Parkinson's Disease
  - ◊ etc.

- Kinesiology and Biomechanics
  - ◊ Rehabilitation
  - ◊ Sports Medicine
  - ◊ Prosthetics
  - ◊ Occupation Disease
  - ◊ etc.

- Alternative medicine
  - ◊ Chinese medicine
  - ◊ Acupuncture
  - ◊ Chinas Medicine
  - ◊ etc.

- Surgery
  - ◊ Planned Operations
  - ◊ Urgent Operations
  - ◊ Postoperative Shock
  - ◊ Plastic Surgery
  - ◊ Reconstructive Surgery
  - ◊ etc.

- Medical Linguistics
  - ◊ Medical Terms
  - ◊ Adaptation of Medical Literature
  - ◊ Translation Problems of Medical Literature
  - ◊ etc.

- New Approaches and Challenges for the Medical Education System
- Authorization, Certification, Licensing Issues in Health Care Institutions, University
- History of medicine
- Philosophy and medicine
- Medical Tourism
- Medical Low
- All about COVID-19
- etc.

DOI 10.51231/2667-9507-2026-005-12-10-17

Blood Rheology as an Indicator of Microcirculatory Changes in Experimental Preterm Labor

Karaman Pagava[1], Nana Momtselidze[2,3], Nino Mirianashvili[4], Fuyong Jiao

[1] *East West European University, Tbilisi, Georgia*
[2] *Ivane Beritashvili Center of Experimental Biomedicine, Tbilisi, Georgia*
[3] *European University, Tbilisi, Georgia*
[4] *Rayman Clinics, Tbilisi, Georgia*
[5] *Children's Hospital of Shaanxi Provincial People's Hospital (SPPH), Xi'an, China*

Abstract

Preterm labor is a multifactorial process involving endocrine, inflammatory, vascular, and uterine mechanisms. Changes in blood rheology may influence microvascular perfusion and therefore provide additional information about circulatory alterations associated with premature delivery. To investigate selected hemorheological characteristics in experimental models of preterm labor induced by mifepristone and oxytocin. Forty pregnant rats were divided into three groups: control (n=20), mifepristone-induced preterm labor (n=10), and oxytocin-induced preterm labor (n=10). Erythrocyte aggregation, erythrocyte deformability, plasma viscosity, and whole blood viscosity were assessed after delivery. Selected conventional coagulation parameters were also measured. Both experimental models were associated with increased erythrocyte aggregation and reduced erythrocyte deformability. The aggregation index increased from 49.8±3.5% in controls to 67.4±4.2% in the mifepristone group and 58.9±3.8% in the oxytocin group ($p<0.001$). Whole blood viscosity increased from 4.15±0.25 mPa·s in controls to 5.35±0.32 mPa·s and 4.85±0.30 mPa·s in the mifepristone and oxytocin groups, respectively ($p<0.001$).

Plasma viscosity also increased, whereas routine coagulation parameters showed comparatively limited changes. Experimental preterm labor was accompanied by measurable changes in blood rheology. Increased erythrocyte aggregation, impaired erythrocyte deformability, and elevated whole blood viscosity may indicate altered blood-flow conditions at the microcirculatory level.

KEYWORDS: preterm labor; hemorheology; erythrocyte aggregation; erythrocyte deformability; blood viscosity; microcirculation.

Introduction

Preterm birth remains an important obstetric and public health problem worldwide. Its frequency and clinical consequences have been extensively documented, while its mechanisms are recognized as heterogeneous rather than attributable to a single pathological pathway [1-4]. Premature activation of uterine activity may occur in association with hormonal changes, inflammation, placental dysfunction, cervical remodeling, and disturbances of maternal-fetal vascular adaptation [3,4]. The rheological characteristics of blood are important determinants of tissue perfusion. Blood viscosity depends on plasma viscosity, hematocrit, erythrocyte deformability, and erythrocyte aggregation. These parameters can substantially influence resistance to blood flow, particularly within the microcirculation [5,6]. Increased erythrocyte aggregation and reduced deformability may impair the passage of red blood cells through small vessels and alter local blood-flow conditions [7-10].

Microcirculatory disturbances are relevant to pregnancy because placental and uterine tissues require adequate vascular adaptation throughout gestation. Alterations in placental vascular function and oxidative stress have been discussed in relation to several pregnancy complications [11]. From a biomechanical perspective, therefore, evaluation of blood rheology may provide information that is not fully reflected by conventional coagulation tests. The present study focused on changes in erythrocyte aggregation, erythrocyte deformability, plasma viscosity, and whole blood viscosity in two experimental models of preterm labor. The objective was to determine whether these parameters demonstrate measurable alterations during experimentally induced premature delivery.

Materials and Methods

Experimental design

The study included 40 pregnant outbred white rats (370-415 gr). Animals were divided into three groups: Control group: n=20; Mifepristone-induced preterm labor: n=10; Oxytocin-induced preterm labor: n=10. The control animals were evaluated at gestational days 21-22, whereas experimental preterm labor was induced at gestational day 20. Blood samples were collected after delivery for hemorheological and coagulation analysis.

Hemorheological assessment

The following parameters were evaluated: erythrocyte aggregation index; erythrocyte deformability index; plasma viscosity; whole blood viscosity. These parameters were selected because erythrocyte aggregation and deformability are important determinants of blood-flow behavior, particularly in the microcirculation [5-10].

Coagulation assessment

Prothrombin time (PT), activated partial thromboplastin time (aPTT), fibrinogen concentration, D-dimer concentration, and platelet count were also determined. We used Counter C1 (Germany). Quantitative results are presented as mean ± standard deviation (SD). Differences were considered statistically significant at $p<0.05$.

Results

The most pronounced differences between the groups concerned the hemorheological parameters. The erythrocyte aggregation index was 49.8±3.5% in the control group, compared with 67.4±4.2% in the mifepristone group and 58.9±3.8% in the oxytocin group ($p<0.001$). Thus, erythrocyte aggregation was increased in both experimental groups, with a greater change observed following mifepristone administration. The erythrocyte deformability index decreased from 0.92± 0.04 in controls to 0.78±0.05 in the mifepristone group and 0.80±0.04 in the oxytocin group ($p<0.001$). Plasma viscosity increased from 1.24±0.05 mPa·s in controls to 1.39±0.07 mPa·s and 1.35±0.06 mPa·s in the mifepristone and oxytocin groups, respectively ($p<0.01$). A similar pattern was observed for whole blood viscosity. The control value was 4.15±0.25 mPa·s, increasing to 5.35±0.32 mPa·s in the mifepristone group and 4.85±0.30 mPa·s in the

oxytocin group (p<0.001). The conventional coagulation profile demonstrated less pronounced changes. PT and aPTT did not differ significantly between groups. Fibrinogen increased from 2.85±0.24 in controls to 3.18±0.31 and 3.05±0.28, while D-dimer increased from 0.42±0.07 to 0.56±0.09 and 0.51±0.08, respectively (p<0.05). Platelet counts did not differ significantly. You can see Fig. 1 and Fig. 2.

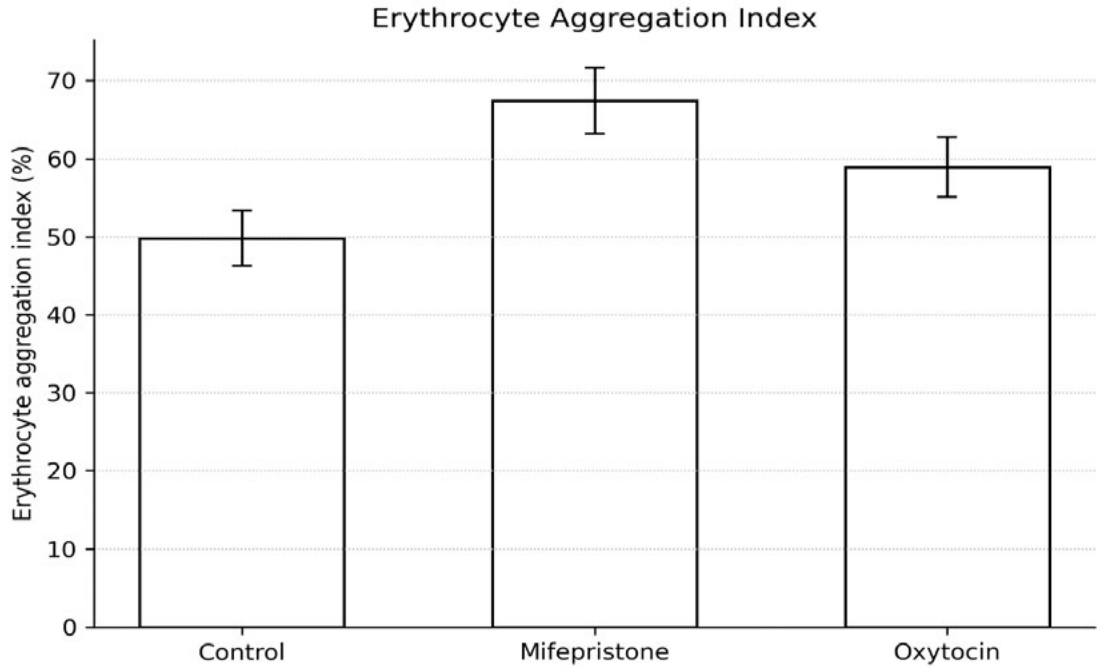


Fig.1. Erythrocy te aggregation index in control, mifepristone, and oxytocin groups. Data are presented as mean±SD.

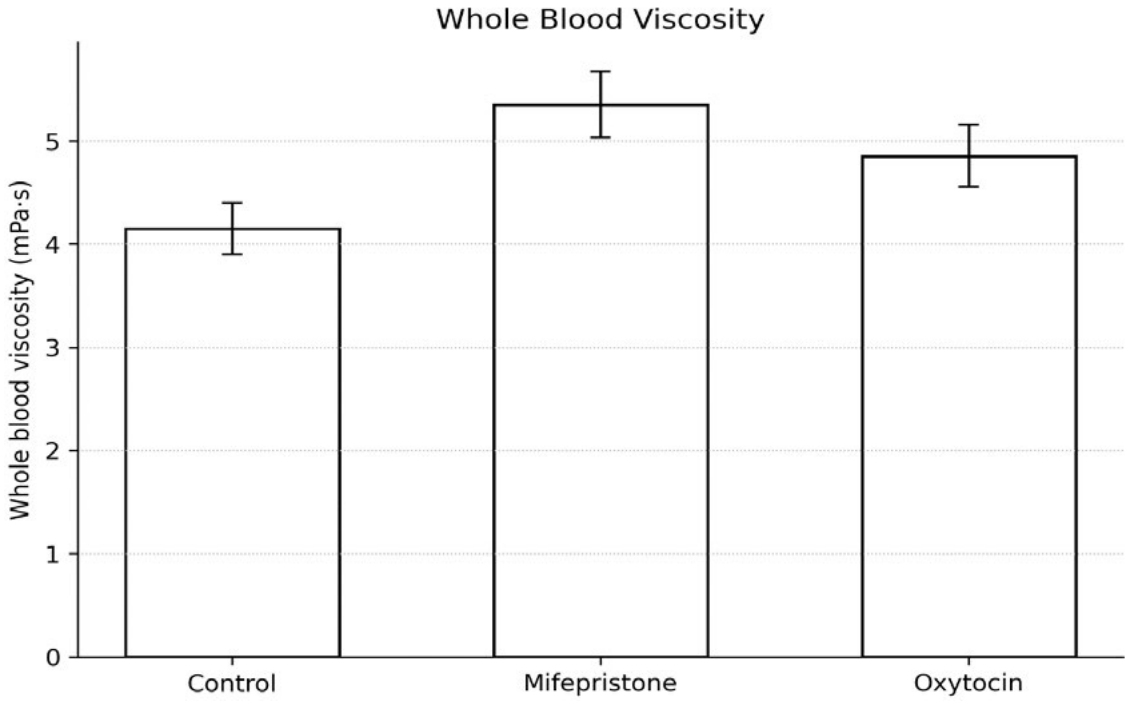


Fig. 2. Whole blood viscosity in control, mifepristone, and oxytocin groups. Data are presented as mean±SD.

Discussion

The present findings demonstrate a coordinated change in several hemorheological characteristics during experimentally induced preterm labor. The increase in erythrocyte aggregation occurred together with a reduction in deformability, suggesting a structural and biophysical shift toward less favorable blood-flow properties [5-10,15-20]. Both parameters are recognized as crucial determinants of whole blood viscosity, vascular wall shear stress, and overall microvascular resistance [5-10,15,17].

The elevation in whole blood viscosity provides additional evidence of altered blood-flow behavior under shear force. Blood viscosity is not a static property; it dynamically changes according to cellular mechanical traits, plasma protein levels (especially fibrinogen), and flow dynamics, playing a particularly vital role in maintaining capillary tissue perfusion in small microvessels [5,6,15,16]. Under low shear rates, increased erythrocyte aggregation promotes the formation of reversible cellular networks and large "rouleaux" clusters [7-10,12,15]. Concurrently, reduced cellular deformability severely impairs the ability of red blood cells to reconfigure and bend when entering and navigating narrow microvascular channels [7-10,17-20].

In the present experiment, the observed changes were noticeably more pronounced in the mifepristone-treated group regarding erythrocyte aggregation and whole blood viscosity. This difference likely reflects the distinct pharmacological and molecular pathways through which different experimental interventions trigger premature myometrial contractions [18]. Mifepristone, as a competitive progesterone receptor antagonist, blocks progesterone-mediated uterine quiescence, triggers a cascade of extracellular matrix breakdown, and promotes local inflammatory alterations in microvascular beds [4,14,18,24]. However, the current study was not specifically designed to isolate the exact cellular signal transduction pathways responsible for this difference.

The relatively modest changes in conventional coagulation parameters – such as prothrombin time (PT), activated partial thromboplastin time (aPTT), and total platelet count – compared with the hemorheological parameters are also noteworthy. Plasma fibrinogen and D-dimer levels were elevated in both experimental groups, signaling an underlying alteration in the procoagulant and fibrinolytic profiles [16]. Nevertheless, the significantly more dominant changes in erythrocyte aggregation, membrane deformability, and whole blood viscosity strongly suggest that evaluating blood rheology provides valuable complementary diagnostic insights beyond traditional coagulation panels.

From a microcirculatory and hemodynamics perspective, these findings hold substantial clinical and physiological relevance. Red blood cell aggregation and deformability govern hydraulic flow resistance, cell-free layer dynamics, and transcapillary oxygen exchange in terminal vascular networks [5-10,15-20]. Previous hemorheological

and uteroplacental research has consistently shown that adverse shifts in erythrocyte biomechanics directly correlate with microvascular perfusion deficits, endothelial stress, disturbances in microvascular blood flow, and tissue hypoxia [8-10,18-21].

These findings should, however, be interpreted within the context of inherent animal model limitations:

1. The number of animals / sample size was relatively small.
2. Inflammatory mediators and cytokines, oxidative stress markers, endothelial function indexes, and placental histopathology were not simultaneously quantified [11].

Therefore, the present results establish a strong physiological association between experimental preterm labor and systemic hemorheological dysregulation, rather than proving a single causal mechanism [1-4].

Conclusion

Experimental preterm labor is associated with profound alterations in systemic hemorheological properties. Significant increases in erythrocyte aggregation, reductions in red cell deformability, and elevations in both plasma and whole blood viscosity were characteristic of both experimental models. Notably, the changes in red cell aggregation and whole blood viscosity were most pronounced in the mifepristone group. These findings strongly support the application of hemorheological profiling as a complementary biomarker tool for investigating microcirculatory, blood-flow, and placental perfusion abnormalities associated with preterm labor [5-10,13,15-20, 22,23].

Acknouledgements

This work was supported by the East West European University Internal Grant.

Conflicts of interest. The authors have no conflict of interest to declare.

References

1. Blencowe H, Cousens S, Oestergaard M Z, et al. National, regional, and worldwide estimates of preterm birth rates in 2010 with time trends since 1990. Lancet. 2012;379(9832):2162-2172.
2. Vogel JP, Chawanpaiboon S, Moller AB, et al. The global epidemiology of preterm birth. Best Practice & Research Clinical Obstetrics & Gynaecology. 2018;52:3-12.
3. Goldenberg, RL, Culhane JF, Iams JD, Romero R. Epidemiology and causes of preterm birth. Lancet. 2008;371(9606):75-84.
4. Romero R, Dey SK, Fisher SJ. Preterm labor: one syndrome, many causes. Science. 2014;345(6198):760-765.
5. Baskurt OK, Meiselman HJ. Blood rheology and hemodynamics. Seminars in Thrombosis and Hemostasis. 2003;29(5):435-450.
6. Baskurt OK, Hardeman MR, Rampling MW, Meiselman HJ. (Eds.). Handbook of Hemorheology and Hemodynamics. IOS Press. 2007.
7. Baskurt, OK, Meiselman HJ. Erythrocyte aggregation: basic aspects and clinical importance. Clinical Hemorheology and Microcirculation. 2013;53(1-2):23-37.
8. Meiselman HJ. Red blood cell aggregation: 45 years being curious. Biorheology. 2009;46(1):1-19.
9. Chien S. Red cell deformability and its relevance to blood flow. Annual Review of Physiology. 1987;49:177-192.
10. Mchedlishvili G. Hemorheological changes in microcirculation: their mechanisms and measurement techniques. Indian Journal of Experimental Biology. 2007;45(1):22-30.
11. Jauniaux E, Burton GJ. Placental oxidative stress and pregnancy complications. Placenta. 2016;48:S2-S6.
12. Rampling MW, Meiselman HJ, Neu B, Baskurt OK. Influence of cell aggregation on blood flow. Biorheology. 2004;41(2):91-112.
13. Baskurt OK, Meiselman HJ. Blood rheology and microvascular function. Clinical Hemorheology and Microcirculation. 2012;49(1-4):133-147.
14. American College of Obstetricians and Gynecologists. ACOG Practice Bulletin No. 234: Preterm Labor. Obstetrics & Gynecology. 2021;138(2):e21-e35.
15. Baskurt OK, Meiselman HJ. Erythrocyte aggregation: basic aspects and clinical importance. Clinical Hemorheology and Microcirculation. 2003;29(1):15-39.
16. Brinkman HJ. Fibrinogen and red blood cell aggregation in vascular disease. Thrombosis Research. 2014;134(4):781-787.
17. Chien S. Physiological and pathophysiological significance of

hemorheology. In: Clinical Hemorheology. Springer, Boston, MA. 1987:11-48.
18. Chien EK. Mifepristone-induced cervical ripening: structural, biomechanical, and molecular events. American Journal of Obstetrics and Gynecology. 2001;184(3):489-496.
19. Fedosov DA, Pan W, Caswell B, Gompper G, & Karniadakis GE. Predictive structure-function modeling of red blood cells in disease. Proceedings of the National Academy of Sciences (PNAS). 2011;108(29):11772-11777.
20. Heilmann L, Rath W. Hemorheology and placental insufficiency. Hypertensive Pregnancy. 2001;20(2):115-128.
21. Kwan MS, Kim S. Red blood cell aggregates and their effect on non-Newtonian blood viscosity in microfluidics. PLOS ONE. 2018;13(6):e0199911.
22. Popel AS, Johnson PC. Microcirculation and Hemorheology. Annual Review of Fluid Mechanics (2005;37:43-69.
23. Simmonds MJ, Meiselman HJ, Baskurt OK. Blood rheology and aging: effects on microvascular perfusion. Microcirculation. 2013;20(3):179-192.
24. Spitzer CA, World SA. The role of mifepristone in cervical maturation and labor induction: pathophysiological mechanisms. Journal of Clinical Medicine. 2025;14(12):4061.

10.51231/2667-9507-2026-005-12-18-33

Extracellular Vesicles in Breast Cancer: Tumor Microenvironment Crosstalk, Organotropic Metastasis, Immune Evasion, and Therapeutic Resistance

Naman Chauhan, Irina Nakashidze

Batumi Shota Rustaveli State University, Batumi, Georgia

Abstract

Breast cancer is a biologically heterogeneous malignancy in which disease progression, metastatic dissemination, immune escape, and therapeutic response are shaped by reciprocal interactions between tumor cells and the surrounding microenvironment. Extracellular vesicles (EVs) have emerged as important mediators of these interactions by transferring proteins, lipids, metabolites, and regulatory nucleic acids among malignant, stromal, endothelial, and immune-cell populations. Within the primary tumor microenvironment, EV-mediated signaling contributes to cancer-associated fibroblast activation, metabolic reprogramming, extracellular-matrix remodeling, angiogenic responses, and immune modulation. Hypoxic stress can further alter EV biogenesis and cargo composition, thereby reinforcing tumor adaptation and vascular remodeling. Beyond the primary tumor, breast-cancer-derived EVs participate in the establishment of organ-specific pre-metastatic niches in the bone, lung, liver, and brain by modifying vascular integrity, stromal-cell behavior, immune-cell function, and tissue-specific signaling networks. EV-associated microRNAs, long non-coding RNAs, proteins, and other bioactive cargos have been implicated in osteoclast activation, endothelial barrier disruption, macrophage reprogramming, suppression of antitumor immunity, and the

intercellular transmission of therapy-resistant phenotypes. These multifaceted functions position EVs as potential circulating biomarkers, therapeutic targets, and delivery platforms in breast cancer. However, their clinical translation remains constrained by EV heterogeneity, methodological variability in isolation and characterization, incomplete definition of cargo specificity and biodistribution, and limited prospective validation. This review critically synthesizes current evidence on EV-mediated microenvironmental crosstalk, organotropic metastasis, immune evasion, and therapeutic resistance in breast cancer, and highlights the methodological and translational priorities required to advance EV-based strategies toward clinical application.

KEYWORDS: Extraccellular vesicles; Breast cancer; tumor microenvironment, organotropic metastasis; immune evasion; therapeutic resistance

Introduction

Breast cancer is a disease characterized by molecular and clinical differences among its subtypes, which include Luminal A, Luminal B, HER2-enriched, and triple-negative breast cancer (TNBC) [1] . According to American Cancer Society, TNBC accounts for approximately 10% to 15% of all cases and is defined by its lack of estrogen receptors, progesterone receptors, and HER2 amplification [2]. Because of this, standard hormone-based or HER2-targeted therapies are not effective, leaving more conventional approach of systemic chemotherapy and surgery as the primary treatment option. The responses to such conventional therapies are commonly short-lived often preceding a rapid relapse often with visceral and brain metastasis. Novel therapies such as combination of AKT inhibitors + EZH2 inhibitors, CDK inhibition primed anti-PDL1, combination epigenetic therapy of a DNA methyltransferase (DNMT) inhibitor and a histone deacetylase (HDAC) inhibitor before ER modulator therapy and several other therapies are being explored but remain under investigation [3-5]. Extracellular vesicles (EVs) are lipid bilayer-enclosed particles released by almost all cell types into biological fluids like plasma and urine. Once considered a mechanism for cellular waste disposal, EVs are now recognized as mediators of communication between cells both locally and systemically [6]. These vesicles are categorized by their size and how they are formed. Exosomes originate from the endosomal pathway, while microves-

icles form through the outward budding of the cell membrane. Other types include apoptotic bodies and large oncosomes. In the tumor microenvironment, breast cancer cells release EVs that deliver microRNAs, such as miR-185-5p, miR-652-5p, and miR-1246, to neighboring cells like fibroblasts. This process can change the state of these fibroblasts, leading to alterations in cellular metabolism that support tumor growth [7]. This communication is bidirectional, as fibroblasts also release vesicles that influence the movement and growth of cancer cells. Additionally, low oxygen levels, or hypoxia, within a tumor increase the release of these vesicles. EVs also enter the bloodstream to reach distant organs like the bone, lungs, liver, and brain. At these sites, they prepare a pre-metastatic niche by increasing vascular permeability. Furthermore, EVs can transfer drug resistance by carrying molecules like P-glycoprotein to sensitive cells. Research into these processes aims to identify new biomarkers and clinical targets for treating metastatic breast cancer.

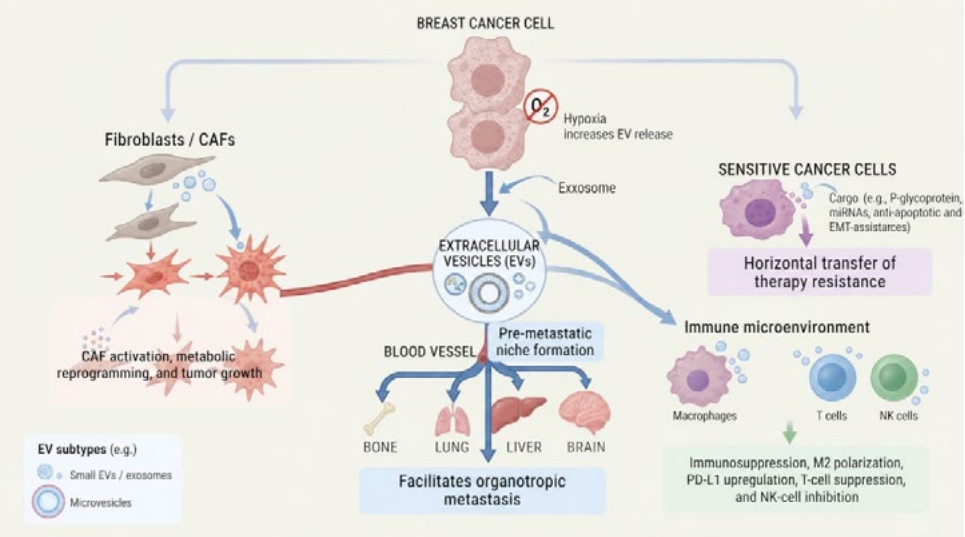


Fig. 1. Extracellular vesicle-mediated communication in breast cancer progression

Breast Cancer Heterogeneity and Extracellular Vesicle Diversity

Breast cancer is characterized by profound molecular and clinical heterogeneity. Standard oncology classifies breast cancer into distinct subtypes based on the expression profiles of estrogen receptors, progesterone receptors, and human epidermal growth factor receptor 2, comprising Luminal A, Luminal B, HER2-enriched, normal-like, and triple-negative (or basal-like) breast cancer; triple-negative breast cancer represents approximately 11%-20% of all cases, exhibiting a highly aggressive clinical

course, early metastatic dissemination, high rates of recurrence, and a complete lack of targetable hormone receptors or HER2 amplification [8]. This absence of receptor targets renders standard endocrine or HER2-targeted therapies ineffective, leaving systemic chemotherapies as the primary standard of care. Standard clinical oncology has also explored combinations such as Trodelvy (sacituzumab govitecan) alongside Keytruda (pembrolizumab) as first-line options for PD-L1-positive metastatic triple-negative breast cancer, or DNA-based therapies like Elenagen, highlighting the need for biomarkers and targeting methods such as PROTAC (Proteolysis Targeting Chimera) alongside delivery systems to counteract the poor cell penetration and instability in vivo [9]. Historically, until the late 1990s, extracellular vesicles were considered simple cellular waste disposal mechanisms. In contemporary cancer biology, however, they are recognized as multifunctional lipid bilayer-enclosed particles released by almost all cell types into biological fluids, such as plasma, urine, saliva, and milk, mediating complex local and systemic intercellular communication. Extracellular vesicles consist of heterogeneous subpopulations that reflect the state of their parental cells at the time of release [10].

TABLE 1. HETEROGENEITY OF EXTRACELLULAR VESICLES

Extracellular Vesicle Class	Diameter Range	Primary Biogenesis Pathway	Key Protein and Regulatory Markers	Lipid Membrane Enrichment
Exosomes (Small EVs)	3-150 nm	Endosomal pathway; inward budding of early endosomes to form intraluminal vesicles within multivesicular bodies.	CD63, CD81,CD9, Alix Hrs, STAM, RAB31, FLOT2	Cholesterol, sphingomyelin, ceramide [8]
Micro vesicles (Ectosomes)	100–1000 nm	Direct outward budding and subsequent fission of the cell's plasma membrane.	Cytoskeletal components, small GTPases, calcium-dependent scramblases	Phosphatidylserine (translocated), cholesterol [8]
Apoptotic Bodies	> 1000 nm	Outward blebbing and cellular disassembly during programmed cell death.	Annexin V, histones, fragmented genomic DNA	Phosphatidylserine (outer leaflet) [8]
Large Oncosomes	1–10 μm	Non-apoptotic plasma membrane shedding from highly active, transformed cancer cells.	Tumor-specific oncoproteins, caveolin-1, lipid raft enzymes	Cholesterol, sphingomyelin

Note: Various classes of vesicles involved in Breast Cancer; they show great heterogeneity

Extracellular Vesicle-Mediated Crosstalk in the Breast Tumor Microenvironment

TME is a regulated network comprising cancer-associated fibroblasts, perivascular-like cells, endothelial cells, immune cells, mesenchymal stem cells, and extracellular matrix components [10]with variations on their methodology and results. The objective of this study is to assess the prevalence of Parkinsonism and its causes in a cohort of individuals age 64 years or older in Bambuí, a Brazilian town. In phase I, 1,186 people older than 64 years responded to a 9-question screening questionnaire for Parkinsonism. In phase II, all subjects who scored > or = 2 points on the test were examined independently by at least 2 movement disorder-trained physicians. A movement disorder senior specialist excluded or confirmed the diagnosis in all suspected cases. The response rate was high for both phases (96% for phase I and 94% for phase II. Single-cell RNA sequencing of triple-negative breast cancer tumors has revealed two distinct functional Cancer-associated fibroblasts (CAF) states (a myofibroblastic phenotype and a state characterized by high growth factor and immunomodulatory gene expression) along with two distinct perivascular-like cell states (differentiated and immature states) [11]. These stromal states exhibit distinct morphologies, spatial relationships, and functional properties in regulating the extracellular matrix. Conventional fibroblast activation is typically tracked using markers such as α-smooth muscle actin α-SMA) and fibroblast activation protein (FAP). Importantly, extracellular vesicles have emerged as primary regulatory players in the activation cascade that activates fibroblasts by the inflammatory mediators and soluble TNF α,β, IL-1,6; as well as direct cell-cell contacts mediated by Jagged1/Notch2 [11,12]. Breast cancer cells actively secrete small extracellular vesicles that deliver regulatory microRNAs-including miR-185-5p, miR-652-5p, and miR-1246-to normal fibroblasts, and therefore support the claim that extracellular vesicles have emerged as a regulatory component in such an activation cascade in breast cancer pathology [12]. Furthermore, small extracellular vesicles support the survival and growth of the primary tumor as the ones containing miR-105 can be transferred from breast cancer cells to cancer associated fibroblasts leading to downregulation of target genes to drive metabolic reprogramming via MYC signaling. Recent studies have revealed that CAFs release their own extracellular vesicles that are internalized by neighboring breast cancer cells, promoting EMT, cell migration, invasion, proliferation, and metabolic alterations thereby facilitating a bidirectional stromal-tumor communication [13]. Moreover, when the extracellular vesicles are mesenchymal stem cell derived, they may contain specific microRNAs, such as miR-205 and miR-31 which support the progression of the primary breast tumor.

Hypoxia, Angiogenesis, and Vascular Remodeling in Breast Cancer

Rapid tumor proliferation lowers the median partial pressure of oxygen to approximately 10mm Hg (1.4%vol/vol$O_{2)}$, relative to 65mm Hg (9.3% vol/vol O_2) in healthy breast tissue. This hypoxia stabilizes hypoxia-inducible factor 1 (HIF-1); its α-subunit is overexpressed in approximately 90% of BRCA1-related breast cancers, correlating with neoadjuvant therapy resistance and reduced survival [14,15].

Under hypoxia, primary breast cancer cells upregulate vascular endothelial growth factor A (VEGFA), von Willebrand factor, and eukaryotic translation elongation factor 1A2 (eEF1A2). This activates the PI3K/AKT and MAPK/ERK pathways, synergistically increasing VEGFA expression, particularly in HER2-enriched subtypes. Elevated HIF-1 additionally activates VE-cadherin, matrix metalloproteinases (MMP2, MMP9), Rac1, and Cdc42, driving cell adhesion, cytoskeletal remodeling, and vasculogenic mimicry (VM) [14,16].

Extracellular Vesicles in Organotropic Metastasis and Pre-Metastatic Niche Formation

Systemic dissemination of breast cancer cells to distant organs remains the primary driver of patient mortality by accounting for over 90% breast cancer related deaths [17]. Before circulating tumor cells colonize distant tissues, primary breast cancer-derived extracellular vesicles travel through the bloodstream to distant organs, preparing a favorable pre-metastatic niche characterized by increased vascular permeability, extracellular matrix remodeling, bone marrow-derived cell recruitment, angiogenesis, and immunosuppression [18].

TABLE 2. VESICLES THAT ARE RESPONSIBLE FOR METASTASIS IN SPECIFIC ORGANS THROUGHOUT THE BODY, THEIR TARGETED GENE OR MOLECULAR PATHWAYS, AND THE KEY PRE METASTATIC MECHANISM FACILITATED BY THE VESICLES

Target Metastatic Organ	Primary Vesicle Cargo	Targeted Gene or Molecular Pathway	Key Pre-Metastatic Mechanism	Reference
Bone	miR-21	Downregulates PDCD4 protein levels	Promotes osteoclast differentiation and activation, inducing osteolytic bone resorption.	[19]
Lung	LncRNA NEAT1	Sponges miR-141-3p, derepressing KLF12	Induces epithelial-mesenchymal transition and upregulates MMPs and ABC transporters.	[18]
	NDPK-B	Activates purinergic receptor P2Y1 and VEGFR2	Regulates purinergic signaling to promote endothelial migration, vascular hyperpermeability, and leakage.	[20]
	miR-105	Downregulates ZO-1 tight junction expression	Destabilizes endothelial cell-cell junctions, enhancing vascular permeability and extravasation.	[18]
Liver	miR-197	Downregulates text PPARG expression	Reduces E-cadherin and upregulates Vimentin, inducing epithelial-mesenchymal transition.	[18]
	miR-9-5p	Upregulates HMGCR, DHCR7,CH25H	Accumulates 25-HC, activating LXR (stemness) and M2 TAMs via IL-6/STAT3.	[18]
	Tspan8	Co-transports E-cadherin and p120-catenin	Induces mesenchymal-epithelial transition (MET) to facilitate macrometastatic colonization.	[18]

Note: Various primary vesicle cargos have been identified specific to organ metastasis.

Highly metastatic breast cancer cells, including the SCP28 subline, secrete exosomes enriched with miR-21. Following internalization by osteoclast precursor cells, exosomal miR-21 directly targets and downregulates programmed cell death protein 4 (PDCD4), accelerating osteoclast differentiation and bone degradation. Concurrently, primary breast cancer cells secrete parathyroid hormone-related protein (PTHrP).

PTHrP acts on osteoblasts to upregulate RANKL and downregulate OPG expression, establishing a RANKL/OPG imbalance that drives pathological osteoclast activity and bone resorption. This osteolytic degradation releases matrix-bound growth factors-specifically TGF-β, VEGF, insulin-like growth factors (IGFs), and calcium ions-creating a positive feedback loop that promotes tumor colonization and survival within the bone marrow niche [21].

Lungs are another target, as Exosomes deliver extracellular matrix (ECM) components, including fibronectin and laminin, altering tumor cell adhesion. Exosome-derived long non-coding RNA NEAT1 functions as a competing endogenous RNA (ceRNA) that sponges and downregulates miR-141-3p, thereby derepressing Kruppel-like factor 12 (KLF12) expression. This KLF12 upregulation activates epithelial-mesenchymal transition (EMT) pathways, increases matrix metalloproteinase (MMP) expression to degrade the local ECM, and elevates ATP-binding cassette (ABC) transporter expression, driving lung-specific invasion. Furthermore, exosomal miR-105 downregulates the tight junction protein zonula occludens-1 (ZO-1) in lung endothelial cells. This disrupts tight junctions and induces hyperpermeability, facilitating the extravasation of circulating tumor cells into the lung parenchyma [18,22].

In liver metastasis, exosomal miR-9-5p is transferred to hepatocytes and hepatic stellate cells, upregulating cholesterol synthesis enzymes, including HMG-CoA reductase (HMGCR), 7-dehydrocholesterol reductase (DHCR7), and cholesterol 25-hydroxylase (CH25H). This drives the localized accumulation of 25-hydroxycholesterol (25-HC), which activates liver X receptor (LXR) signaling to enhance tumor cell stemness. This 25-HC accumulation additionally drives M2-like macrophage polarization via the IL-6/STAT3 pathway, establishing an immunosuppressive hepatic niche [18].

In triple-negative breast cancer, tumor-derived extracellular vesicles stimulate resident hepatic endothelial cells to release CX3CL1, recruiting CX3CR1-expressing macrophages to the pre-metastatic niche. These recruited macrophages overexpress matrix metalloproteinase 9 (MMP9), causing vascular leakage and facilitating circulating tumor cell extravasation. Finally, tetraspanin 8-positive (Tspan8+) extracellular vesicles transfer E-cadherin and p120-catenin to the hepatic parenchyma, triggering mesenchymal-epithelial transition (MET) to facilitate circulating cancer cell colonization [18].

In Brain metastasis, Small extracellular vesicles (sEVs) serve as critical mediators throughout breast cancer via two primary mechanisms Blood-Brain Barrier (BBB) Disruption in which sEVs cross and physically disrupt the BBB by downregulating tight junction proteins and activating brain endothelial cells, which facilitates the transmigration of circulating tumor cells into the central nervous system, and Niche Induction where Within the brain parenchyma, sEVs target resident astrocytes and microglia to induce a neuro-inflammatory, immunosuppressive pre-metastatic niche that promotes metastatic colonization and subsequent tumor cell proliferation.

Extracellular Vesicle-Mediated Immune Modulation and Therapeutic Resistance

Neoplastic cells utilize EVs to suppress anti-tumor immunity through distinct paracrine pathways. First, EVs induce the polarization of macrophages into a tumor-supportive, M2-like phenotype within the tumor microenvironment (TME). Specifically, triple-negative breast cancer cells undergoing chemotherapy-induced apoptosis secrete apoptotic EVs enriched with the chemokine CXCL1. Phagocytosis of these vesicles by macrophages upregulates the infiltration of programmed death-ligand 1-positive PD-L1+ tumor-associated macrophages, a process inhibitable by Baohuoside I or the XIAOPI formula [10]with variations on their methodology and results. The objective of this study is to assess the prevalence of Parkinsonism and its causes in a cohort of individuals age 64 years or older in Bambuí, a Brazilian town. In phase I, 1,186 people older than 64 years responded to a 9-question screening questionnaire for Parkinsonism. In phase II, all subjects who scored > or = 2 points on the test were examined independently by at least 2 movement disorder-trained physicians. A movement disorder senior specialist excluded or confirmed the diagnosis in all suspected cases. The response rate was high for both phases (96% for phase I and 94% for phase II.

Second, tumor-derived exosomes metabolically reprogram tissue-resident macrophages within the pre-metastatic niche. These exosomes stimulate glycolysis via nuclear factor kappa B (NF-kB) signaling, thereby increasing glucose uptake and accelerating the conversion of pyruvate to lactate. The subsequent intracellular accumulation of lactate upregulates macrophage surface expression of PD-L1, which suppresses adaptive T-cell responses.

Third, tumor vesicles directly impair effector lymphocyte function. HER2-positive breast cancer cells overexpressing Neuromedin U secrete EVs enriched with TGFβ1 and PD-L1, which inhibit cytolytic CD8+ T cells, expand regulatory T-cell populations, and induce T-cell exhaustion. Concurrently, mesenchymal stem cell-derived EVs suppress natural killer (NK) cell cytotoxicity by downregulating key activating receptors, thereby impairing innate elimination of circulating tumor cells.

Beyond immunomodulation, EVs operate as functional vectors for the horizontal transfer of drug resistance. Breast cancer cells resistant to Paclitaxel, Adriamycin, Doxorubicin, or Cisplatin encapsulate resistance-associated biomolecules-including P-glycoprotein efflux transporters, anti-apoptotic factors targeting PTEN and BIM, and epithelial-mesenchymal transition regulators acting via the Wntβ-catenin or TGF-β pathways-into secreted vesicles. Internalization of these vesicles by sensitive recipient cells transfers the drug-resistant phenotype [10]with variations on their methodology and results. The objective of this study is to assess the prevalence of Parkinsonism and its causes in a cohort of individuals age 64 years or older in Bambuí, a Brazilian town.

In phase I, 1,186 people older than 64 years responded to a 9-question screening questionnaire for Parkinsonism. In phase II, all subjects who scored > or = 2 points on the test were examined independently by at least 2 movement disorder-trained physicians. A movement disorder senior specialist excluded or confirmed the diagnosis in all suspected cases. The response rate was high for both phases (96% for phase I and 94% for phase II. Furthermore, vesicles selectively incorporate membrane-type matrix metalloproteinases, such as MT1-MMP and ADAM10, which maintain proteolytic activity in the extracellular space and degrade the extracellular matrix to facilitate invasion and metastasis [23].

Discussion

Collectively, the studies reviewed here support extracellular vesicles (EVs) as important mediators of communication between breast cancer cells and the surrounding stromal, vascular, and immune compartments. Their biological effects are unlikely to reflect a single conserved mechanism; rather, they depend on EV source, molecular cargo, recipient-cell phenotype, breast cancer subtype, microenvironmental conditions, and treatment exposure. EVs should therefore be considered components of a broader intercellular signaling network rather than independent determinants of tumor behavior. This distinction is particularly important because much of the mechanistic evidence summarized in this review derives from experimental systems that may not fully reproduce the complexity and heterogeneity of human breast tumors. Within the primary tumor microenvironment, EV-mediated signaling may contribute to reciprocal adaptation between malignant and stromal cells. Breast cancer-derived EVs can alter fibroblast phenotype and metabolism, whereas EVs released by cancer-associated fibroblasts can influence tumor-cell migration, invasion, proliferation, epithelial-mesenchymal plasticity, and metabolic adaptation. These interactions occur alongside cytokine signaling, direct cell-cell communication, and extracellular-matrix remodeling, indicating that EVs represent one component of an integrated tumor-stroma signaling system. Hypoxic conditions further modify this network by increasing EV release and altering EV cargo composition. Together with established hypoxia-responsive pathways, these changes may contribute to endothelial dysfunction, vascular remodeling, angiogenic signaling, and tumor adaptation. However, the relative contribution of EV-mediated signaling to these processes is likely to vary across tumor subtypes and experimental models.

The systemic effects of tumor-derived EVs may be particularly relevant to metastatic progression. Experimental evidence indicates that circulating EVs can modify

distant tissues by influencing vascular permeability, stromal-cell behavior, extracellular-matrix organization, local metabolism, and immune responses. The organ-specific examples discussed in this review illustrate the diversity of these mechanisms. EV-associated miR-21 has been linked to PDCD4 downregulation and osteoclast activation in bone; miR-105-mediated ZO-1 disruption and NEAT1/miR-141-3p/KLF12 signaling have been associated with endothelial and metastatic changes relevant to the lung; EV-associated miR-9-5p and other signaling pathways may contribute to metabolic and immune remodeling in the liver; and breast cancer-derived EVs may influence blood–brain barrier integrity and neuroglial responses during brain metastatic progression. These examples should be regarded as representative rather than exhaustive. Organotropism remains a multifactorial process that also depends on tumor-intrinsic characteristics, survival of circulating tumor cells, vascular accessibility, immune surveillance, and tissue-specific host factors. EV-mediated pre-metastatic niche formation is therefore best interpreted as one component of a broader metastatic cascade.

EV-mediated immune modulation and therapeutic resistance provide additional examples of how intercellular communication may influence disease progression. Tumor-associated EVs have been reported to alter macrophage phenotype and metabolism, contribute to PD-L1-associated immunosuppressive signaling, impair T-cell responses, and reduce natural killer-cell activity in selected experimental settings. In parallel, drug-resistant breast cancer cells can transfer P-glycoprotein, regulatory miRNAs, and other resistance-associated cargo to therapy-sensitive recipient cells. Such transfer may influence drug efflux, survival and apoptosis pathways, epithelial-mesenchymal signaling, and therapeutic responsiveness. These findings support EV-mediated horizontal transfer as one potential mechanism contributing to the spread of resistant phenotypes within heterogeneous tumors. Nevertheless, treatment resistance is inherently multifactorial and also involves clonal selection, genomic and epigenetic adaptation, altered drug transport and metabolism, and microenvironmental protection. EV-dependent mechanisms should therefore be interpreted within this wider biological context.

The ability of EV cargo to reflect aspects of parental-cell biology has generated considerable interest in their use as minimally invasive biomarkers and therapeutic platforms. EV-associated proteins and nucleic acids may provide information about tumor state, metastatic behavior, or therapeutic response, while the intrinsic capacity of EVs to transport biologically active molecules has stimulated investigation of engineered EV-based delivery approaches. However, substantial barriers remain before these applications can be translated reliably into routine clinical practice. EV populations are heterogeneous, and differences in sample collection, separation, purification, characterization, normalization, and functional testing complicate comparisons across studies. Terminology also requires careful standardization; operational descriptors such

as small extracellular vesicles should be preferred when vesicle biogenesis has not been directly demonstrated. In addition, many proposed EV biomarkers and therapeutic strategies remain supported primarily by preclinical evidence. Prospective clinical studies, independent replication, standardized analytical workflows, and quantitative assessment of EV abundance and cargo will therefore be required to establish reproducibility and clinical utility.

A further limitation of the current literature is the predominance of cell-culture and animal-model studies for many specific EV cargos and signaling pathways. These studies provide important mechanistic insight but do not necessarily establish the magnitude or clinical relevance of the same mechanisms in patients. Differences in EV isolation methods, experimental dose, tumor subtype, recipient-cell model, and disease stage may also contribute to variability between studies. Future work should therefore integrate standardized EV characterization with physiologically relevant models and well-annotated patient cohorts. Combining EV profiling with tumor genomics, transcriptomics, proteomics, immune phenotyping, and longitudinal treatment data may help distinguish reproducible disease-associated signals from model-specific observations and identify the EV-associated mechanisms most likely to have diagnostic, prognostic, or therapeutic value.

More broadly, breast cancer is a biologically and molecularly heterogeneous disease in which differences in gene and epigenetic regulation, non-coding RNA activity, and metabolic state may contribute to variability in tumor behavior, invasiveness, biomarker profiles, and therapeutic response [24-27]. This broader heterogeneity provides important context for interpreting EV-mediated signaling as one component of the complex and dynamic breast cancer ecosystem

Fig. 2 integrates the principal themes of this review by linking breast cancer heterogeneity and EV diversity with tumor-stroma communication, hypoxia-associated adaptation, selected mechanisms involved in organ-specific metastatic niche formation, immune modulation, and therapy resistance. The pathways depicted are representative and context dependent rather than exhaustive. Taken together, the available evidence supports EVs as biologically relevant participants in the evolving breast cancer ecosystem, while also emphasizing that their effects occur within a larger network of tumor-intrinsic, stromal, vascular, metabolic, and immune processes. A clearer definition of reproducible EV-associated mechanisms, together with methodological standardization and prospective clinical validation, will be essential for determining which findings can ultimately support clinically useful biomarkers or therapeutic strategies.

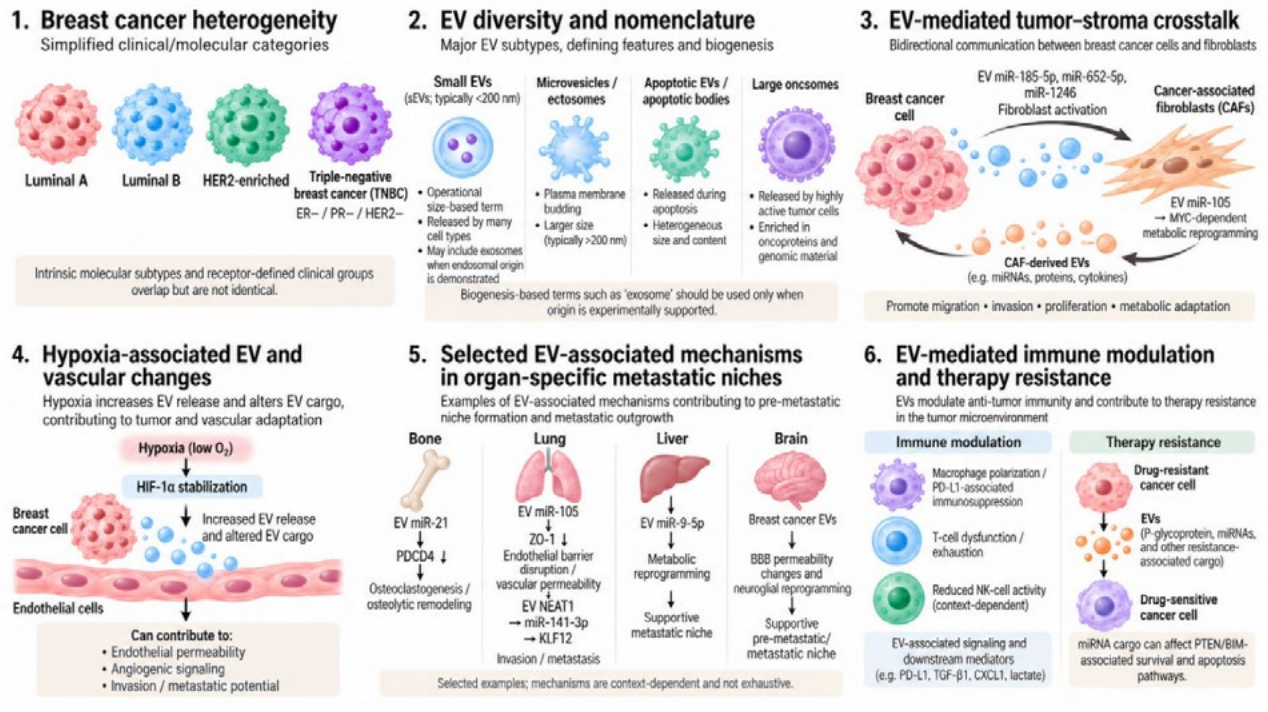


Fig. 2. Extracellular vesicle–mediated mechanisms in breast cancer progression, metastasis, and therapy resistance. The schematic summarizes representative EV-associated processes discussed in this review, including EV diversity, tumor-stroma crosstalk, hypoxia-associated adaptation, selected mechanisms contributing to organ-specific metastatic niches, immune modulation, and horizontal transfer of therapy-resistance-associated phenotypes. The illustrated pathways are context dependent and are not intended to represent an exhaustive model of breast cancer progression.

Conclusion

Extracellular vesicles (EVs) are mediators of communication in breast cancer, particularly in subtypes like triple-negative breast cancer that lack standard therapeutic targets. These vesicles, including exosomes and microvesicles, transfer cargo such as microRNAs and proteins to surrounding cells. Within the tumor microenvironment, this interaction activates fibroblasts and changes cellular metabolism to support tumor growth. Factors such as low oxygen levels, or hypoxia, increase EV secretion, which further supports blood vessel growth and tissue remodeling. Beyond the local environment, EVs travel through the bloodstream to prepare distant organs for metastasis. In the bone, lungs, liver, and brain, these vesicles increase vascular permeability and create conditions that allow cancer cells to survive and grow. This process involves the delivery of molecules that reprogram local cells and suppress immune responses

through signaling pathways like PD-L1 and TGFβ1. Furthermore, EVs carry components that transfer drug resistance between cells, such as efflux transporters and anti-apoptotic factors. Because EVs reflect the state of their origin cells and contribute to cancer progression, they are used to study new biomarkers and treatments for managing metastasis and drug resistance.

References

1. Guo L, et al. Breast cancer heterogeneity and its implication in personalized precision therapy. Exp. Hematol. Oncol. 2023;12(1):3. doi: 10.1186/s40164-022-00363-1.
2. Yin L, Duan J-J, Bian X-W, Yu S. Triple-negative breast cancer molecular subtyping and treatment progress. Breast Cancer Res. 2020;22(1):61. doi: 10.1186/s13058-020-01296-5.
3. Schade AE, et al. AKT and EZH2 inhibitors kill TNBCs by hijacking mechanisms of involution, Nature. 2024;635(8039):755-763. doi: 10.1038/s41586-024-08031-6.
4. Cheung A, et al. CDK Inhibition Primes for Anti-PD-L1 Treatment in Triple-Negative Breast Cancer Models. Cancers. 2022;14(14):3361. doi: 10.3390/cancers14143361.
5. Sharma D, Saxena NK, Davidson NE, Vertino PM. Restoration of Tamoxifen Sensitivity in Estrogen Receptor-Negative Breast Cancer Cells: Tamoxifen-Bound Reactivated ER Recruits Distinctive Corepressor Complexes. Cancer Res. 2006;66(12):6370-6378. doi: 10.1158/0008-5472.CAN-06-0402.
6. Saviana M, Romano G, Del Valle-Morales D, Acunzo M, Nana-Sinkam P. Look Who Is Talking: Extracellular Vesicles as Mediators of Intercellular and Interorgan Communication. Compr. Physiol. 2026;16(2):e70128. doi: 10.1002/cph4.70128.
7. De Luca G, et al. Fibroblasts activated by miRs-185-5p, miR-652-5p, and miR-1246 shape the tumor microenvironment in triple-negative breast cancer via PATZ1 downregulation. Cell. Mol. Life Sci. 2025;82(1):287. doi: 10.1007/s00018-025-05781-y.
8. Schwich E, Rebmann V. The Inner and Outer Qualities of Extracellular Vesicles for Translational Purposes in Breast Cancer. Front. Immunol. 2018;9:584. doi: 10.3389/fimmu.2018.00584.
9. Erwin N, et al. Proteolysis Targeting Chimera Loaded Extracellular Vesicles for Developing Triple Negative Breast Cancer Treatment. J. Extracell. Vesicles. 2025;14(12):e70211. doi: 10.1002/jev2.70211.
10. Loric S, Denis, JA, Desbene C, Sabbah M, Conti M. Extracellular

Vesicles in Breast Cancer: From Biology and Function to Clinical Diagnosis and Therapeutic Management. International Journal of Molecular Sciences. 2023;24:7208. doi:10.3390/ijms24087208.

11. Muttiah B, Ng SL, Lokanathan Y, Ng MH, Law JX, Extracellular Vesicles in Breast Cancer: From Intercellular Communication to Therapeutic Opportunities. Pharmaceutics. 2024;16(5):654. doi: 10.3390/pharmaceutics16050654.
12. Naito Y, Yoshioka Y, Ochiya T. Intercellular crosstalk between cancer cells and cancer-associated fibroblasts via extracellular vesicles. Cancer Cell Int. 2022:22(1):367. doi: 10.1186/s12935-022-02784-8.
13. Castillo-Sanchez R, Churruca-Schuind A, Martinez-Ival M, Salazar EP. Cancer-associated Fibroblasts Communicate with Breast Tumor Cells Through Extracellular Vesicles in Tumor Development. Technol. Cancer Res. Treat. 2022;21:15330338221131647. doi: 10.1177/15330338221131647.
14. Zhou Z, et al. Microenvironmental regulation and remodeling of breast cancer angiogenesis: from basic mechanisms to clinical therapeutic implications. Discov. Oncol. 2025;16(1):1973. doi: 10.1007/s12672-025-03797-1.
15. Ahn M, Mun J-G, Han Y, Seo JH. Cancer cell-derived extracellular vesicles: a potential target for overcoming tumor immunotherapy resistance and immune evasion strategies. Front. Immunol. 2025;16:1601266. doi: 10.3389/fimmu.2025.1601266.
16. Todorova D, Simoncini S, Lacroix R, Sabatier F, Dignat-George F. Extracellular Vesicles in Angiogenesis. Circ. Res. 2017;120(10):1658-1673. doi: 10.1161/CIRCRESAHA.117.309681.
17. Balaji P, Ragothaman S, Maddaly R, Breast cancer metastasis research: current approaches and future possibilities. Curr. Sci. 2026;130(3):208-219. doi: 10.18520/cs/v130/i3/208-219.
18. Shang H, Zhang Y, Chao T. Unveiling the Involvement of Extracellular Vesicles in Breast Cancer's Organotrophic Metastasis: Molecular Mechanisms and Translational Prospects. Int. J. Mol. Sci. 2025;26(12):5430. doi: 10.3390/ijms26125430.
19. Yuan X, et al. Breast cancer exosomes contribute to pre-metastatic niche formation and promote bone metastasis of tumor cells. Theranostics. 2021;11(3):1429-1445. doi: 10.7150/thno.45351.
20. Patel U, Susman D, Allan AL. Influence of Extracellular Vesicles on Lung Stromal Cells during Breast Cancer Metastasis. Int. J. Mol. Sci. 2023;24(14):11801. doi: 10.3390/ijms241411801.
21. Tran MT. Metastatic breast cancer-derived exosomes and osteoclast-mediated bone metastasis. J. Breast Cancer Res. 2023;3(1):8-10. doi: 10.46439/breastcancer.3.019.
22. Q, Liu X, Cheng K, Sheng J, Kong J, Liu T. Pre-metastatic Niche Formation in Different Organs Induced by Tumor Extracellu-

lar Vesicles. Front. Cell Dev. Biol. 2021;9:733627. doi: 10.3389/fcell.2021.733627.

23. Ciferri MC, TassoR. Extracellular vesicle-mediated chemoresistance in breast cancer: focus on miRNA cargo. Extracell. Vesicles Circ. Nucleic Acids. 2025:6(1):112-27. doi: 10.20517/evcna.2024.90.
24. Petrović N, Nakashidze I, Nedeljković M. Breast Cancer Response to Therapy: Can microRNAs Lead the Way? Journal of Mammary Gland Biology and Neoplasia. 2021;26:157-178. doi:10.1007/s10911-021-09478-3.
25. Parveen Shaikh N, Murvanidze I, Shaikh AP, Khurana R, Nakashidze I. The Altered Gene Expression and Epigenetic Mechanisms in Breast Cancer. Journal of Biomedical Research & Environmental Sciences. 2023;4(10):1461-1469. doi:10.37871/jbres1819.
26. Nishanthan AF, Jahja E, Peshkova T, Shaikh NP, Shaikh AP, Barua JD, Nakashidze I. The predictive value of metabolomic-related biomarkers in breast cancers: Current approaches in biotechnology. EUCHEMBIOJ Reviews. 2026;2(1):e26001. doi:10.62063/rev-22.
27. Petrović N, Sami A, Martinović J, Zarić M, Nakashidze I, Lukić S, Jovanović-Ćupić S. TIMP-3 mRNA expression levels positively correlates with levels of miR-21 in in situ BC and negatively in PR positive invasive BC. Pathology – Research and Practice. 2017;213(10):1264-1270. doi:10.1016/j.prp.2017.08.012.

10.51231/2667-9507-2026-005-12-34-47

Clinical Outcomes Following Percutaneous Coronary Intervention, as Determined by Rheological Properties in Patients with Stable Ischemic Heart Disease

Spartak Lekveishvili, Vera Kapetivadze, Maka Mantskava

Tbilisi State Medical University, Tbilisi, Georgia

Abstract

Background: Hemorheological abnormalities contribute to impaired microcirculation and myocardial ischemia in coronary artery disease (CAD). Their prognostic significance after percutaneous coronary intervention (PCI) remains insufficiently defined.

Objective: To evaluate changes in blood cell aggregation after PCI and their association with long-term clinical outcomes in patients with stable CAD.

Materials and Methods: This prospective observational study included patients with stable angina undergoing PCI between March and September 2025. Blood samples were collected before PCI and at 3, 8, and 90 days after intervention. Erythrocyte, leukocyte, and platelet aggregation were assessed using standardized laboratory techniques. Patients were followed for 12 months and divided into two groups according to clinical outcome: Group I (favorable outcome without recurrent ischemia) and Group II (repeat intervention due to recurrent angina and/or restenosis). Statistical analysis included repeated-measures ANOVA and Student's t-test.

Results: Patients with stable CAD demonstrated significantly increased erythrocyte and leukocyte aggregation compared with controls ($p < 0.05$).

Patients with favorable outcomes showed progressive normalization of hemorheological parameters during follow-up, whereas patients requiring repeat PCI demonstrated persistent erythrocyte hyperaggregation and elevated leukocyte aggregation. Platelet aggregation showed less pronounced intergroup differences.

Conclusion: Persistent hemorheological abnormalities, particularly erythrocyte hyperaggregation, are associated with recurrent ischemia and repeat coronary intervention after PCI. Assessment of blood rheology may improve risk stratification in stable CAD.

KEYWORDS: coronary artery disease; hemorheology; erythrocyte aggregation; microcirculation; PCI; restenosis.

Introduction

Coronary artery disease (CAD) remains one of the leading causes of mortality and disability worldwide [1]. Stable angina is among the most common clinical manifestations of CAD and is characterized by transient myocardial ischemia resulting from an imbalance between myocardial oxygen demand and coronary blood supply [1]. Despite major advances in diagnostic and therapeutic strategies, recurrent ischemic events and repeated coronary interventions remain significant clinical challenges [2]. Current European guidelines for chronic coronary syndromes emphasize that revascularization is only one component of management and that long-term outcome depends equally on secondary prevention and on the control of residual risk factors [17].

Percutaneous coronary intervention (PCI) is currently one of the standard methods for myocardial revascularization in patients with symptomatic CAD [2]. Restoration of epicardial coronary blood flow substantially improves symptoms and quality of life. Nevertheless, the long-term clinical effect of PCI varies among patients. Some individuals experience sustained clinical improvement, whereas others develop recurrent ischemia requiring repeat revascularization [2,3].

In-stent restenosis remains the principal cause of repeat target-lesion revascularization after PCI. Although drug-eluting stents have markedly reduced its incidence compared with bare-metal stents, restenosis has not been eliminated, and its treatment remains technically demanding and associated with further recurrence [13]. The established predictors of restenosis are largely procedural and anatomical, including small vessel diameter, long lesions, stent underexpansion and diabetes mellitus [2]. Systemic

factors that modify the local hemodynamic and inflammatory environment of the treated segment have received considerably less attention.

In addition to structural coronary artery lesions, increasing attention has been directed toward abnormalities in blood rheology and microcirculation [4,5]. Blood rheological properties play a critical role in tissue perfusion and oxygen delivery [4]. Elevated blood viscosity, increased aggregation of blood cells, impaired erythrocyte deformability, and endothelial dysfunction may contribute to myocardial ischemia independently of the degree of coronary stenosis [5]. Hemorheological abnormalities have been documented across the whole spectrum of CAD: erythrocyte aggregation, plasma viscosity and whole-blood viscosity are elevated in stable angina and increase further in unstable angina and acute myocardial infarction, suggesting that rheological disturbance tracks disease severity [9]. In patients with unstable angina, increased plasma viscosity and erythrocyte aggregation have been associated with an unfavorable clinical course [10], and in population studies higher blood viscosity and plasma fibrinogen predict future cardiovascular events [11,12].

Erythrocyte aggregation is considered one of the principal determinants of blood viscosity, particularly in low-flow conditions characteristic of the microcirculatory bed [5,6]. Excessive erythrocyte aggregation impairs capillary perfusion, increases peripheral vascular resistance, and reduces oxygen transport efficiency [6]. Leukocyte activation and aggregation additionally contribute to endothelial injury and inflammatory responses, while platelet activation promotes thrombosis and vascular obstruction [7].

The coronary microcirculation is the segment of the coronary tree in which these properties matter most. Coronary microvascular dysfunction can cause angina and myocardial ischemia in the absence of obstructive epicardial disease and frequently coexists with it [15]. After PCI, impaired microvascular perfusion may persist despite a widely patent epicardial artery; in its most severe form this is recognized as the no-reflow phenomenon, in which embolization, endothelial injury and plugging of capillaries by blood cells limit tissue perfusion [14]. Blood with increased cellular aggregation is therefore expected to be particularly disadvantageous in the post-PCI microcirculation.

Previous studies have demonstrated the importance of hemorheological abnormalities in cardiovascular disease [8]. However, limited data are available regarding the relationship between blood cell aggregation and long-term clinical outcomes after PCI [3,8]. Identification of rheological markers associated with recurrent ischemia may improve risk stratification and facilitate individualized therapeutic strategies [2]. The aim of this study was to evaluate changes in blood cell aggregation after PCI and to investigate their association with long-term clinical outcomes in patients with stable CAD. Specifically, the study examined whether the trajectory of erythrocyte, leukocyte and platelet aggregation during the first three months after PCI differs between patients with a favorable 12-month outcome and those who require repeat intervention.

Materials and Methods

Study design and population

This prospective observational study included patients with stable angina who underwent PCI at the Cardiology Department of the University Hospital between March 2025 and September 2025. The study population consisted of patients aged 55 ± 5.4 years with documented stable CAD requiring coronary intervention according to current clinical guidelines [2].

Inclusion criteria:

- Stable angina pectoris;
- Indication for PCI confirmed by a cardiologist;
- Age > 45 years.

Exclusion criteria:

- Anemia;
- Active inflammatory disease;
- Malignancy;
- History of chemotherapy or radiation therapy within the previous year;
- Type 2 diabetes mellitus;
- Severe renal or hepatic dysfunction.

Patients were followed for 12 months after PCI.

Study groups

Patients were divided into two subgroups according to clinical outcomes during follow-up:

- **Group I (Favorable outcome group):** patients without recurrent ischemic symptoms or repeat coronary intervention during follow-up.
- **Group II (Repeat intervention group):** patients who required repeat PCI because of recurrent angina and/or angiographically confirmed restenosis [2].

The control group consisted of apparently healthy age- and sex-matched volunteers.

Laboratory assessment

Venous blood samples were collected before PCI and at 3 days, 8 days, and 3 months after intervention. Parameters assessed included fibrinogen, total cholesterol,

low-density lipoprotein cholesterol (LDL-C), high-density lipoprotein cholesterol (HDL-C), and triglycerides.

Blood rheology assessment

Erythrocyte aggregation was evaluated using the Georgian quantitative aggregation technique described by Mchedlishvili [5]. Blood samples were diluted in autologous plasma and analyzed using the Texture Analysis System (TAS-plus, Leitz, Germany). The erythrocyte aggregation index (EAI) was defined as the ratio of aggregated erythrocyte area to total erythrocyte area [5,6].

Platelet aggregation was assessed using a dual-channel laser platelet aggregation analyzer according to standard principles [7].

Leukocyte aggregation was determined using a hematological counter.

Statistical analysis

Continuous variables are presented as mean ± standard deviation (SD). Normality was assessed via the Shapiro–Wilk test. Between-group comparisons were performed using Student's t-test or Welch's t-test. Repeated measurements were analyzed using repeated-measures ANOVA with post hoc Bonferroni correction. Categorical variables were analyzed using the χ^2 test. A p-value < 0.05 was considered statistically significant (SPSS v27.0).

Results

Baseline characteristics

A total of 62 patients with stable CAD undergoing PCI were enrolled. During 12-month follow-up, 32 patients (51.6%) demonstrated favorable clinical outcomes (Group I), whereas 30 patients (48.4%) required repeat PCI (Group II). The control group consisted of 25 healthy volunteers. Age and sex distribution were comparable between the control group and the patient cohort (Table 1).

Compared with controls, patients with stable CAD had higher total cholesterol (by approximately 29%), LDL-C (by approximately 42%) and fibrinogen (by approximately 41%). The erythrocyte aggregation index was approximately 48% higher in patients than in controls (0.43 ± 0.06 vs. 0.29 ± 0.04; $p < 0.05$). These differences are shown in Fig. 2.

TABLE 1. BASELINE CHARACTERISTICS OF THE CONTROL GROUP AND PATIENTS WITH STABLE CAD

Parameter	Control group	CAD patients
Age (years)	54 ± 4.8	55 ± 5.4
Male sex (%)	62	65
Total cholesterol (mmol/L)	4.5 ± 0.7	5.8 ± 0.9*
LDL-C (mmol/L)	2.6 ± 0.5	3.7 ± 0.8*
Fibrinogen (g/L)	2.9 ± 0.4	4.1 ± 0.6*
Erythrocyte aggregation index	0.29 ± 0.04	0.43 ± 0.06*

*p < 0.05 vs. control group.

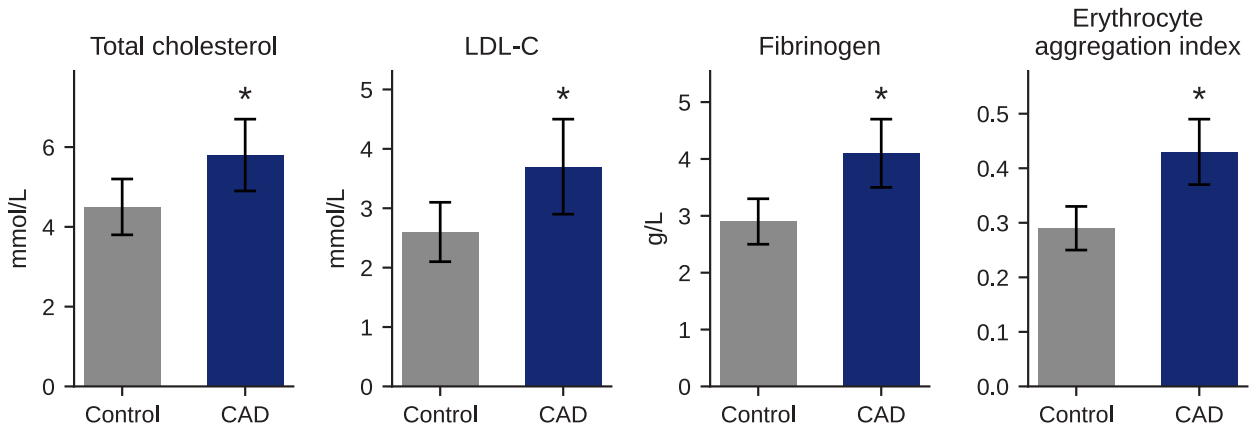


Fig. 2. Lipid parameters, fibrinogen and erythrocyte aggregation index in the control group and in patients with stable CAD before PCI. Data are presented as mean ± SD. *p < 0.05 vs. control group.

Changes in erythrocyte aggregation after PCI

Before PCI, erythrocyte aggregation was elevated in both patient groups compared with controls. Patients with favorable outcomes demonstrated progressive reduction during follow-up, whereas patients requiring repeat intervention showed persistent elevation.

In Group I, the erythrocyte aggregation index decreased from 0.42 ± 0.05 before PCI to 0.31 ± 0.03 at 3 months, a relative reduction of approximately 26%; the 3-month value approached that of the control group (0.29 ± 0.04). In Group II, the index changed from 0.46 ± 0.07 to 0.44 ± 0.06 over the same period, a relative reduction of approximately 4%, and remained at the level observed in the overall CAD cohort before intervention. Group II also had a numerically higher erythrocyte aggregation index before PCI (0.46 vs. 0.42). The time course in both groups is presented in Table 2 and Fig. 1.

TABLE 2. ERYTHROCYTE AGGREGATION INDEX AFTER PCI BY OUTCOME GROUP

Time point	Group I (Favorable)	Group II (Repeat Intervention)
Before PCI	0.42 ± 0.05	0.46 ± 0.07
Day 3	0.39 ± 0.05	0.45 ± 0.06
Day 8	0.35 ± 0.04*	0.43 ± 0.05
3 months	0.31 ± 0.03*	0.44 ± 0.06**

*p < 0.05 vs. baseline; **p < 0.05 vs. Group I.

Leukocyte and platelet aggregation

Leukocyte aggregation decreased significantly after PCI in Group I but remained elevated in Group II. Platelet aggregation showed less pronounced differences between groups, likely reflecting routine dual antiplatelet therapy.

Statistical analysis of hemorheological changes

Repeated-measures ANOVA demonstrated a significant reduction in erythrocyte aggregation over time in Group I ($F = 16.8$, $p < 0.001$; Bonferroni $p < 0.01$ at Day 8 and Month 3). Group II demonstrated a non-significant reduction ($F = 2.4$, $p = 0.084$). At 3 months, erythrocyte aggregation was significantly higher in Group II vs. Group I (0.44 ± 0.06 vs. 0.31 ± 0.03, $p < 0.001$; partial $\eta^2 = 0.31$). Leukocyte aggregation decreased significantly in Group I ($F = 11.2$, $p < 0.001$) but remained elevated in Group II ($F = 3.1$, $p = 0.051$). Platelet aggregation showed no between-group difference ($p = 0.18$).

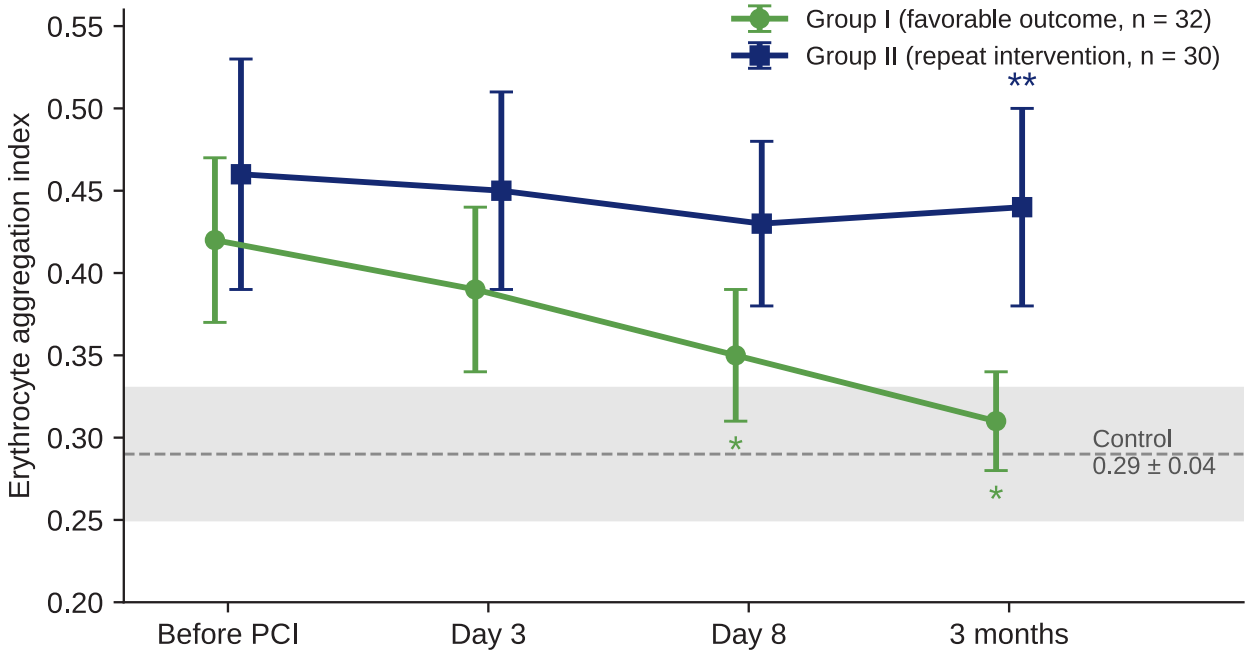


Fig. 1. Erythrocyte aggregation index before and after PCI in patients with a favorable outcome (Group I) and patients who required repeat intervention (Group II). Data are presented as mean ± SD. The dashed line and shaded band show the control group (mean ± SD). *p < 0.05 vs. baseline; **p < 0.05 vs. Group I.

TABLE 3. REPEATED-MEASURES ANOVA OF ERYTHROCYTE AND LEUKOCYTE AGGREGATION OVER THE FOLLOW-UP PERIOD

Parameter	Group	F	p
Erythrocyte aggregation	Group I	16.8	< 0.001
	Group II	2.4	0.084
Leukocyte aggregation	Group I	11.2	< 0.001
	Group II	3.1	0.051

Erythrocyte aggregation at 3 months, Group II vs. Group I: $p < 0.001$, partial $\eta^2 = 0.31$. Platelet aggregation, between-group comparison: $p = 0.18$.

Discussion

The present study demonstrated significant disturbances in blood rheology in patients with stable CAD undergoing PCI [4,8]. Sustained clinical improvement after PCI was associated with persistent normalization of blood rheology, whereas patients requiring repeat intervention demonstrated persistent hyperaggregation [2,3].

The baseline findings are consistent with earlier reports. Increased erythrocyte aggregation and blood viscosity have been described in stable angina, with greater abnormalities in acute coronary syndromes [9], and an adverse rheological profile has been linked to a worse course in unstable angina [10]. The present data extend these observations to the period after elective PCI and suggest that the direction of rheological change after revascularization, rather than the baseline value alone, separates patients with different long-term outcomes. In patients with a favorable outcome, the erythrocyte aggregation index returned close to the control level within three months, whereas in patients who later required repeat intervention it remained essentially unchanged.

Role of fibrinogen

Fibrinogen is the main plasma protein promoting erythrocyte aggregation, and patients in this study had markedly higher fibrinogen than controls. Large prospective data show that plasma fibrinogen is associated with the risk of coronary heart disease and stroke [12], and blood viscosity has likewise been linked to cardiovascular events in the general population [11]. Elevated fibrinogen may therefore be one of the links between systemic inflammation, erythrocyte hyperaggregation and adverse outcome after PCI. Analysis of fibrinogen dynamics during follow-up in relation to aggregation would help to clarify whether the persistent hyperaggregation in Group II reflects a persistent plasma-protein abnormality or an intrinsic change in erythrocyte properties.

Leukocyte aggregation and vascular inflammation

The behavior of leukocyte aggregation paralleled that of erythrocyte aggregation: it decreased significantly in patients with a favorable outcome and remained elevated in patients who required repeat intervention. Atherosclerosis is fundamentally an inflammatory disease in which activated leukocytes interact with the endothelium, migrate into the vessel wall and sustain the local response to injury [18]. Balloon dilatation and stent implantation add an acute mechanical injury to this chronic process. Persistent leukocyte activation after PCI may therefore indicate an ongoing inflammatory response, and the parallel course of erythrocyte and leukocyte aggregation in the present study suggests that both may reflect a common systemic state rather than independent abnormalities. Because leukocyte aggregation was determined by a hematological counter and

its values are reported here only descriptively, this interpretation should be confirmed by quantitative analysis and by concurrent measurement of established inflammatory markers.

Baseline aggregation and the course after PCI

Patients who later required repeat intervention already had a numerically higher erythrocyte aggregation index before PCI than patients with a favorable outcome (0.46 vs. 0.42). The present analysis focused on the change over time and on the comparison at 3 months, and it cannot establish whether the pre-procedural value alone carries prognostic information. Two interpretations are possible: patients with a more pronounced rheological disturbance at baseline may be less likely to normalize after revascularization, or the failure to normalize may itself be the relevant factor. Distinguishing between these possibilities requires a larger cohort in which baseline values, their change after PCI and clinical covariates can be analysed together in a multivariable model.

Relationship with coronary microvascular dysfunction

Coronary microvascular dysfunction represents an important mechanism linking hemorheological abnormalities with adverse outcomes after PCI. Restoration of epicardial patency does not automatically ensure microvascular normalization. Erythrocyte hyperaggregation increases blood viscosity at low shear rates, impairing capillary perfusion and oxygen transport [6]. Microvascular dysfunction is increasingly recognized as a cause of persistent angina after technically successful revascularization [15], and capillary obstruction by aggregated blood cells is one of the mechanisms implicated in impaired post-procedural reperfusion [14]. Persistent hyperaggregation may therefore produce recurrent ischemic symptoms even in the absence of significant restenosis, which may partly explain why recurrent angina and angiographic restenosis were combined in the definition of the adverse outcome group.

Potential mechanisms of restenosis

Persistent erythrocyte hyperaggregation promotes local flow disturbances and increases shear stress heterogeneity. Elevated fibrinogen further accelerates thrombo-inflammatory responses. Activated leukocytes release cytokines and reactive oxygen species, driving smooth muscle proliferation and neointimal hyperplasia. Low and oscillatory wall shear stress is a recognized promoter of endothelial dysfunction and atherogenesis [16], and the neointimal response within a stent is sensitive to the local flow environment. In this context, the relatively small change in platelet aggregation is not unexpected: all patients received routine antiplatelet therapy after PCI [17], which likely at-

tenuated differences between groups, whereas erythrocyte and leukocyte aggregation are not directly targeted by standard post-PCI pharmacotherapy.

Clinical implications

Assessment of erythrocyte aggregation provides prognostic insight beyond angiography. Hemorheological monitoring during follow-up can identify high-risk individuals who may benefit from intensified secondary prevention. The erythrocyte aggregation index is obtained from a small venous blood sample, and its absolute values in the two outcome groups differed substantially at 3 months. If confirmed in larger cohorts, a persistent elevation of the index at follow-up could serve as a signal for closer clinical surveillance and stricter control of modifiable risk factors in line with current recommendations [17]. At present, however, the data do not support any specific rheology-targeted treatment.

Future directions

Larger multicenter cohorts and extended longitudinal follow-up beyond 12 months are necessary to evaluate MACE outcomes and potential targeted hemorheological therapies.

Study Limitations

Single-center observational design, limited sample size, indirect microvascular assessment, and lack of direct whole-blood viscosity measurements represent the main limitations.

Several further points should be considered when interpreting the results. First, with 62 patients the study is not powered to assess hard clinical endpoints, and the findings should be regarded as hypothesis-generating. Second, the analysis compares outcome groups without adjustment for potential confounders such as lesion characteristics, stent type, lipid-lowering therapy and treatment adherence. Third, erythrocyte deformability, plasma viscosity and whole-blood viscosity were not measured, so the contribution of aggregation to overall blood fluidity cannot be quantified. Fourth, leukocyte and platelet aggregation are reported mainly descriptively. Finally, because the outcome groups were defined by events during the 12-month follow-up, the timing of repeat intervention relative to the 3-month blood sampling should be taken into account; the association observed is not evidence of a causal relationship.

Conclusion

Patients with stable CAD demonstrate significant abnormalities in blood rheology before PCI. Improvement in hemorheological parameters post-PCI correlates with favorable long-term outcomes, whereas persistent erythrocyte hyperaggregation is associated with recurrent ischemia and restenosis.

Ethics approval. Approved by the Ethics Committee of Tbilisi State Medical University (TSMU1.05/2024).

Funding. None declared.

Conflict of interest. None declared.

Data availability. Available upon reasonable request from the corresponding author.

References

1. Pastena P, Frye JT, Ho C, Goldschmidt ME, Kalogeropoulos AP. Ischemic cardiomyopathy: epidemiology, pathophysiology, outcomes, and therapeutic options. Heart Fail Rev. 2024;29(1):287-299.
2. Ullrich H, Olschewski M, Münzel T, Gori T. Coronary in-stent restenosis: predictors and treatment. Dtsch Arztebl Int. 2021;118(38):637-644.
3. Heusch G. Coronary blood flow in heart failure: cause, consequence and bystander. Basic Res Cardiol. 2022;117(1):1.
4. Saldanha C. Hemorheology, microcirculation and macrocirculation. Rev Port Cardiol. 2020;39(1):25-26.
5. Mchedlishvili G. Red blood cell aggregability in blood. Criteria for scoring the techniques. Clin Hemorheol Microcirc. 1998;19(2):161-162.
6. Baskurt OK, Meiselman HJ. Hemodynamic effects of red blood cell aggregation. Indian J Exp Biol. 2007;45(1):25-31.
7. Jackson SP. The growing complexity of platelet aggregation. Blood. 2007;109(12):5087-5095.
8. Mantskava M, Jung F, Sanikidze T, Momtselidze N. Parallel study of the rheological status, vascular changes and intracardiac hemodynamics in heart failure in coronary artery disease. Clin Hemorheol Microcirc. 2023;84(2):185-192.
9. Lee BK, Durairaj A, Mehra A, Wenby RB, Meiselman HJ, Alexy T. Hemorheological abnormalities in stable angina and acute coronary syndromes. Clin Hemorheol Microcirc. 2008;39(1-4):43-51.
10. Neumann FJ, Katus HA, Hoberg E, et al. Increased plasma viscosity and erythrocyte aggregation: indicators of an unfavourable clinical outcome in patients with unstable angina pectoris. Br Heart J. 1991;66(6):425-430.
11. Lowe GD, Lee AJ, Rumley A, Price JF, Fowkes FG. Blood viscosity and risk of cardiovascular events: the Edinburgh Artery Study. Br J Haematol. 1997;96(1):168-173.
12. Fibrinogen Studies Collaboration; Danesh J, Lewington S, Thompson SG, et al. Plasma fibrinogen level and the risk of major cardiovascular diseases and nonvascular mortality: an individual participant meta-analysis. JAMA. 2005;294(14):1799-1809.
13. Alfonso F, Byrne RA, Rivero F, Kastrati A. Current treatment of in-stent restenosis. J Am Coll Cardiol. 2014;63(24):2659-2673.
14. Niccoli G, Burzotta F, Galiuto L, Crea F. Myocardial no-reflow in humans. J Am Coll Cardiol. 2009;54(4):281-292.

15. Taqueti VR, Di Carli MF. Coronary microvascular disease pathogenic mechanisms and therapeutic options: JACC state-of-the-art review. J Am Coll Cardiol. 2018;72(21):2625-2641.
16. Malek AM, Alper SL, Izumo S. Hemodynamic shear stress and its role in atherosclerosis. JAMA. 1999;282(21):2035-2042.
17. Vrints C, Andreotti F, Koskinas KC, et al. 2024 ESC Guidelines for the management of chronic coronary syndromes. Eur Heart J. 2024;45(36):3415-3537.
18. Ross R. Atherosclerosis – an inflammatory disease. N Engl J Med. 1999;340(2):115-126.

10.51231/2667-9507-2026-005-12-48-56

An Integrated Methodological Framework for Comparative Assessment of Coastal Seawater in the Black Sea Basin

Maka Mantskava[1], Giorgi Kuchava[1,2], Irina Imerlishvili[3], Gulnara Abashidze[3], Nino Mirianashvili[4], Nadia Antonova[5], Nana Momtselidze[1,6]

[1]*Ivane Beritashvili Center of Experimental Biomedicine, Tbilisi, Georgia*

[2] *Georgian Technical University, Tbilisi, Georgia*

[3]*BAU International University, Batumi, Georgia*

[4] *Rayman Clinics, Tbilisi, Georgia*

[5]*Institute of Mechanics, Bulgarian Academy of Sciences, Sofia, Bulgaria*

[6] *European University, Tbilisi, Georgia*

Abstract

The Black Sea is a unique semi-enclosed marine ecosystem heavily impacted by coastal urbanization, port infrastructure, and industrial activity. Traditional monitoring approaches predominantly focus on quantifying specific chemical pollutants, providing crucial yet piecemeal information regarding individual water body components. This study presents an integrated methodological framework combining physical, physicochemical, rheological, and chemical analyses to establish a comprehensive multi-parameter evaluation of coastal seawater quality across three distinct Black Sea basins: Batumi (Georgia), Varna (Bulgaria), and Istanbul (Turkey). Spatial stratification was structured using a three-tier station design (port/industrial zone, urban/recreational area, and spatial control). Preliminary assessment

under representative summer conditions revealed estimated dynamic viscosities of 0.94 mPa·s (Batumi, 25.0 ∘C), 0.98 mPa·s (Istanbul, 23.5 ∘C), and 1.00 mPa·s (Varna, 22.5 ∘C), demonstrating a clear inverse relationship with temperature. Dynamic viscosity is established as a complementary physical indicator reflecting the holistic state of the fluid, which must be normalized against natural controlling factors (temperature and salinity) rather than interpreted as a standalone pollution metric. The developed protocol standardizes field sampling, temperature-controlled rheometry, GC-MS/HPLC organic contaminant profiling, and multi-variable data integration, providing a robust operational standard for regional Black Sea ecological monitoring.

KEYWORDS: Black Sea; environmental monitoring; seawater rheology; dynamic viscosity; petroleum hydrocarbons; integrated methodology; coastal zone management; standardized sampling

Introduction

The Black Sea constitutes one of the most critical semi-enclosed marine ecosystems globally, uniting the ecological, economic, and social interests of six riparian countries [1,2]. Its coastal zones are characterized by dense urban populations, major shipping routes, expanding port infrastructure, and seasonal tourist hubs [3,4]. These anthropogenic drivers impose intense pressure on marine ecosystems through the Introduction of petroleum hydrocarbons, combustion byproducts, heavy metals, nutrients, and synthetic organic pollutants [5,6]. Traditional marine environmental monitoring relies almost exclusively on direct chemical determinations of specific target contaminants [7,8]. While chemical analysis yields precise quantitative data for individual substances, it frequently fails to capture the aggregate physical and structural transformations occurring within the complex multicomponent seawater matrix [9,10]. In recent years, physical and rheological parameters have gained attention as potential complementary metrics in aquatic ecosystem assessment [11,12]. Seawater dynamic viscosity (η) reflects the macroscopic deformation and flow resistance of the fluid, integrating the combined influences of temperature, salinity, suspended particulate matter, surfactant films, and dissolved organic matter [13,14]. However, a major scientific gap persists: seawater rheological properties are rarely integrated into standardized ecological monitoring protocols, and non-specific physical variations are frequently

misinterpreted without proper baseline normalization [15,16]. This paper introduces a comprehensive, multi-parameter methodological framework designed for comparative coastal water assessment across three major Black Sea coastal nodes: Batumi (Georgia), Varna (Bulgaria), and Istanbul (Turkey). The study defines standardized protocols for spatial sampling, field parameters, physical-chemical characterization, rheological measurement, chemical identification, and multi-variable data integration.

Experimental Part

Study Design and Spatial Stratification

The study employs a comparative spatial design focused on peak summer conditions to evaluate spatial variability while controlling for major seasonal fluctuations. Three major coastal basins of the Black Sea were selected: Batumi (Georgia), Varna (Bulgaria), and Istanbul (Turkey). To capture anthropogenic gradients within each coastal basin, a standardized three-level spatial stratification scheme is established: Station A (High Impact Zone): Located inside or in immediate proximity to primary commercial port infrastructure and industrial maritime channels; Station B (Urbanized Coastal Zone): Located along municipal beach lines and recreational areas characterized by moderate urbanization and seasonal runoff; Station C (Spatial Reference/Control Zone): Located in relatively undisturbed marine waters removed from major direct point-source discharges.

Standardized Sampling and Field Measurements

Sampling is conducted using a unified protocol across all basins. Samples are collected at a standard surface depth of 0.5 m using pre-cleaned, inert fluorinated container vessels to prevent organic contamination. Sample handling minimizes mechanical agitation, bubble entrainment, and phase separation. Each sample is assigned a standardized unique code: BASIN-STATION-NUMBER-DATE (e.g., BAT-A-01-2026). Standardized field registrations include precise GPS coordinates, sampling timestamp, sea state, surface weather conditions, ambient water temperature, Secchi disk transparency, visual surface oil film observations, and proximity to active vessel traffic.

Physicochemical and Rheological Analytical Protocols

Basic physicochemical parameters (pH, electrical conductivity, salinity, and turbidity) are determined immediately using calibrated multi-parameter field probes (WTW MultiLine / YSI ProDSS). Rheological measurements are performed using a temperature-controlled rotational rheometer (e.g., Anton Paar MCR series or Haake Viscotester) equipped with a double-gap coaxial cylinder geometry optimized for low-viscosity

fluids. To eliminate thermal artifacts, rheological measurements are standardized at precise target temperatures (20.0 ^{0}C, 25.0 ^{0}C) using a Peltier temperature control unit (± 0.01 ∘C). Dynamic viscosity (η, mPa·s) is measured across a controlled shear rate range ($\dot{\gamma}$=10–1000 s−1) to verify Newtonian behavior and evaluate potential non-Newtonian anomalies induced by heavy organic loads or colloidal dispersions.

Chemical Contaminant Identification

Chemical analysis targets priority organic pollutants, total petroleum hydrocarbons (TPH), and polycyclic aromatic hydrocarbons (PAHs). Volatile and semi-volatile organic fractions are extracted via liquid-liquid extraction with dichloromethane (DCM) and quantified using Gas Chromatography-Mass Spectrometry (GC-MS, Agilent 7890B/5977B). Polar organic surfactants and specific chemical markers are identified via High-Performance Liquid Chromatography (HPLC-DAD/FLD).

Results and Discussion

Preliminary Physicochemical and Rheological Baseline Assessment

A preliminary baseline model was established for the three representative Black Sea coastal areas (Batumi, Istanbul, and Varna) based on representative summer sea surface temperatures and a standard Black Sea surface salinity of approximately 18. The values represent baseline physical calculations and reference models for standardizing future field campaigns. The assumed summer surface water temperatures were highest in Batumi (25.0 ∘C), intermediate in Istanbul (23.5 ∘C), and lowest in Varna (22.5 ∘C). Correspondingly, the estimated dynamic viscosity values increased from 0.94 mPa·s in Batumi to 0.98 mPa·s in Istanbul and 1.00 mPa·s in Varna (Table 1). The total viscosity difference between Varna and Batumi was 0.06 mPa·s, representing a 6.4% variation relative to the Batumi baseline. The observed ordering for viscosity (Batumi < Istanbul < Varna) was exactly inverse to the temperature ordering (Batumi > Istanbul > Varna), adhering strictly to the pure thermophysical fluid behavior governed by the Andrade-Arrhenius equation for liquid water viscosity.

TABLE 1. PRELIMINARY BASELINE TEMPERATURE AND ESTIMATED SEAWATER DYNAMIC VISCOSITY ACROSS THE STUDY AREAS

Study Area	Assumed Water Temp. (^{0}C)	Estimated Dynamic Viscosity (mPa·s)	Relative Rheological Position
Batumi (Georgia)	25.0	0.94	Lowest estimated viscosity
Istanbul (Turkey)	23.5	0.98	Intermediate estimated viscosity
Varna (Bulgaria)	22.5	1.00	Highest estimated viscosity

Preliminary Seawater pH Profiling

Preliminary reference ranges for seawater pH across the three basins were established (Table 2). All three regions exhibit weakly alkaline conditions characteristic of carbonate-buffered Black Sea surface waters.

TABLE 2. PRELIMINARY ESTIMATED PH RANGES AND PRIMARY ENVIRONMENTAL CONTROLLING FACTORS

Study Area	Preliminary pH Range	Range Midpoint	Main Factors Requiring Field Verification
Batumi (Georgia)	8.0-8.2	8.10	Freshwater discharge (Rioni/Chorokhi), localized precipitation, primary production
Istanbul (Turkey)	8.1-8.2	8.15	Bosphorus hydrodynamic mixing, steep salinity gradients, organic turnover
Varna (Bulgaria)	8.2-8.3	8.25	Coastal freshwater inputs, regional circulation, seasonal phytoplankton blooms

Integrated Multidimensional Profile

Combining thermal, rheological, pH, and anthropogenic exposure parameters yields a unified data structure for baseline comparative monitoring (Table 3). The baseline calculations clearly highlight that raw dynamic viscosity cannot be directly utilized as a standalone pollution indicator. The 6.4% difference in viscosity between Batumi and Varna is fully accounted for by the 2.5^{0}C thermal gradient. Consequently, ranking water bodies by pollution level based on uncorrected field viscosity would lead to erroneous ecological Conclusions (e.g., misinterpreting colder, cleaner water in Varna as more polluted than warmer, heavily impacted water in Batumi) [17,18]. Therefore, all com-

parative monitoring protocols must either execute laboratory rheometry under identical temperature conditions (e.g., strictly at 20.0^{0}C or 25.0^{0}C) or mathematically normalize viscosity values to a standard reference temperature (Tref=20^{0}C) using empirical thermophysical state equations for seawater [19,20]. A vital distinction established in this framework is the physical separation between bulk seawater dynamic viscosity and floating surface petroleum films. A visible petroleum slick on the sea surface represents a distinct immiscible phase [21,22]. Unless oil is emulsified into sub-micron droplets or dissolved as light aromatic fractions, it does not alter the dynamic viscosity of the underlying bulk water column. Therefore, visual surface oil films must be recorded as categorical field descriptors, while dissolved and emulsified petroleum hydrocarbons (TPH) in bulk water are quantified via GC-MS and correlated with normalized rheological residual values [23,24,25,26].

TABLE 3. INTEGRATED PRELIMINARY PHYSICOCHEMICAL AND RHEOLOGICAL PROFILE OF THE BLACK SEA STUDY AREAS

Parameter	Batumi (Georgia)	Istanbul (Turkey)	Varna (Bulgaria)
Assumed Temperature (0C)	25.0	23.5	22.5
Estimated Viscosity (mPa·s)	0.94	0.98	1.00
Estimated pH Range	8.0-8.2	8.1-8.2	8.2-8.3
Anthropogenic Exposure Category	High/Port & Tourist	High/Urban & Maritime	High/Port & Industrial
Viscosity Interpretation	Temperature-sensitive	Temperature-sensitive	Temperature-sensitive
Data Status	Calculated baseline	Calculated baseline	Calculated baseline

Conclusions

This study successfully establishes an integrated methodological framework for multi-parameter assessment of coastal seawater across the Black Sea basin. By combining standardized spatial sampling, field registrations, physicochemical profiling, temperature-controlled rheometry, and GC-MS organic chemical identification, the framework bridges physical fluid mechanics and marine environmental chemistry. The key findings include:

1. Seawater dynamic viscosity (η) is a valuable bulk physical parameter that integrates structural changes in liquid media, but it cannot be used as an isolated

pollution metric.

2. Temperature exerts the primary control on raw seawater viscosity. Uncorrected field viscosity measurements across different temperatures will lead to misleading ecological assessments.
3. Comparative ecological assessments require strict thermal standardization during laboratory rheometry or mathematical normalization to reference conditions (20.0 ◦C).
4. The three-tier station scheme (Batumi – Istanbul – Varna) provides a scalable operational blueprint for transboundary Black Sea environmental monitoring.

Acknowledgements

This work was supported by the Shota Rustaveli National Science Foundation of Georgia (Grant No. BS-26-077).

Conflict of Interest. The authors declare no conflict of interest.

References

1. Deng S, Zhao D, Chen Y, Chen Z, Wang K. Spatiotemporal characteristics and potential drivers of global compound dry-wet events. Environ. Impact Assess. Rev. 2027;110:108619.
2. Allan RP, Barlow MA, Byrne MP, Wilcox LJ, Zolina OG. Advances in understanding large-scale responses of the water cycle to climate change. Ann. N.Y. Acad. Sci. 2020;1472:49.
3. Benjamini Y, Hochberg Y. Controlling the false discovery rate: a practical and powerful approach to multiple testing. J. R. Stat. Soc. Series B Stat. Methodol. 1995;57:289.
4. Terenko G, Krakhmalnyi A, Krakhmalnyi M, Sokolovska O, Lazar L. Blixaea quinquecornis (Dinoflagellata): An Overlooked Blooming Species in the Black Sea. Turk. J. Fish. Aquat. Sci. 2026;26:TRIFAS29993.
5. Klimova T, Vdodovich I, Petrova T, Mashukova O, Zabrodin D. Seasonal Changes in the Ichthyoplankton of the Crimean Peninsula (Northern Black Sea) in 2023. Turk. J. Fish. Aquat. Sci. 2026;26:10421.
6. Malakhova L, Tamoikin I, Voitsekhovskaya V, Malakhova T,

Vdodovich I. Organochlorine contamination in common and rare fish species of the Crimean coastal waters (Black Sea). Mar. Pollut. Bull. 2026;231:119912.

7. Baki OT. Examination of electrical conductivity changes in the sunrise and midday in Değirmendere stream watershed. Phys. Chem. Earth. 2026;144:104497.
8. Ozcan F, Em A, Gasso VY, Arserim NB. A species-specific thermal risk index for cage aquaculture: Spatio-temporal analysis of marine heatwaves in the Turkish Black Sea. Aquaculture. 2026;624:744210.
9. Komorin V, Leposhkin O, Titiapkyn A, Vyshnevskyi V, Oleinik Y. War-related pollution in Black Sea coastal waters: Hydrochemistry, priority pollutant profiles and shoreline oil backtracking. Mar. Pollut. Bull. 2026;230:119835.
10. Sezgin R, Durmus T, Krock B, Balkis-Ozdelice N, Balci M. First phylogenetic and amphidinol-based evidence of benthic Amphidinium species from Turkish coastal waters. Harmful Algae. 2026;158:103168.
11. Solomonova E, Shoman N., Akimov A. Modulation of toxic effects of zinc oxide nanoparticles by nutrient supply conditions: deficiency and excess of nutrients as factors of stress enhancement in the phytoplankton of the Black Sea. Aquat. Toxicol. 2026;298:107895.
12. Liu J, Yang H, Guan H, Ji Z, Ganchev I. Machine learning-guided predictive modeling and optimization of polyamide-based thin-film nanocomposite reverse osmosis membranes. Environ. Res. 2026;305;124981.
13. Talib M, Choudhary A, Ghosh K, Darbha GK. Hybrid ML-driven simulation exploring the fate of environmentally relevant nanoplastics in complex aqueous matrices: Mechanistic insight into colloidal behavior via explainable AI. Water Res. 2026;301:126016.
14. Agirbas E, Dizman S, Sahin A, Yener Helvaci M, Feyzioglu AM. Climate-driven restructuring of phytoplankton productivity and community composition in the south-eastern black sea: Insights from seasonal CO2-Temperature manipulation experiments. Mar. Environ. Res. 2026;218: 108029.
15. Shoman N, Solomonova E, Akimov A. Assessing the ecological risks of ZnO and CuO nanoparticles to black sea picophytoplankton. Comp. Biochem. Physiol. C Toxicol. Pharmacol. 2026;304: 110490.
16. Celik MA, Bilik A, Akiner ME. A Spatiotemporal Analysis of Land Surface Temperature Trends in Türkiye's Biodiversity Hotspot: The Case of Artvin (2000-2024). Pure Appl. Geophys. 2026;183:1120.
17. Solbakov VV, Zatsepa SN, Diansky NA, Panasenkova II, Fomin VV. Simulation of a Fuel Oil Spill Using the Oil-Spill Model SPILLMOD. Phys. Oceanogr. 2026;33:145.

18. Jagelaviciute J, Simkute S, Kaire A, Basinskiene L, Cizeikiene D. Physicochemical Characterization of Soluble and Insoluble Fibers from Berry Pomaces. Gels. 2025;11:796.
19. Yalman V, Turkoglu N, Sahin YM. Development of gelatine and alginate based inks for 3D bioprinters and characterization. Int. J. Biol. Macromol. 2025;295:139666.
20. Fazil AZ, Gomes PIA, Sandamal RMK. Applicability of machine learning techniques to analyze Microplastic transportation in open channels with different hydro-environmental factors. Environ. Pollut. 2024;357:124389.
21. Gao L, Sun H, Nagassa M, Gu Y, He S. Edible film preparation by anthocyanin extract addition into acetylated cassava starch/sodium carboxymethyl cellulose matrix for oxidation inhibition of pumpkin seeds. Int. J. Biol. Macromol. 2024;267:131439.
22. Demyshev SG. Finite-Difference Approximation of the Potential Vorticity Equation for a Stratified Incompressible Fluid and an Example of its Application for Modeling the Black Sea Circulation. Phys. Oceanogr. 2024;31:88.
23. Wang S, Gao Z, Qi X, Bi J, Liu Z. Superhydrophobic carbon black-loaded polyurethane sponge for efficient oil-water separation and solar-driven cleanup of high-viscosity crude oil. J. Water Process Eng. 2023;53:103812.
24. Chen J, Sun M, Ni Y, Li X, Lai Y. Superhydrophobic polyurethane sponge for efficient water-oil emulsion separation and rapid solar-assisted highly viscous crude oil adsorption and recovery. J. Hazard. Mater. 2023;445:130541.
25. Geng T, Yi W, Zhang Y, Wang C, Sun H. Enhancement of rheological properties of water-based drilling fluids using modified nanosilica for deep-sea drilling. J. Eng. Appl. Sci. 2026;73:211.
26. Osmanpour S, Saeedi Dehaghani AH, Behnam Motlagh MA, Simjoo M. Rheology and gelation kinetics of sulfonated polyacrylamide/Cr(III) acetate gels for water shut-off: effects of salinity, temperature, and shear. Sci. Rep. 2026;16:16293.

10.51231/2667-9507-2026-005-12-57-77

Self-Inflicted Denial-of-Service in Digital Healthcare Systems: A Simulation Study of Retry Storms, Metastable Failure, and Mitigation Policies

Teimuraz Sturua[1,2]

[1] *Georgian Technical University, Tbilisi, Georgia*
[2] *European University, Tbilisi, Georgia*

Abstract

Modern healthcare increasingly depends on distributed digital services, including electronic health record systems, telemedicine platforms, patient portals, laboratory information systems, and clinical decision-support applications. Temporary overload or degradation of such services may trigger automatic client retries, potentially increasing system load and converting a short disturbance into a prolonged service disruption. This phenomenon represents a form of self-inflicted denial-of-service and may threaten the availability and continuity of digital healthcare services. This study evaluates the behavior of retry and load-shedding policies under transient overload and identifies conditions associated with metastable failure in distributed healthcare-oriented service architectures. A discrete-event simulation model of an open-loop client fleet and a multi-worker server was developed. The model incorporated client timeouts, retries, bounded server queues, wasted processing of abandoned requests, load spikes, and temporary capacity reductions. Eight policies were compared: no retry, immediate retry, exponential backoff, exponential backoff with jitter, retry budget, circuit breaker, server-side deadline checking, and a combination of retry budget with server-side deadline check-

ing. A total of 2,220 simulation runs were performed, varying trigger magnitude and duration, baseline utilization, server capacity, queue capacity, and retry-budget size. Under the reference scenario of a 2-fold load spike lasting 10 s at 70% baseline utilization, immediate retry, exponential backoff, and backoff with jitter resulted in persistent metastable failure in all 10 simulation runs, with request success of only 2.6-2.7% and retry amplification of approximately 3.9. In contrast, retry-budget and circuit-breaker policies prevented metastable failure under the tested conditions. Server-side deadline checking alone reduced wasted processing but resulted in a degraded state with approximately 22% request success. Combining retry-budget control with server-side deadline checking produced 93.9% request success and the lowest peak queue among the tested policies. A trigger-severity index based on accumulated backlog relative to the amount of work that can be completed during one client timeout period corresponded closely with the simulated transition to instability. In distributed digital healthcare services, retry timing mechanisms such as exponential backoff and jitter should not be considered sufficient protection against self-inflicted overload. Limiting the rate of retries, controlling queueing delay, and discarding requests that have exceeded their useful deadline can substantially improve service resilience. The findings provide a simulation-based framework for assessing the reliability of digital healthcare infrastructure and for designing safer fault-injection and resilience-testing strategies.

KEYWORDS: digital healthcare; healthcare information systems; telemedicine; electronic health records; self-inflicted denial of service; retry storm; metastable failure; distributed systems resilience; retry budget; circuit breaker; simulation; healthcare IT infrastructure

Introduction

Digital technologies have become an essential component of modern healthcare delivery. Electronic health record (EHR) platforms, telemedicine services, patient portals, laboratory and diagnostic information systems, appointment platforms, and clinical decision-support applications increasingly rely on distributed software architectures.

The availability of these systems can therefore influence the continuity and timeliness of access to healthcare information and digital services.

The reliability of distributed healthcare systems is commonly discussed in terms of external cyberattacks, hardware failures, network disruptions, or software defects. However, a service may also become unavailable as a consequence of its own normal reliability mechanisms. A relatively short disturbance-such as a temporary increase in demand, degradation of a dependent service, infrastructure maintenance, garbage-collection pause, or partial system outage-may increase response latency beyond the timeout configured by clients. Automated clients may then retransmit failed requests. The additional requests further increase system load, causing additional delays and generating still more retries.

This positive feedback loop (Fig. 1) can result in a situation in which the original disturbance has already ended but the service remains overloaded. Importantly, the server may continue processing requests for which the requesting client has already stopped waiting. Processing capacity is consequently consumed by work that no longer produces useful output. In healthcare information systems, this type of failure may reduce the availability of patient-facing services or delay access to digital clinical information even though the initial technical disturbance was relatively short.

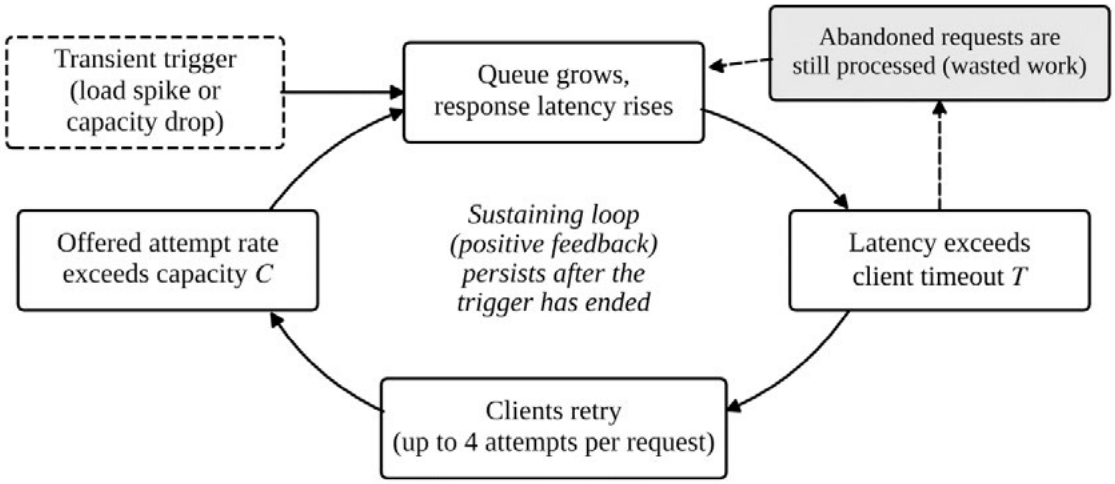


Fig. 1. Retry-storm feedback loop underlying self-inflicted denial-of-service. A transient trigger (dashed box) increases queueing delay; once latency exceeds the client timeout, retries raise the offered attempt rate above server capacity, which sustains the overload after the trigger has ended. Processing of abandoned requests (grey box) consumes further capacity.

Bronson et al. described this behavior as a ***metastable failure***: a system may remain in an undesirable state after the initial trigger has disappeared because a sustaining mechanism continues to generate load [1]. Huang et al. investigated 22 such incidents

across 11 organizations and identified retry policies as a common sustaining mechanism [2]. From the perspective of service availability, this phenomenon resembles a distributed denial-of-service event, although the additional traffic originates from legitimate clients of the service. In this study, the phenomenon is referred to as **self-inflicted denial-of-service (self-DDoS)** [1].

Several engineering mechanisms have been proposed to reduce retry-related overload, including exponential backoff, jitter, retry budgets, circuit breakers, deadline propagation, and server-side load shedding [3-7]. These mechanisms are frequently recommended for resilient distributed systems. However, their individual contribution under comparable operating conditions is less frequently quantified.

This issue is particularly relevant to digital healthcare because healthcare services may involve large numbers of simultaneously connected users and automated systems. For example, a temporary increase in requests to a patient portal or telemedicine platform may cause repeated client requests, while an overloaded backend may continue processing requests that have already exceeded the useful response deadline.

The objective of this study was therefore to investigate, using a reproducible discrete-event simulation, how different retry and load-shedding policies affect the stability of distributed services that may support digital healthcare applications.

The study had four main objectives:

1. To develop a reproducible simulation model of a distributed service with client timeouts, retries, bounded queues, and multiple server workers.
2. To compare eight, retry and load-shedding policies under systematic variations of transient overload and service capacity.
3. To determine whether exponential backoff and jitter are sufficient to prevent metastable failure in an open-loop client population.
4. To identify simple indicators that can help estimate the vulnerability of a digital service to self-inflicted overload.

Background and Related Work

1. Metastable failures in distributed services

Metastable failure describes a state in which a system that was initially functioning normally remains degraded after the original trigger has disappeared [1]. The distinction between stable, vulnerable, and metastable states is particularly useful for distributed healthcare systems because a temporary infrastructure disturbance may become prolonged when interacting with automatic recovery mechanisms (Fig. 2).

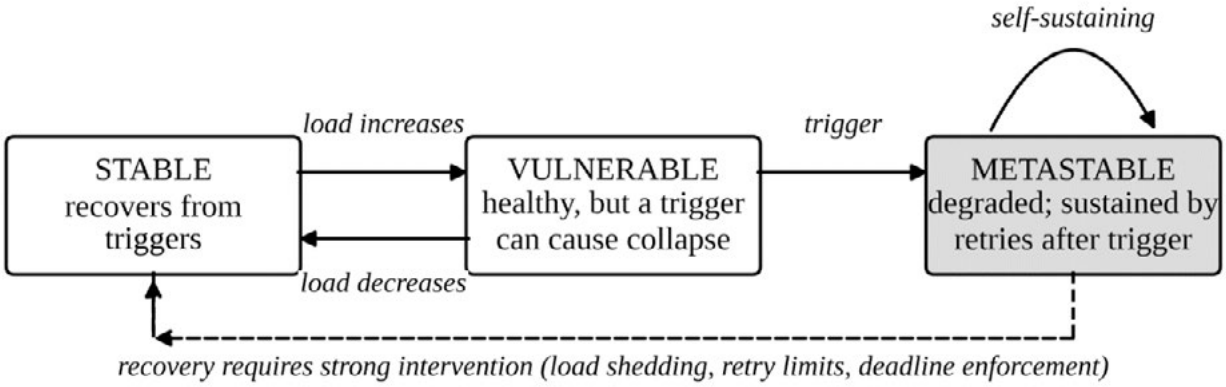


Fig. 2. Stable, vulnerable and metastable states of a distributed service, following the state model of Bronson et al. Movement between the stable and vulnerable states depends on load; a trigger can move a vulnerable system into a self-sustaining metastable state, from which recovery requires explicit intervention.

Huang et al. analysed real-world metastable failures and identified retry behaviour as one of the most frequent sustaining mechanisms [2]. Other research has developed probabilistic, queueing, and formal models for identifying conditions under which distributed systems become vulnerable [8-11].

These findings suggest that resilience cannot be evaluated only by asking whether a system survives an initial fault. It is also necessary to determine whether the system can recover after the fault has been removed.

2. Retry mechanisms and overload control

Exponential backoff with jitter is a widely recommended mechanism for reducing synchronized retries [3]. Backoff increases the interval between successive attempts, while jitter introduces randomization. These mechanisms can reduce simultaneous request bursts.

However, backoff does not necessarily reduce the total number of attempts generated by a large population of independent clients. Brooker has argued that backoff can defer rather than eliminate work in such environments [5]. Retry token buckets and circuit breakers provide an additional mechanism by limiting the amount of retry traffic reaching the service [4].

The Google Site Reliability Engineering literature recommends retry budgets, deadline propagation, and load shedding as mechanisms for reducing cascading failures [6]. The circuit-breaker pattern provides another approach by temporarily preventing requests from reaching a failing service [7].

3. Queueing and response deadlines

Large queues can transform overload into excessive latency [12]. A request may remain technically processable while becoming clinically or operationally useless because its response arrives after the client has timed out. This phenomenon is related to the concept of buffer bloat in computer networks, where excessive buffering produces large delays [13]. Queue-delay control mechanisms such as CoDel demonstrate that limiting delay can be more important than simply maximizing buffer utilization [14]. The same principle may apply to healthcare information systems: a request that remains in a queue beyond the useful response deadline may consume computing resources without contributing to effective service delivery.

4. Relevance to digital healthcare

The increasing dependence of healthcare organizations on distributed digital infrastructure makes availability an important component of healthcare service continuity. A disruption in an EHR interface, telemedicine platform, appointment system, laboratory information system, or patient portal does not necessarily represent a clinical failure in itself, but it can interfere with access to information and digital services.

Consequently, resilience testing of healthcare IT infrastructure should consider not only external attacks but also failure amplification caused by legitimate automated clients.

Chaos engineering provides a structured approach for testing system resilience using controlled faults [15]. However, deliberately triggering a metastable failure in a production healthcare environment may be inappropriate because of the potential impact on users and services. Simulation can therefore be used as a preliminary method for identifying potentially unsafe parameter regions.

System Model and Mitigation Policies

1. Simulation model

The simulated system consists of three components: users, a client fleet, and a server (Fig. 3).

Users generate requests according to a Poisson process with rate λ. The client fleet sends each request to the server as an attempt. Each attempt has a client timeout T and may be retried up to three times, resulting in a maximum of four attempts per original request.

The server contains four parallel workers. Service times are exponentially distributed with a mean of 20 ms. The resulting nominal server capacity is 200 requests/s. Requests enter a FIFO queue with a finite capacity of 5,000 attempts.

The reference baseline utilization is 70%, corresponding to an incoming rate of 140 requests/s.

An attempt fails when its timeout expires or when the server queue is full. Unless server-side deadline checking is enabled, the server continues processing an abandoned attempt even after the client has stopped waiting. The response is subsequently discarded. This mechanism represents wasted processing capacity.

The model uses an open-loop client population: new users continue to generate requests at the specified rate independently of the current system state.

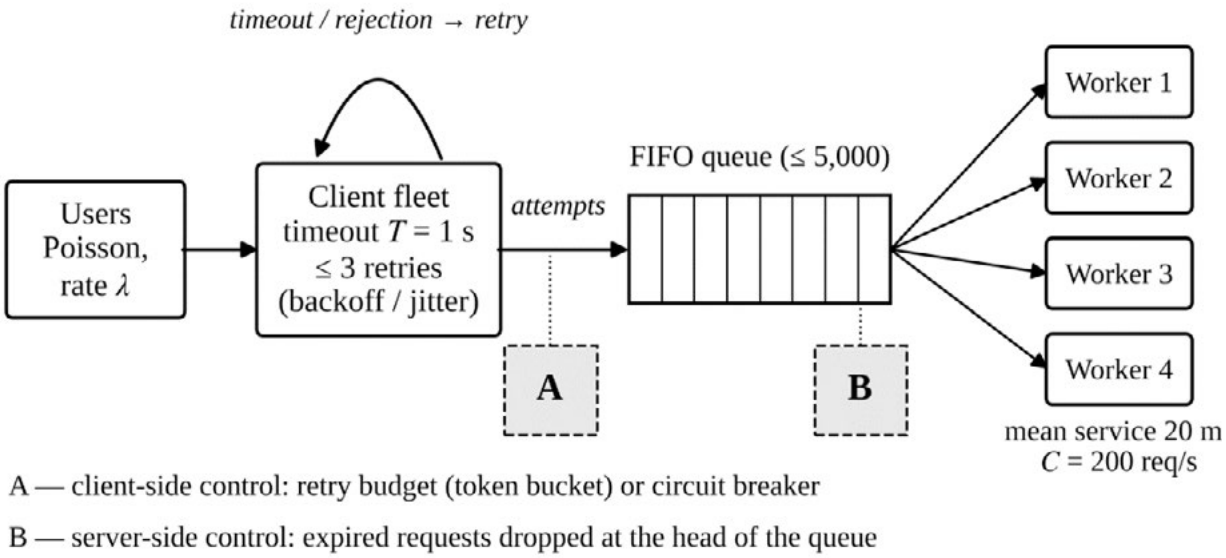


Fig. 3. Simulation model. Users generate requests (Poisson process, rate λ); the client fleet sends attempts with timeout T and up to three retries to a bounded FIFO queue served by four parallel workers (nominal capacity C = 200 requests/s). Dashed boxes mark where the mitigation policies act: (A) client-side retry budget or circuit breaker; (B) server-side deadline check at the head of the queue.

Two types of transient trigger were investigated:

- **Load spike:** the incoming request rate is multiplied by a specified factor.
- **Capacity drop:** the mean service time is multiplied by a specified factor, thereby reducing server capacity.

These triggers represent simplified versions of situations that may occur in digital healthcare infrastructure, such as sudden increases in portal or telemedicine traffic, temporary degradation of a dependent service, or partial loss of processing capacity.

2. Mitigation policies

Eight policies were compared (Table 1):

TABLE 1. RETRY AND LOAD-SHEDDING POLICIES COMPARED IN THE SIMULATION

Policy	Description
No retry	Baseline; failed requests are not retried
Immediate retry	Failed requests are retransmitted immediately
Exponential backoff	Retry delay increases exponentially
Backoff + jitter	Exponential backoff combined with randomised retry delay
Jitter + retry budget	Backoff with jitter plus a fleet-wide retry token budget
Jitter + circuit breaker	Backoff with jitter plus a client-side circuit breaker
Immediate + server deadline	Immediate retry with server-side rejection of expired requests
Budget + server deadline	Retry budget combined with server-side deadline checking

All retrying policies use a maximum of three retries.

The retry budget uses a fleet-wide token-bucket mechanism. Each new request contributes tokens, while each retry consumes one token. This limits the proportion of traffic that can be generated through retries.

The circuit breaker opens for 2 s when more than 50% of attempts in a 1-s observation window fail, with a minimum of 20 observations. While open, new requests and retries fail immediately without reaching the server.

The server-side deadline mechanism discards a request when its deadline has expired by the time it reaches the head of the queue.

3. Analytical indicators

Three quantities were used to characterize system vulnerability.

Vulnerability condition

If each failed request generates four attempts, the offered attempt rate may substantially exceed the original request rate. When the resulting attempt rate exceeds server capacity, the system cannot drain its backlog.

For a retry-budget ratio (r), the maximum retry contribution can be approximated as (r\lambda). The resulting stability condition can therefore be expressed as a relationship between baseline utilization and the permitted retry ratio.

For the reference utilization of 0.70, the theoretical retry-budget boundary is approximately:

$$r^* = \frac{1}{p_0} = 1 + 0.43 = 1.43$$

Trigger-severity index

We define the trigger-severity index as the backlog accumulated during the trigger divided by the amount of work that the server can complete during one client timeout:

$$S = \frac{B_{trigger}}{C \cdot T}$$

where

$$B_{trigger}$$

is the additional backlog produced by the trigger, (C) is server capacity, and (T) is the client timeout.

A value of approximately 1 represents a situation in which the accumulated backlog corresponds to roughly one timeout period of server work.

Queue-capacity threshold

The same reasoning suggests a queue-capacity threshold:

$$Q^* \approx CT$$

If the queue is maintained at or below this level, an attempt should generally not remain queued for longer than approximately one client timeout under the simplified model.

These indicators are first-order approximations and are not intended as exact clinical or operational thresholds.

Experimental Methodology

1. Simulator

The simulator was implemented in Python 3.13 using a discrete-event architecture and NumPy for aggregation.

Each simulation run lasted 240 s (Fig. 4) and included:

- 60 s of baseline operation;
- the transient trigger;
- at least 150 s of post-trigger observation.

The simulator is deterministic for a given random seed.

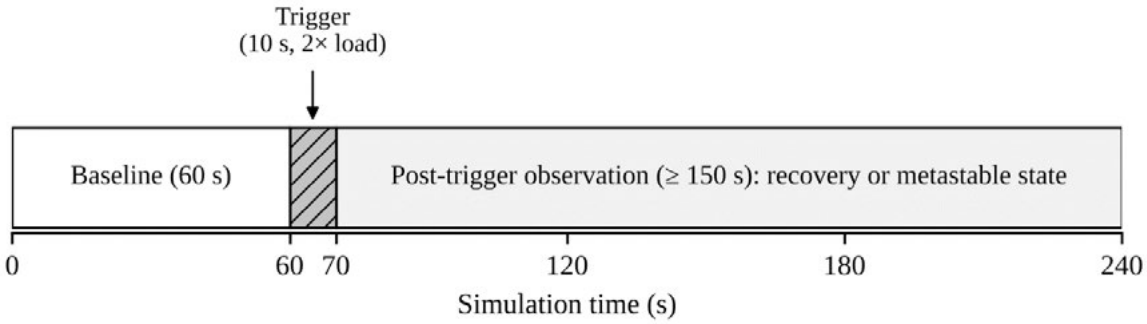


Fig. 4. Timeline of a single simulation run, shown for the reference trigger (2-fold load spike lasting 10 s). Recovery time is measured from the end of the trigger.

The principal reference parameters are summarised in Table 2:

TABLE 2. PRINCIPAL PARAMETERS OF THE REFERENCE CONFIGURATION

Parameter	Reference value
Number of workers	4
Mean service time	20 ms
Server capacity	200 requests/s
Baseline utilisation	0.70
Client timeout	1 s
Maximum retries	3
Backoff base/cap	0.1 / 5 s
Retry-budget ratio	0.1
Token-bucket size	50
Circuit breaker	1 s / 50% / 2 s
Queue capacity	5,000 attempts
Trigger	2× load spike
Trigger duration	10 s
Simulation duration	240 s

2. Experimental design

Each configuration was executed with 10 independent random seeds.
Six experiments produced a total of 2,220 simulation runs (Table 3):

TABLE 3. EXPERIMENTAL DESIGN: VARIED PARAMETERS, POLICIES AND NUMBER OF RUNS

Experiment	Variable	Values	Policies	Runs
E1	Reference scenario	Reference configuration	8	80
E2	Trigger magnitude/duration	1.25–3×; 2–20 s	8	1,280
E3	Baseline utilisation	0.5–0.9	8	400
E4	Capacity reduction	1.5–3× service time	8	240
E5	Queue capacity	50–5,000	4	160
E6	Retry-budget ratio	0.05–1.0	Budget	60

3. Outcome measures

The following metrics were calculated:

- **Goodput:** requests successfully completed within the client timeout per second.
- **Recovery time:** time from the end of the trigger until goodput remained at or above the predefined recovery level for 10 consecutive seconds.
- **Metastable run:** a run that had not recovered by the end of the simulation.
- **Request success:** proportion of requests that ultimately succeeded after retries.
- **Retry amplification:** total attempts divided by original requests.
- **Wasted work:** proportion of completed service associated with responses arriving after client timeout.
- **p99 latency:** 99th percentile of end-to-end latency for successful requests.
- **Peak queue:** maximum queue length.

Means are reported with 95% confidence intervals calculated across the independent simulation seeds.

Results

1. Reference scenario

Under the reference trigger-a 2-fold load increase for 10 s at 70% baseline utilization-policies that allowed unrestricted retries entered persistent metastable failure (Fig. 5, Table 4).

TABLE 4. REFERENCE-SCENARIO OUTCOMES BY POLICY (2-FOLD LOAD SPIKE, 10 S, P_0 = 0.70; MEANS OF 10 RUNS)

Policy	Metastable runs	Recovery, median	Request success	Retry amplification	Wasted work	p99 latency	Peak queue
No retry	0/10	14 s	86.9%± 0.9	1.00	13.1%	0.80 s	813
Immediate retry	10/10	—	2.7% ± 0.3	3.91	98.0%	0.98 s	5,000
Exponential backoff	10/10	—	2.7% ± 0.3	3.90	98.0%	0.98 s	5,000
Backoff + jitter	10/10	—	2.6% ± 0.3	3.91	98.0%	0.98 s	5,000
Jitter + retry budget	0/10	24 s	82.2% ± 1.6	1.02	19.4%	0.84 s	1,089
Jitter + circuit breaker	0/10	14 s	93.8% ± 0.6	0.97	3.7%	0.83 s	428
Immediate + server deadline	10/10	—	22.2% ± 0.8	3.57	83.6%	4.00 s	1,149
Budget + server deadline	0/10	16.5 s	93.9% ± 0.3	1.01	3.9%	0.99 s	371

Before the trigger, all policies produced similar behavior, with a p99 latency of approximately 0.11 s.

During and after the load spike, immediate retry, exponential backoff, and backoff with jitter generated approximately 560 attempts/s. This was approximately four times the original user request rate and substantially exceeded server capacity.

The server therefore remained continuously busy, while approximately 98% of completed processing represented work whose response arrived after the corresponding client timeout.

The similarity between exponential backoff and jitter indicates that these mechanisms altered the timing of retries but did not sufficiently reduce the total amount of retry-generated work in the simulated open-loop environment.

Server-side deadline checking substantially reduced the queue size but did not prevent the system from remaining in a degraded state. Request success remained approximately 22%, with p99 latency increasing to approximately 4 s.

Both retry-rate limiting approaches prevented metastable collapse. The retry budget maintained amplification near 1.02, while the circuit breaker reduced peak queue length and wasted work. Combining the retry budget with server-side deadline checking resulted in the highest request success (93.9%) and the lowest peak queue (371) in the reference experiment.

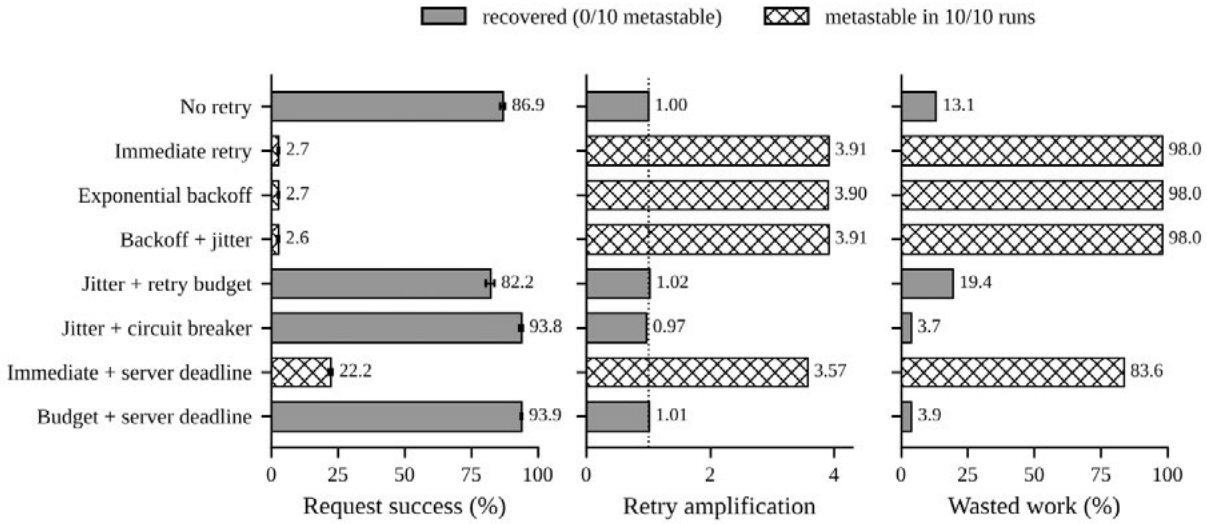


Fig. 5. Reference-scenario outcomes by policy (2-fold load spike, 10 s, $\rho_0 = 0.70$; means of 10 runs). Error bars in the left panel show 95% confidence intervals. Hatched bars denote policies that remained metastable in all 10 runs; the dotted line in the middle panel marks an amplification of 1. Values correspond to the reference-scenario Table 4.

2. Trigger magnitude and duration

The probability of metastable failure increased sharply once the trigger generated a sufficiently large backlog.

At a trigger magnitude of 1.25, the increased load remained below server capacity and no runs collapsed.

For example, a 1.5-fold increase lasting 10 s generated a trigger-severity index close to the transition region. A 1.5-fold increase lasting 20 s generated an index of approximately 1 and resulted in metastable behavior in 6-7 of 10 runs.

For more severe triggers, all runs using immediate retry, exponential backoff, backoff with jitter, or server-deadline checking collapsed.

In contrast, the retry-budget, circuit-breaker, budget-plus-deadline, and no-retry

policies did not produce metastable runs in the tested trigger grid.

These results support the use of backlog relative to timeout-period capacity as a simple preliminary indicator of vulnerability (Fig. 6).

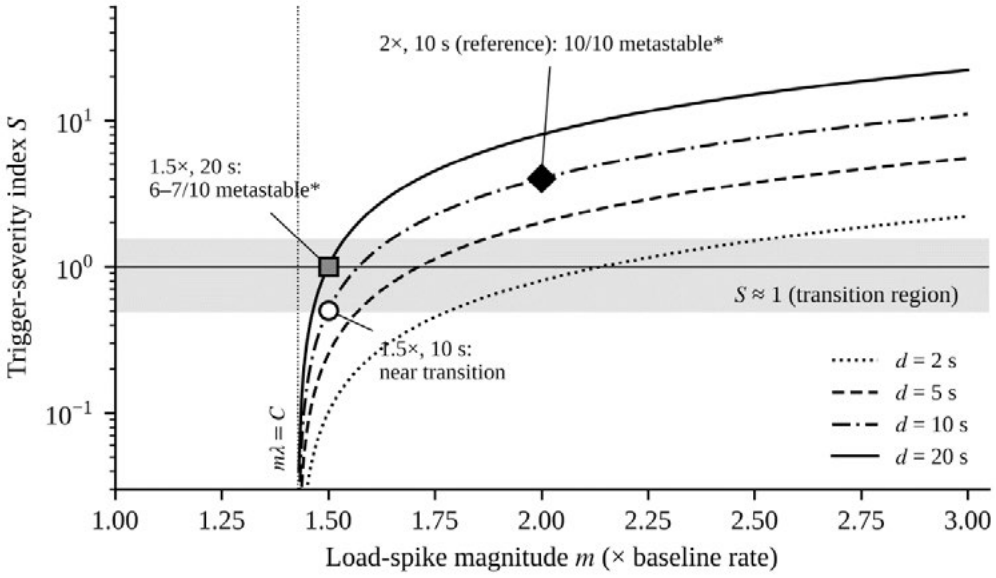


*Fig. 6. Trigger-severity index S = B_trigger / (C·T) for load spikes as a function of spike magnitude m and duration d (λ = 140 requests/s, C = 200 requests/s, T = 1 s), computed analytically from the model parameters. S = 0 when mλ ≤ C (dotted vertical line). Markers show configurations discussed in Section 5.2; * refers to policies without retry-rate limiting.*

3. Baseline utilization

Higher baseline utilization reduced the amount of spare capacity available for recovery (Fig. 7).

At 50% baseline utilization, the 2-fold load spike approximately reached server capacity, and all policies recovered with 100% request success.

At 60% utilization and above, the unlimited-retry policies consistently entered metastable failure.

The server-deadline policy remained functional at 60% utilization but collapsed from 70% upwards.

The retry budget remained stable up to approximately 80% utilization but collapsed at 90%. This corresponded to the theoretical stability boundary for the selected retry-budget ratio.

The circuit breaker and budget-plus-deadline combination maintained request success above 90% across the tested utilization range, including the 90% baseline-utilization condition.

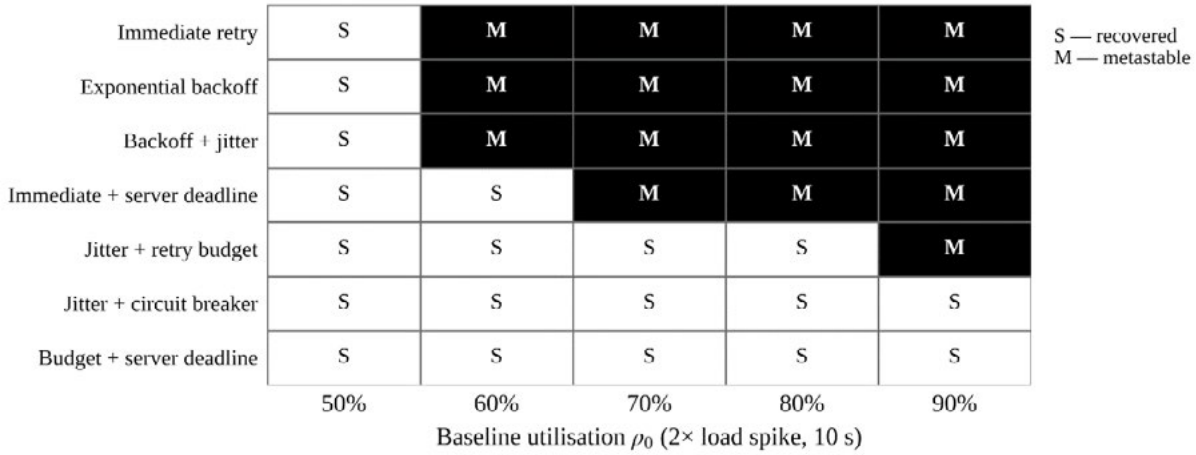


Fig. 7. Outcome of a 2-fold, 10-s load spike across baseline utilisation levels for the seven retrying policies (Experiment E3). S – recovered; M – metastable.

4. Capacity-drop trigger

Temporary reductions in processing capacity produced a pattern similar to that observed with load spikes.

A 1.5-fold increase in service time reduced capacity to approximately 133 requests/s against a baseline workload of 140 requests/s. Under this condition, one of 10 runs collapsed for each of the immediate-retry, backoff, jitter, and deadline policies.

More severe capacity reductions resulted in collapse in all runs for these policies.

The retry budget, circuit breaker, and combined budget-plus-deadline approach prevented metastable failure in the tested configurations.

The combined approach achieved request-success rates of 99.9%, 97.1%, and 95.8% for the three capacity-reduction magnitudes.

5. Queue capacity

Reducing queue capacity substantially improved resilience.

With queue capacities of 50 or 200 attempts, immediate retry and backoff with jitter recovered in every tested run, achieving approximately 94-97% request success.

With queue capacities of 1,000 and 5,000, both policies collapsed in every run.

The observed transition occurred around the analytically estimated threshold of approximately 200 attempts, corresponding to the amount of work that the server can complete during one 1-s client timeout.

Short queues also improved the no-retry baseline. At a queue capacity of 50, request success increased to 97.1%, compared with 86.9% at a queue capacity of 5,000. p99 latency decreased from 0.80 s to approximately 0.31 s.

These results indicate that excessive queueing may convert transient overload into prolonged delay and wasted processing.

6. Retry-budget size

The retry budget behaved consistently with the theoretical stability boundary (Fig. 8).

At low retry-budget ratios, all runs recovered. At ratios of 0.5 and 1.0, all runs collapsed, with retry amplification increasing to 1.48 and 1.96, respectively.

For the reference scenario, the estimated stability boundary was:

$$r^* \approx 0.43$$

Within the stable region, smaller retry budgets produced higher request success and shorter recovery times. This indicates that a retry budget should primarily be interpreted as a **safety mechanism** rather than a performance optimization.

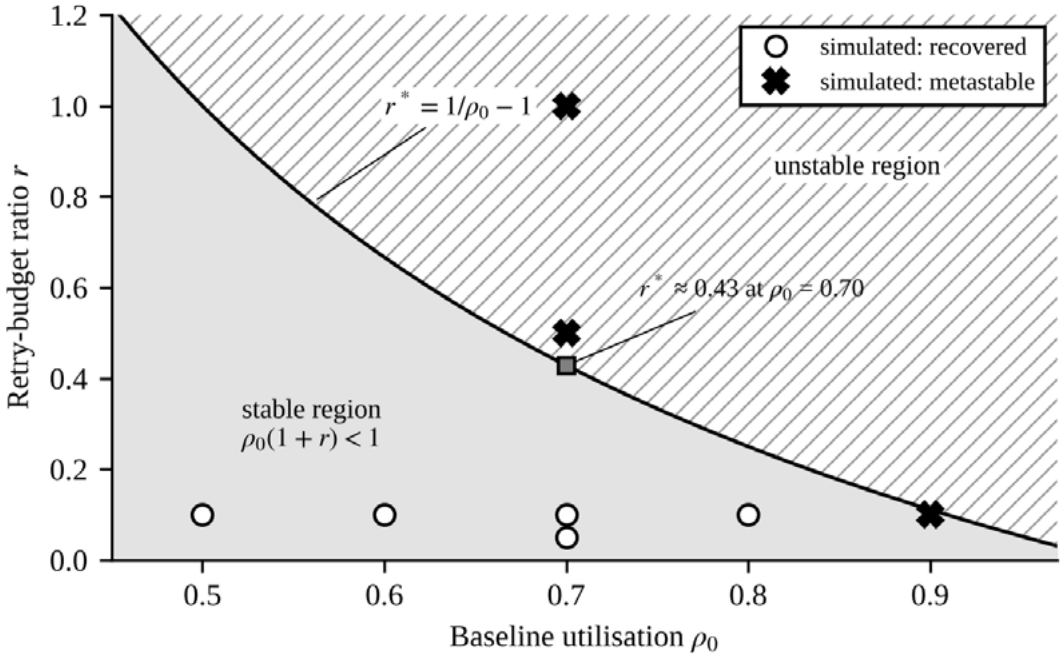


Fig. 8. Theoretical retry-budget stability boundary $r^* = 1/\rho_0 - 1$ with simulated outcomes from Experiments E3 and E6 overlaid. The run at $\rho_0 = 0.9$, $r = 0.1$ lies close to the first-order boundary ($r^* \approx 0.11$) and collapsed in simulation.

Discussion

1. Relevance to digital healthcare

The results demonstrate that automated recovery mechanisms can unintentionally amplify a transient disturbance in a distributed service. This finding has direct relevance to healthcare information infrastructure. Modern healthcare organizations often operate multiple interconnected digital services, and temporary degradation of one component may generate repeated requests from dependent systems, user interfaces, mobile applications, or automated integrations. For example, a temporary slowdown

in a patient portal backend could result in repeated browser or application requests. Similarly, a telemedicine platform experiencing transient latency may generate repeated connection or API attempts. An EHR interface or laboratory information system may also depend on multiple backend services, increasing the potential for cascading retry behavior [2,6]. The present study does not demonstrate that such failures cause specific clinical outcomes. Rather, it identifies a systems-engineering mechanism that may threaten the availability of digital healthcare services.

2. Exponential backoff is not sufficient by itself

In the simulated open-loop environment, exponential backoff and full jitter did not prevent metastable failure. This does not imply that backoff and jitter are inappropriate. They remain useful for reducing synchronisation and instantaneous retry bursts [3]. However, the findings indicate that they should not be considered a complete defence against retry storms. For healthcare systems with strict availability requirements, backoff should therefore be combined with mechanisms that place an explicit upper bound on retry traffic.

3. Retry-rate limiting

Retry budgets and circuit breakers were the most effective client-side mechanisms in the simulation.

A retry budget is particularly attractive because its operating principle is simple: only a controlled fraction of normal traffic may be converted into retries [4,6].

The appropriate budget should be derived from the peak expected utilization rather than the average utilization. A budget that is safe under moderate load may become unsafe when the service operates close to capacity. For healthcare organizations, this principle is relevant when configuring applications and integrations that communicate with shared backend services. Retry policies should be coordinated rather than independently configured by multiple client applications.

4. Queueing delay and deadline propagation

The results also demonstrate the importance of preventing servers from processing requests that have already exceeded their useful deadline [6]. In a healthcare information system, the value of a response is time-dependent. A delayed response may be technically correct while no longer being useful to the requesting application or user. Server-side deadline checking reduces the amount of capacity spent on stale requests. However, the simulation indicates that deadline checking alone may not be sufficient because the system can continue generating excessive retries. The combination of retry-rate limiting and deadline checking therefore provides two complementary protections:

1. **client-side control** limits the amount of additional work entering the system;
2. **server-side control** prevents expired work from consuming processing capacity.

5. Queue configuration as a resilience parameter

Large queues may appear desirable because they prevent immediate rejection of requests. However, the simulation shows that excessive buffering can increase latency and allow a large volume of stale work to accumulate [13,14].

For digital healthcare services, queue size should therefore be considered together with expected service time and client timeout rather than as an independent capacity parameter.

The relationship

$$Q^* \approx CT$$

provides a simple starting point for evaluating whether a queue can contain more work than the service can process within one client timeout. This relationship should not be interpreted as a universal operational rule because real healthcare systems have multiple service classes, priorities, dependencies, and latency distributions.

6. Trigger severity as a resilience-testing indicator

The trigger-severity index provides a potentially useful planning metric for resilience testing. Before conducting controlled fault injection against a digital healthcare service, engineers could estimate whether the expected temporary backlog is likely to exceed the amount of work the system can process during one timeout period. This may help distinguish between relatively safe and potentially destabilizing chaos-engineering experiments [15]. Importantly, the indicator was derived and tested within the simplified simulation model and should therefore be independently validated before being used as an operational decision rule.

Threats to Validity

Several limitations should be considered.

First, the model represents a single service tier with exponentially distributed service times and negligible network latency. Real healthcare IT systems often consist of multiple interconnected services, databases, caches, message brokers, authentication systems, and external dependencies. Such architectures may produce more complex amplification effects.

Second, the client population is open-loop. Real users and applications may com-

bine open-loop and closed-loop behavior. In a closed-loop system, backoff can reduce offered load because a client may wait before initiating another transaction [5]. Therefore, the present results should not be interpreted as demonstrating that backoff is ineffective in all environments. Third, only one set of circuit-breaker and backoff parameters was tested. Alternative thresholds and timeout values may change quantitative results. Fourth, the analytical indicators were evaluated using a relatively coarse experimental grid. For example, queue capacities between 200 and 1,000 attempts were not systematically evaluated. The indicators should therefore be considered hypotheses for engineering analysis rather than validated universal thresholds. Fifth, all findings are based on simulation. No clinical environment, patient data, or real healthcare service was used. The next stage of research should evaluate the proposed mechanisms using a containerized testbed that reproduces representative digital healthcare workloads.

Implications for Healthcare IT Resilience

The findings suggest several practical principles for organizations operating digital healthcare services. First, retry policies should be treated as part of the overall reliability architecture rather than as isolated client configuration parameters. Second, healthcare applications should impose explicit limits on retry traffic. A failure condition should not automatically allow every client to multiply its request rate. Third, request deadlines should propagate through service layers so that servers can avoid processing work that is already obsolete. Fourth, queue capacity should be evaluated in relation to service capacity and client timeout rather than maximized without considering latency. Fifth, resilience testing should include scenarios in which a temporary fault triggers an increase in legitimate application traffic. Finally, healthcare organizations should consider self-inflicted overload as a distinct failure mode in business continuity and digital-service resilience planning.

Conclusion

A distributed healthcare-oriented service can effectively deny service to itself when transient overload causes client timeouts and uncontrolled retries. In 2,220 simulation runs, immediate retry, exponential backoff, and backoff with jitter were unable to prevent metastable failure under sufficiently severe triggers. In the reference scenario, request success decreased to approximately 3%, while approximately 98% of completed server work was wasted because responses arrived after client timeout. Retry budgets and

circuit breakers substantially reduced this risk by limiting the rate at which additional requests entered the system. Server-side deadline checking reduced stale processing, although it was insufficient as a stand-alone mechanism. Combining retry-budget control with deadline checking produced approximately 93.9% request success in the reference scenario and the lowest peak queue. The results indicate that the resilience of digital healthcare services depends not only on increasing computational capacity but also on controlling the feedback mechanisms created by automated clients. Exponential backoff and jitter remain useful for controlling the timing of retries, but they should be complemented by explicit retry-rate limits, queue-delay control, and server-side deadline enforcement. The trigger-severity index and queue-capacity threshold provide simple simulation-derived indicators that may assist in preliminary resilience assessment. Their application to real healthcare infrastructures requires further validation. Future work should evaluate these mechanisms in multi-tier healthcare architectures, including EHR systems, telemedicine platforms, patient-facing applications, and service-to-service integrations. Validation on a containerized testbed with representative workloads and controlled fault injection will be an important next step.

References

1. Gelishvili T, Kuchava G, Sturua T. Self-Inflicted Denial of Service (Self-DDoS) in Distributed Systems, Mechanisms and Mitigating Architectural Strategies: When a System „Attacks“ Itself, An Analysis of Retry Storms, Thundering Herds, and Cascading Failure. Computational and Applied Science. 2026;1(2):141-148. doi:10.68218/2ddp5705.
2. Huang L, Magnusson M, Muralikrishna AB, Estyak S, Isaacs R, Aghayev A, Zhu T, Charapko A. Metastable failures in the wild. In: Proceedings of the 16th USENIX Symposium on Operating Systems Design and Implementation (OSDI '22). 2022:73-90.
3. Brooker M. Exponential backoff and jitter. AWS Architecture Blog. 2015.
4. Brooker M. Fixing retries with token buckets and circuit breakers. 2022.
5. Brooker M. What is backoff for? 2022.
6. Beyer B, Jones C, Petoff J, Murphy NR, eds. Site Reliability Engineering: How Google Runs Production Systems. Sebastopol, CA: O'Reilly Media. 2016.
7. Nygard MT. Release It! Design and Deploy Production-Ready Software. 2nd ed. Raleigh, NC: Pragmatic Bookshelf. 2018.

8. Isaacs R, Alvaro P, Majumdar R, Reddy K, Salamati M, Soudjani S. Analyzing metastable failures. In: Proceedings of the Workshop on Hot Topics in Operating Systems (HotOS '25). ACM. 2025.
9. Alvaro P, Isaacs R, Majumdar R, Muniswamy-Reddy KK, Salamati M, Soudjani S. Formal analysis of metastable failures in software systems. arXiv:2510.03551. 2025.
10. Habibi F, Lorido-Botran T, Showail A, Sturman DC, Nawab F. MSF-Model: Queuing-based analysis and prediction of metastable failures in replicated storage systems. In: Proceedings of the 43rd International Symposium on Reliable Distributed Systems (SRDS). IEEE. 2024.
11. Farahbakhsh A, Lu Q, Alvisi L, Haeberlen A, Van Renesse R. Characterizing metastable faults and failures. arXiv:2606.00942. 2026.
12. Dean J, Barroso LA. The tail at scale. Communications of the ACM. 2013;56(2):74-80.
13. Gettys J, Nichols K. Bufferbloat: Dark buffers in the Internet. Communications of the ACM. 2012;55(1):57-65.
14. Nichols K, Jacobson V. Controlling queue delay. Communications of the ACM. 2012;55(7):42-50.
15. Basiri A, Behnam N, de Rooij R, Hochstein L, Kosewski L, Reynolds J, Rosenthal C. Chaos engineering. IEEE Software. 2016;33(3):35-41.

10.51231/2667-9507-2026-005-12-78-89

Machine Learning in Genomics, A Critical Review of Model Classes, Validation Practices, and Barriers to Translation

Ketevan Kartvelishvili[1], Giorgi Kuchava[1,2]

[1] *Ivane Beritashvili Center of Experimental Biomedicine, Tbilisi, Georgia*

[2] *Georgian Technical University, Tbilisi, Georgia*

Abstract

Machine learning (ML), and deep learning in particular, has become a standard tool in genomics, with applications ranging from prediction of regulatory activity from DNA sequence to variant-effect prediction, single-cell analysis, and polygenic risk estimation. Reported performance, however, depends strongly on evaluation design, and several independent benchmarks indicate that headline results do not always generalize to the tasks that matter biologically or clinically. This review addresses three questions: (i) which model classes are applied to which genomic tasks; (ii) how evaluation practices influence reported performance and where they risk overestimation; and (iii) which factors currently limit translation into biological and clinical use. We organize the literature by task, summarize evidence of performance limits, and illustrate the effect of sample dependence on validation using a controlled simulation. We conclude with a minimum reporting checklist and identify open problems: leakage-resistant benchmarks, evaluation on variant – and individual-level tasks, comparison with tuned simple baselines, ancestry-aware validation, and interpretable, privacy-preserving modeling.

KEYWORDS: machine learning; deep learning; genomics; validation; data leakage; variant-effect prediction; single-cell; polygenic risk

Introduction

In genomics, data generation is no longer the rate-limiting step; interpretation is [1]. Machine-learning methods, particularly deep neural networks, are now applied across the field to predict regulatory activity from sequence, prioritize genetic variants, model cell states, and estimate disease risk [2,3]. Their appeal lies in the ability to learn features directly from raw data and to capture nonlinear and long-range dependencies that hand-engineered features miss.

Genomic data, however, have properties that make standard ML practice hazardous. Dimensionality often exceeds sample size by orders of magnitude. Observations are not independent: adjacent genomic windows share sequence context, paralogous sequences and repeat families recur across the genome, and individuals share haplotypes through common ancestry. Technical variation and population structure can confound biological signal, and labels are frequently noisy, sparse, or biased. As a consequence, reported performance depends heavily on how models are evaluated, and recurrent pitfalls have been catalogued [4].

Existing reviews have mainly described architectures and applications [2,3]. Here we adopt a critical, evaluation-centered perspective and address three questions: (i) which model classes are applied to which genomic tasks; (ii) how do evaluation practices influence reported performance, and where do they risk overestimation; and (iii) which factors currently limit translation into biological and clinical use? Beyond synthesizing the literature, we provide a task-to-model map (Fig. 1, Table 1), a summary of independent evidence on performance limits (Table 2), a controlled simulation illustrating the effect of the data-splitting strategy (Fig. 2 and Fig. 3), and a minimum validation checklist (Table 3).

Scope and Literature Search

This review covers supervised and self-supervised learning on nucleic-acid-derived data in human and model-organism genomics, specifically sequence-based prediction of regulatory activity, variant calling and interpretation, transcriptomic and single-cell modeling, and polygenic prediction. Protein structure prediction, medical imaging, and models based solely on clinical records are outside the scope.

[Literature search strategy: databases searched (e.g., PubMed, Scopus, Web of Science), date of the last search, search strings, inclusion and exclusion criteria, and the number of records screened and included. To be completed by the authors.]

Model Classes and Genomic Tasks

Fig. 1. maps the principal input data types to the model classes and tasks discussed below, and Table 1 summarizes representative models and their main limitations.

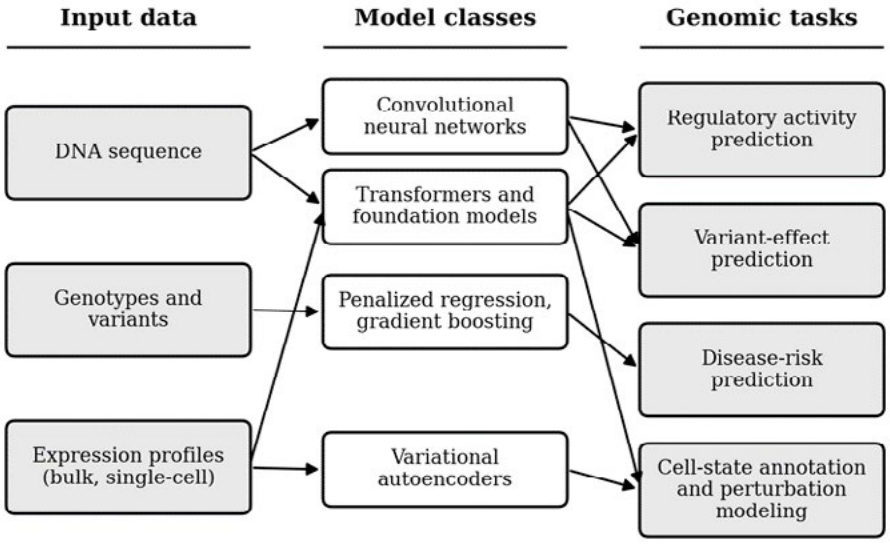


Fig. 1. Relationship between input data, model classes, and genomic tasks. Arrows indicate common pairings and are not exhaustive.

1. Regulatory Genomics from DNA Sequence

Convolutional neural networks (CNNs) were among the first deep architectures applied to genomic sequence. DeepBind predicted the sequence specificities of DNA – and RNA-binding proteins, DeepSEA predicted chromatin features and the effects of noncoding variants directly from sequence, and Basset modeled chromatin accessibility across cell types [5-7]. Subsequent work extended the receptive field: Enformer combined convolutional layers with transformer attention to integrate interactions over long genomic distances (on the order of 100 kb) when predicting expression and chromatin tracks [8]. More recently, self-supervised pretraining on genomic sequence, analogous to language modeling, has produced DNA language models such as DNABERT and the Nucleotide Transformer which are subsequently fine-tuned for downstream tasks [9,10]. A central caveat, examined in Section 4, is that accurate prediction of genome-wide regulatory profiles across loci does not imply accurate prediction of the effects of individual variants.

2. Variant Calling and Variant-Effect Prediction

DeepVariant recast variant calling as image classification on read pileups using a CNN [11]. For variant interpretation, integrative scores such as CADD combined heterogeneous annotations in a linear model [12]; later approaches learned directly from se-

quence, as in SpliceAI, which predicts splice-altering effects of variants from pre-mRNA sequence using a deep residual network [13]. For missense variants, AlphaMissense adapted a protein structure prediction architecture to estimate pathogenicity across the proteome [14]. A recurring difficulty is the nature of the labeled data: clinically classified variants are few, unevenly distributed across genes, and often classified using evidence related to the features used by predictors, which creates circularity between training and benchmarking [15].

3. Single-Cell and Transcriptomic Modeling

Single-cell RNA sequencing yields sparse, high-dimensional count matrices. Probabilistic deep generative models such as scVI use variational autoencoders with count-based likelihoods to model technical noise, batch, and latent cell state [16]. Following the transformer paradigm, foundation models pretrained on tens of millions of cells, such as Geneformer and scGPT, aim to transfer knowledge to tasks including cell-type annotation, gene-network inference, and prediction of perturbation responses [17,18]. Whether pretraining provides gains over simpler approaches on these downstream tasks remains under active evaluation.

4. Polygenic Prediction

Polygenic scores aggregate the effects of many variants, typically estimated by penalized or Bayesian regression on genome-wide association data, to estimate disease risk. Genome-wide scores for several common diseases were shown to identify individuals whose risk approaches that conferred by rare monogenic mutations [19]. Although deep learning has been explored for genotype-phenotype prediction, linear models remain strong baselines in many settings, because common-variant effects are largely additive and sample sizes are small relative to the number of variants.

TABLE 1. PRINCIPAL MACHINE-LEARNING APPROACHES IN GENOMICS, ORGANIZED BY TASK

Task	Input → output	Representative models	Principal limitations
Regulatory activity prediction	DNA sequence → chromatin accessibility, factor binding, expression	DeepBind, DeepSEA, Basset, Enformer [5-8]	Weak prediction of variant effects at the individual level; dependence on cell types present in training data
Self-supervised sequence models	Unlabeled genomes → representations for downstream tasks	DNABERT, Nucleotide Transformer [9,10]	Benefit over supervised baselines must be established task by task; high computational cost
Variant calling	Aligned reads → genotypes	DeepVariant [11]	Performance depends on sequencing platform and training data

Task	Input → output	Representative models	Principal limitations
Variant-effect prediction	Sequence and annotations → pathogenicity or splicing effect	CADD, SpliceAI, AlphaMissense [12-14]	Sparse and biased labels; circularity between training and benchmark data [15]
Single-cell modeling	Count matrices → latent states, annotations, perturbation effects	scVI, Geneformer, scGPT [16-18]	Batch effects; advantage over simple baselines not consistently shown
Polygenic prediction	Genotypes → disease risk	Penalized and Bayesian regression [19]	Reduced accuracy in ancestry groups underrepresented in training data [26]

Evaluation and Its Pitfalls

1. Sample Dependence and Data Leakage

Standard ML validation assumes that training and test examples are independent draws from the same distribution. In genomics this assumption is routinely violated. Adjacent genomic windows share sequence context and regulatory elements, paralogous genes share sequence, and related individuals share haplotypes. If such related observations are divided at random between training and test sets, models can exploit local or family-specific signatures instead of learning generalizable rules, and test performance is inflated [4]. Chromosome-level hold-out has therefore become common practice in sequence-to-function modeling (Fig. 2), although it does not remove homology between chromosomes [20].

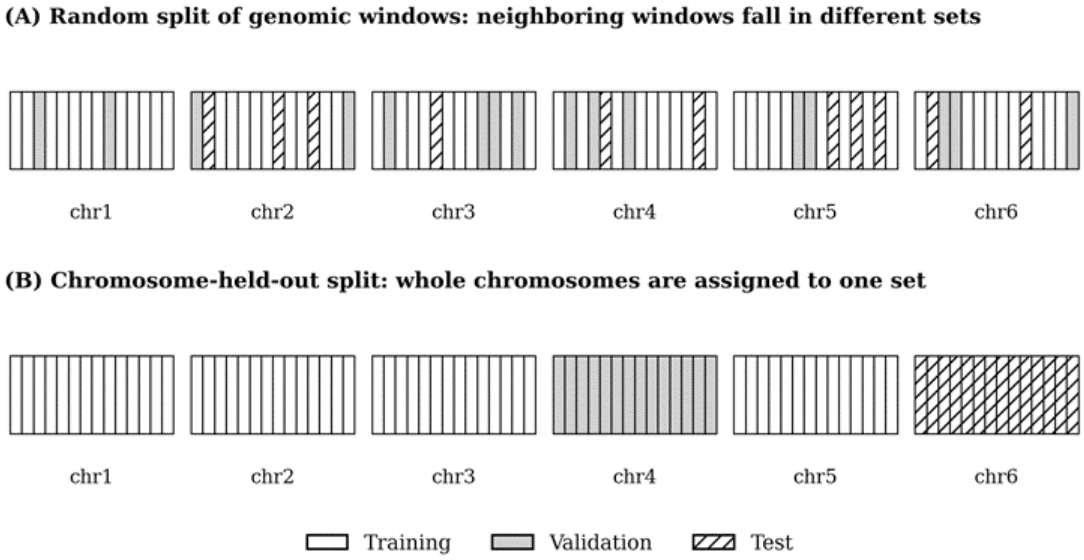


Fig. 2. Data-splitting strategies for genomic windows. (A) In a random split, neighboring windows are distributed across training, validation, and test sets, allowing information to leak between them. (B) In a chromosome-held-out split, entire chromosomes are assigned to a single set.

To illustrate the magnitude of the effect in a controlled setting, we simulated 10 “chromosomes” of 300 windows each, with 20 features. Each feature vector was the sum of a chromosome-specific signature (representing locus, batch, or local sequence context), a weak label-related signal in three features, and random noise; label prevalence differed across chromosomes. A random forest classifier evaluated with random five-fold cross-validation reached a mean area under the receiver operating characteristic curve (AUROC) of 0.70 (SD 0.02; 15 replicate simulations), because it could learn chromosome-specific signatures that predict label prevalence. When entire chromosomes were held out, mean AUROC fell to 0.54 (SD 0.07), close to chance, reflecting the weak signal that actually generalizes (Fig. 3). The simulation is deliberately simple and does not represent any specific published model; its purpose is to show that the gap can be large even when the algorithm and data are identical and only the splitting rule differs.

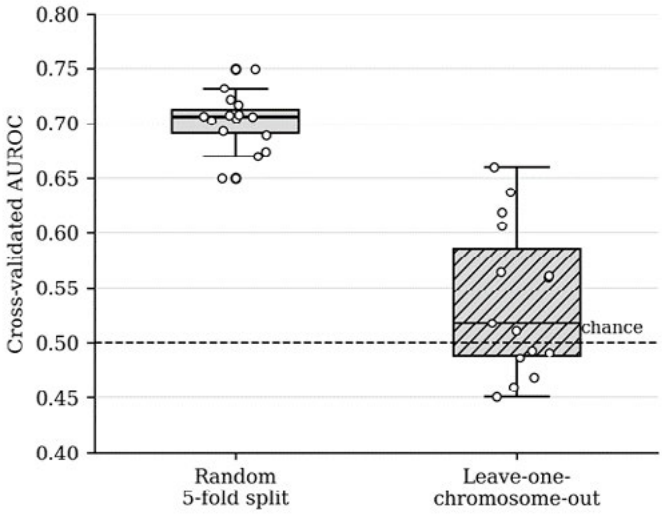


Fig. 3. Effect of the splitting strategy on apparent performance in a simulation (15 replicates; points are individual replicates, boxes show the interquartile range). The dashed line indicates chance performance (AUROC=0.5).

2. Confounding, Bath Effects, and Preprocessing Leakage

High-throughput data are affected by technical variation arising from platform, laboratory, reagent lot, and processing date, which can exceed the biological effects of interest [21]. A model trained on data in which biology is confounded with batch may learn batch. Population structure plays an analogous role in genotype-based prediction. Leakage also arises from preprocessing: normalization, feature selection, or hyperparameter tuning performed on the full dataset before splitting allows information from test data to influence training [4]. Mitigation includes designing splits that hold out entire batches or cohorts, fitting all preprocessing within training folds, and reporting performance stratified by cohort.

3. Performance Limits Reported by Independent Benchmarks

Independent benchmarks have documented gaps between headline performance and performance on biologically or clinically relevant tasks (Table 2). Two studies evaluated sequence-to-expression models on paired personal genomes and transcriptomes and found that current models, including Enformer, explain little of the variation in gene expression between individuals and often predict the wrong direction of effect of variants [22,23]. A comparison of deep-learning models for predicting the effects of gene perturbation, including single-cell foundation models, found that none outperformed simple linear baselines [24]. These findings do not imply that the models are without value: they perform well on the tasks for which they were trained, such as predicting genome-wide regulatory profiles across loci. They indicate that transfer to a different task, such as predicting the effect of a single variant in an individual, cannot be assumed and must be demonstrated.

TABLE 2. SELECTED STUDIES REPORTING LIMITS OF CURRENT MACHINE-LEARNING MODELS IN GENOMICS

Study	Task evaluated	Principal finding
Sasse et al. 2023 [22]; Huang et al. 2023 [23]	Prediction of between-individual gene expression from personal genomes	Current sequence-to-expression models, including Enformer, explained little of the variation in expression between individuals, and the predicted direction of variant effects was often incorrect
Ahlmann-Eltze et al. 2025 [24]	Prediction of transcriptional responses to genetic perturbation	Deep-learning models, including single-cell foundation models, did not outperform simple linear baselines
Martin et al. 2019 [26]	Transferability of polygenic risk scores across ancestries	Prediction accuracy was lower in individuals of non-European ancestry, reflecting the composition of the underlying association studies
Whalen et al. 2022 [4]	Survey of evaluation practice in genomic machine learning	Recurrent pitfalls include distributional differences between training and deployment data, dependence among examples, confounding, and leaky preprocessing

4. Baselines and Metrics

Comparisons are informative only if baselines are competitive. Simple models, such as k-mer-based linear models for sequence tasks, additive or linear models for perturbation prediction, and penalized regression for genotype-based prediction, should be tuned with effort comparable to that invested in the proposed model [4,24]. Metric choice also matters. The AUROC can appear high in imbalanced problems,

such as rare regulatory elements or pathogenic variants, for which precision–recall measures and calibration are more informative. Metrics computed across loci, such as the correlation between predicted and observed expression across genes, can mask failure to explain variation across individuals within a locus [22,23].

Barriers to Translation

1. Interpretability

Attribution methods such as DeepLIFT and integrated gradients assign importance scores to input nucleotides and are widely used to derive sequence motifs and to nominate candidate causal variants [27,28]. Their outputs are, however, explanations of model behavior, not of biology: they may reflect artifacts of the training data and require experimental validation, for example by reporter assays or genome editing. For high-stakes decisions, it has been argued that inherently interpretable models should be preferred over post hoc explanations of black-box models when their performance is comparable [29].

2. Ancestry Bias and Equity

Genomic datasets used to train and evaluate models are dominated by individuals of European ancestry [25]. Polygenic scores derived from such data are less accurate in other ancestry groups, and their clinical use may therefore widen health disparities [26]. Comparable concerns apply to variant-effect predictors trained on reference data with unequal representation. Ancestry-stratified evaluation should accordingly be a reporting requirement rather than an option.

3. Privacy and Governance

Genomic data are inherently identifying: even de-identified genomic data can be linked to individuals through auxiliary information, as demonstrated by the inference of surnames from Y-chromosome markers [30]. Training ML models on human genomic data therefore raises consent and governance issues. Federated learning, in which models are trained across institutions without pooling raw data, is one approach studied for health data, but it does not by itself provide formal privacy guarantees and must be combined with additional safeguards such as differential privacy or secure aggregation [31].

Recommendations and Open Problems

The evidence reviewed above suggests a set of minimum practices for studies applying ML to genomic data (Table 3).

TABLE 3. MINIMUM VALIDATION AND REPORTING CHECKLIST FOR MACHINE-LEARNING STUDIES IN GENOMICS

Issue	Mechanism of bias	Recommended safeguard
Sample dependence	Neighboring windows, paralogs, and related individuals share information across training and test sets	Split by chromosome, locus, homology cluster, or kinship; report the splitting rule
Confounding	Models learn batch, cohort, or ancestry signals rather than biology	Hold out entire cohorts or batches; stratify results by cohort and ancestry
Preprocessing leakage	Normalization, feature selection, or tuning uses test-set information	Fit all preprocessing and tuning within training folds only
Weak baselines	Gains are overstated when comparators are untuned or absent	Include simple linear or k-mer baselines tuned with equal effort
Metric mismatch	Aggregate or threshold-free metrics hide failure on the intended task	Report precision–recall, calibration, and task-specific metrics (e.g., within-locus correlation across individuals)
No external validation	Performance reflects idiosyncrasies of a single dataset	Validate on independent cohorts and, where feasible, with experimental data

Beyond these practices, we identify the following open problems:

1. Community benchmarks with standardized, leakage-resistant splits and held-out cohorts, maintained over time.
2. Evaluation on the tasks that matter, such as variant-level and individual-level effects, rather than on proxy tasks alone.
3. Systematic comparison with strong, tuned, simple baselines.
4. Ancestry-diverse training and evaluation data, with stratified reporting.
5. Uncertainty quantification and calibration that support decision-making.
6. Integration of experimental perturbation data, such as reporter assays and genome-editing screens, for validation.
7. Privacy-preserving training methods with formal guarantees.

Conclusion

Machine learning has expanded what can be predicted from genomic data, but the reliability of reported performance depends on evaluation design at least as much as on model architecture. Sample dependence, confounding, weak baselines, and mismatched metrics can inflate results, and independent benchmarks show that success on proxy tasks does not guarantee success on individual-level or clinically relevant tasks. Progress will require leakage-resistant benchmarks, transparent reporting, ancestry-aware validation, and closer integration of computational predictions with experimental evidence.

Code availability

The code used for the simulation in Figures 2 and 3 is available at [repository URL].

```
import numpy as np, json
from sklearn.ensemble import RandomForestClassifier
from sklearn.model_selection import KFold, LeaveOneGroupOut
from sklearn.metrics import roc_auc_score
def run(seed, n_chr=10, n_per=300, p=20, effect=0.35):
 rng = np.random.default_rng(seed)
 chrom = np.repeat(np.arange(n_chr), n_per)
 prev = rng.uniform(0.2, 0.8, n_chr)
 y = (rng.random(n_chr * n_per) < prev[chrom]).astype(int)
 offsets = rng.normal(0, 1.0, (n_chr, p)) # chromosome-specific (locus/batch) signature
 signal = np.zeros(p); signal[:3] = effect # weak, generalizable signal
 X = offsets[chrom] + np.outer(y, signal) + rng.normal(0, 1.0, (n_chr * n_per, p))
 def cv_auc(splitter, groups=None):
 preds = np.zeros(len(y));
 for tr, te in splitter.split(X, y, groups):
 m = RandomForestClassifier(n_estimators=40, min_samples_leaf=10, n_jobs=1, random_
state=seed)
 m.fit(X[tr], y[tr]); preds[te] = m.predict_proba(X[te])[:, 1]
 return roc_auc_score(y, preds)
 return (cv_auc(KFold(5, shuffle=True, random_state=seed)),
 cv_auc(LeaveOneGroupOut(), chrom))
res = np.array([run(s) for s in range(15)])
json.dump({"random": res[:,0].tolist(), "chrom": res[:,1].tolist()}, open("sim.json","w"))
print("random mean %.3f sd %.3f" % (res[:,0].mean(), res[:,0].std()))
print("chrom mean %.3f sd %.3f" % (res[:,1].mean(), res[:,1].std()))
```

References

1. Stephens ZD, et al. Big Data: Astronomical or Genomical? PLoS Biol. 2015;13(7):e1002195.
2. Eraslan G, Avsec Ž, Gagneur J, Theis FJ. Deep learning: new computational modelling techniques for genomics. Nat Rev Genet. 2019;20:389-403.
3. Zou J, Huss M, Abid A, Mohammadi P, Torkamani A, Telenti A. A primer on deep learning in genomics. Nat Genet. 2019;51:12-18.
4. Whalen S, Schreiber J, Noble WS, Pollard KS. Navigating the pitfalls of applying machine learning in genomics. Nat Rev Genet. 2022;23:169-181.
5. Alipanahi B, Delong A, Weirauch MT, Frey BJ. Predicting the sequence specificities of DNA – and RNA-binding proteins by deep learning. Nat Biotechnol. 2015;33:831-838.
6. Zhou J, Troyanskaya OG. Predicting effects of noncoding variants with deep learning–based sequence model. Nat Methods. 2015;12:931-934.
7. Kelley DR, Snoek J, Rinn JL. Basset: learning the regulatory code of the accessible genome with deep convolutional neural networks. Genome Res. 2016;26:990-999.
8. Avsec Ž, et al. Effective gene expression prediction from sequence by integrating long-range interactions. Nat Methods. 2021;18:1196-1203.
9. Ji Y, Zhou Z, Liu H, Davuluri RV. DNABERT: pre-trained Bidirectional Encoder Representations from Transformers model for DNA-language in genome. Bioinformatics. 2021;37:2112-2120.
10. Dalla-Torre H, et al. Nucleotide Transformer: building and evaluating robust foundation models for human genomics. Nat Methods. 2025;22:287-297.
11. Poplin R, et al. A universal SNP and small-indel variant caller using deep neural networks. Nat Biotechnol. 2018;36:983-987.
12. Kircher M, et al. A general framework for estimating the relative pathogenicity of human genetic variants. Nat Genet. 2014;46:310-315.
13. Jaganathan K, et al. Predicting splicing from primary sequence with deep learning. Cell. 2019;176:535-548.
14. Cheng J, et al. Accurate proteome-wide missense variant effect prediction with AlphaMissense. Science. 2023;381:eadg7492.
15. Grimm DG, et al. The evaluation of tools used to predict the impact of missense variants is hindered by two types of circularity. Hum Mutat. 2015;36:513-523.
16. Lopez R, Regier J, Cole MB, Jordan MI, Yosef N. Deep gener-

ative modeling for single-cell transcriptomics. Nat Methods. 2018;15:1053-1058.
17. Theodoris CV, et al. Transfer learning enables predictions in network biology. Nature. 2023;618:616-624.
18. Cui H, et al. scGPT: toward building a foundation model for single-cell multi-omics using generative AI. Nat Methods. 2024;21:1470-1480.
19. Khera AV, et al. Genome-wide polygenic scores for common diseases identify individuals with risk equivalent to monogenic mutations. Nat Genet. 2018;50:1219-1224.
20. Kelley DR, et al. Sequential regulatory activity prediction across chromosomes with convolutional neural networks. Genome Res. 2018;28:739-750.
21. Leek JT, et al. Tackling the widespread and critical impact of batch effects in high-throughput data. Nat Rev Genet. 2010;11:733-739.
22. Sasse A, et al. Benchmarking of deep neural networks for predicting personal gene expression from DNA sequence highlights shortcomings. Nat Genet. 2023;55:2060-2064.
23. Huang C, et al. Personal transcriptome variation is poorly explained by current genomic deep learning models. Nat Genet. 2023;55:2056-2059.
24. Ahlmann-Eltze C, Huber W, Anders S. Deep-learning-based gene perturbation effect prediction does not yet outperform simple linear baselines. Nat Methods. 2025;22:1657-1661.
25. Popejoy AB, Fullerton SM. Genomics is failing on diversity. Nature. 2016;538:161-164.
26. Martin AR, et al. Clinical use of current polygenic risk scores may exacerbate health disparities. Nat Genet. 2019;51:584-591.
27. Shrikumar A, Greenside P, Kundaje A. Learning important features through propagating activation differences. Proc Mach Learn Res (ICML). 2017;70:3145-3153.
28. M, Taly A, Yan Q. Axiomatic attribution for deep networks. Proc Mach Learn Res (ICML). 2017;70:3319-3328.
29. C. Stop explaining black box machine learning models for high stakes decisions and use interpretable models instead. Nat Mach Intell. 2019;1:206-215.
30. M, McGuire AL, Golan D, Halperin E, Erlich Y. Identifying personal genomes by surname inference. Science. 2013;339:321-324.
31. N, et al. The future of digital health with federated learning. npj Digit Med. 2020;3:119.

DOI 10.51231/2667-9507-2026-005-12-90-101

Effects of Vitamin D on Erythrocyte Deformability in STZ-Induced Diabetes Mellitus

Nino Sakhanberidze[1], Manana Namoradze[1], Nino Charkviani[2], Maia Mantskava[3,4]

[1] *Department of Pathophysiology, Tbilisi State Medical University, Tbilisi, Georgia*

[2] *Department of Endocrinology, Tbilisi State Medical University, Tbilisi, Georgia*

[3] *Department of Physics, Biophysics, Biomechanics and Informational Technologies, Tbilisi State Medical University, Tbilisi, Georgia*

[4] *Ivane Beritashvili Experimental Center of Biomedicine, Tbilisi, Georgia*

Abstract

Objectives: Diabetes mellitus is a systemic metabolic disorder characterized by chronic hyperglycemia, which contributes to progressive cellular and vascular dysfunction and the development of microvascular and macrovascular complications. Given the role of altered erythrocyte mechanical properties in diabetic microvascular dysfunction, this study aimed to assess temporal changes in erythrocyte deformability and compare the effects of preventive and therapeutic vitamin D administration in streptozotocin-induced diabetic rats on days 7, 14 and 21.

Methods: The study included 64 male rats randomly allocated to four experimental groups: intact control, streptozotocin (STZ)-induced diabetic control, preventive vitamin D and therapeutic vitamin D groups. Experimental diabetes was induced by a single intraperitoneal injection of STZ (30 mg/kg). Vitamin D was administered orally at a dose of 300 IU/day, starting 14 days before STZ administration in the preventive group and on Day 3 after STZ administration in the therapeutic group. Erythrocyte deformability was assessed using a standardized microfiltration technique at three time points (Days 7, 14 and 21). Data were expressed as mean ± standard deviation and statistical significance was set at $p < 0.05$.

Results: Erythrocyte deformability progressively declined in STZ-induced diabetic rats, with a significant reduction in EDI by Day 14 ($p < 0.05$), reaching a 19.5% decrease by Day 21 compared with intact controls. Preventive vitamin D administration resulted in slightly higher EDI values compared with the diabetic control group, although the differences were not statistically significant. In contrast, therapeutic vitamin D administration significantly improved erythrocyte deformability, with EDI increasing by 7.55% on Day 14 and 16.2% on Day 21 compared with the STZ control group ($p < 0.05$).
Conclusions: STZ-induced diabetes progressively reduced erythrocyte deformability with minor changes on Day 7, significant deterioration by Day 14 and the most pronounced alterations on Day 21. Preventive vitamin D administration showed no significant protective effect, whereas therapeutic administration significantly improved deformability by Day 14, with greater improvement observed on Day 21.

KEYWORDS: Vitamin D; STZ-induced diabetes mellitus; Erythrocyte deformability; Preventive and therapeutic approaches.

Introduction

Diabetes mellitus is a systemic metabolic disorder characterized by chronic hyperglycemia, which, over time, contributes to progressive cellular and vascular dysfunction and the development of microvascular and macrovascular complications [1,2]. Alterations in blood rheological properties, together with endothelial dysfunction, are important pathophysiological components of diabetic vascular impairment, collectively compromising vascular homeostasis and microcirculatory blood flow [2-4]. A substantial body of evidence indicates that hyperglycemic conditions induce significant changes in blood rheological properties, with impaired erythrocyte mechanical properties, particularly reduced erythrocyte deformability, being consistently reported [5-7].

One of the principal mechanisms underlying these changes is hyperglycemia-induced oxidative stress, which can damage erythrocyte membrane lipids and proteins, thereby altering membrane structure, fluidity, and mechanical stability [8,9]. Hemoglobin auto-oxidation may further contribute to reactive oxygen species (ROS) generation, while oxidative modifications of erythrocyte membrane lipids and cytoskeletal proteins, including spectrin, may impair membrane integrity and reduce erythrocyte deformability [8,13,22].

It is worth noting that glucose transport into erythrocytes occurs independently of insulin [21]. Consequently, erythrocytes are directly exposed to circulating glucose concentrations, making them particularly susceptible to hyperglycemia-induced biochemical modifications [5,10,11]. One major consequence is the non-enzymatic glycation of hemoglobin as well as membrane-associated and cytoskeletal proteins [9,11,12]. Glycation-induced modification of key structural proteins can disrupt membrane-cytoskeleton interactions and cytoskeletal organization, thereby reducing membrane elasticity [11,12]. In parallel, increased glucose flux through the polyol pathway may contribute to erythrocyte metabolic disturbances under hyperglycemic conditions [7,14]. Aldose reductase utilizes NADPH during the conversion of glucose to sorbitol, potentially reducing NADPH availability for glutathione regeneration [14,23]. Because NADPH-dependent glutathione recycling is essential for maintaining erythrocyte redox homeostasis, alterations in these pathways may increase susceptibility to oxidative membrane damage [8,22]. Collectively, these interconnected hyperglycemia-associated processes promote structural and biophysical alterations in the erythrocyte membrane, driving a shift toward increased erythrocyte rigidity [8,12].

Vitamin D is a secosteroid with a broad range of biological functions beyond its classical role in calcium and bone homeostasis, including antioxidant, anti-inflammatory and immunomodulatory effects [17-19]. Despite growing interest in the pleiotropic effects of vitamin D, its influence on erythrocyte mechanical properties remains insufficiently characterized, particularly with regard to the temporal evolution of erythrocyte deformability and potential differences between preventive and therapeutic administration. Although our previous study reported erythrocyte deformability and the effects of preventive and therapeutic vitamin D administration at the Day 21 endpoint, it did not characterize the temporal development of these effects [20]. The present study extends this work by examining erythrocyte deformability at Days 7, 14 and 21 in an expanded analytical cohort, with particular emphasis on the time-dependent patterns associated with preventive and therapeutic supplementation.

Materials and Methods

1. Experimental Animals and Ethical Approval

Male laboratory rats, 10 weeks of age and weighing approximately 201.70 ± 8.48 g, were maintained under controlled environmental conditions (24 ± 1 °C, relative humidity 55 ± 5%, and a 12-h light/dark cycle) and received a standard diet formulated

for laboratory rats. Male animals were used to minimize potential variability related to sex-dependent hormonal influences and differences in susceptibility to streptozotocin (STZ). All experimental procedures were approved by the Institutional Animal Ethics Committee (Protocol No. 79) and were conducted in accordance with applicable guidelines for the care and use of laboratory animals.

2. Study Design and Experimental Groups

The animals were assigned to four experimental groups: an intact control group, an STZ-induced diabetic group without vitamin D supplementation, a preventive vitamin D group and a therapeutic vitamin D group. In the preventive group, vitamin D administration was initiated 14 days before STZ injection and continued throughout the experimental period. In the therapeutic group, supplementation was started on Day 3 after STZ administration, following confirmation of hyperglycemia and was maintained until the corresponding experimental endpoint.

A total of 64 rats were included in the study: Intact Control Group (n=10): Healthy animals that received no STZ or vitamin D supplementation and were administered sodium citrate buffer as the vehicle control. This group served as a common baseline reference for all observation time points.

STZ-Induced Diabetes Group: Evaluated at three observation time points (6 rats per time point: Days 7, 14 and 21).

Preventive Vitamin D Group: Vitamin D supplementation was initiated before STZ administration (6 rats per time point: Days 7, 14 and 21).

Therapeutic Vitamin D Group: Vitamin D administration was initiated after confirmation of hyperglycemia (6 rats per time point: Days 7, 14, and 21).

3. Induction of Experimental Diabetes

Experimental diabetes was induced in accordance with an established STZ-based protocol with modifications described previously [20]. Before STZ administration, the animals were fasted and subsequently received a single intraperitoneal injection of streptozotocin at a dose of 30 mg/kg. STZ was dissolved immediately before use in freshly prepared 50 mM sodium citrate buffer (pH 4.5) and administered within 10 min of preparation to minimize degradation. Control animals received an equivalent intraperitoneal injection of sodium citrate buffer without STZ. Following STZ administration, animals were provided with a 10% sucrose solution for 24 h. Development of diabetes was confirmed on Day 3 after injection by blood glucose measurement using a glucometer. Successful induction was defined by persistent hyperglycemia exceeding 19 mmol/L, accompanied by polyuria.

4. Vitamin D Administration

Vitamin D was administered orally once daily at a dose of 300 IU/day. In the preventive group, supplementation was initiated 14 days before STZ administration and continued throughout the experimental period. In the therapeutic group, vitamin D treatment was initiated on Day 3 after STZ injection, following confirmation of hyperglycemia and continued until the corresponding experimental endpoint. Vitamin D administration was discontinued 24 h before blood collection.

5. Assessment of Erythrocyte Deformability

Erythrocyte deformability was assessed using a standardized microfiltration technique through microporous membrane filters under controlled suction pressure. The erythrocyte deformability index (EDI,%) was recorded as the primary experimental measure of erythrocyte mechanical behavior. Lower EDI values indicate reduced erythrocyte deformability.

6. Statistical Analysis

Statistical analysis was performed using OriginPro software (version 8.1; OriginLab Corp., Northampton, MA, USA). The erythrocyte deformability index (EDI) is expressed as mean ± standard deviation (SD). Data normality within each group and observation time point was evaluated using the Shapiro-Wilk test and homogeneity of variances across groups was assessed using Levene's test. Statistical comparisons between the intact control group and experimental sub-groups across Days 7, 14 and 21 were performed using one-way analysis of variance (ANOVA) followed by Tukey's post hoc test for multiple comparisons. Pairwise comparisons between specific groups at individual time points were verified using Student's two-tailed independent t-test. Differences were considered statistically significant at a threshold of $p<0.05$.

Results

Erythrocyte deformability index (EDI) values varied across experimental groups and observation time points during the 21-day study period (Table 1). In the Intact Control Group , healthy baseline EDI was 2.46±0.17%.

In the untreated STZ Control Group, a progressive impairment of erythrocyte deformability was observed over time: On Day 7, EDI slightly decreased to 2.32±0.08% ($p>0.05$); On Day 14, EDI significantly declined to 2.12±0.09% ($p<0.05$ vs. Control); On Day 21, EDI reached its lowest value of 1.98±0.10% ($p<0.05$ vs. Control), repre-

senting a total reduction in deformability of approximately 19.5% relative to healthy controls.

In the preventive vitamin D group, EDI was higher than in the diabetic control group at all time points, but the differences were not statistically significant.

In the therapeutic vitamin D group, erythrocyte deformability improved significantly compared with the untreated diabetic control group. EDI was 7.55% higher on Day 14 and 16.2% higher on Day 21 than in the corresponding STZ control groups ($p < 0.05$).

TABLE 1. TEMPORAL DYNAMICS OF ERYTHROCYTE DEFORMABILITY INDEX (EDI) ACROSS EXPERIMENTAL GROUPS (MEAN ± SD)

Experimental Group	N	Time (Days)	EDI (%)
Intact Control	10	Baseline	2.46±0.17
STZ Control	6	Day 7	2.32±0.08
	6	Day 14	2.12±0.09*
	6	Day 21	1.98±0.10*
Preventive STZ + Vit D	6	Day 7	2.33±0.07
	6	Day 14	2.15±0.08*
	6	Day 21	2.00±0.08*
Therapeutic STZ + Vit D	6	Day 7	2.38±0.09
	6	Day 14	2.28±0.10**
	6	Day 21	2.30±0.12**

*Note: Data expressed as Mean ± SD. *p<0.05 vs. Intact Control; **p<0.05 vs. STZ Control at the same time point.*

Discussion

The present study evaluated temporal changes in erythrocyte deformability in an STZ-induced diabetic rat model and examined the effects of preventive and therapeutic oral vitamin D supplementation over a 21-day observation period. By assessing the erythrocyte deformability index (EDI) at three experimental time points, this study provides a more detailed characterization of erythrocyte mechanical alterations during the progression of experimental diabetes and following vitamin D administration.

Temporal Dynamics of Erythrocyte Biomechanical Impairment

A central finding of this investigation is the progressive, time-dependent reduction in erythrocyte deformability in untreated STZ-diabetic animals. In healthy intact controls, red blood cells maintain high mechanical compliance (EDI: 2.46±0.17), which is essential for negotiating capillaries whose diameters are smaller than those of relaxed erythrocytes [3, 4]. Following STZ administration, erythrocyte deformability showed a modest, statistically non-significant initial decline on Day 7 (EDI: 2.32 ± 0.08%). However, erythrocyte deformability decreased significantly by Day 14 (EDI: 2.12 ± 0.09%, $p < 0.05$ vs. intact control) and reached its lowest value on Day 21 (EDI: 1.98 ± 0.10%, $p < 0.05$ vs. intact control), representing an approximately 19.5% reduction relative to healthy controls. The reduction in erythrocyte deformability observed at Day 21 is consistent with our previously published findings at the same experimental endpoint [20]. However, the present study extends these observations by including additional animals and evaluating the temporal dynamics of erythrocyte deformability at Days 7, 14 and 21.

The progressive reduction in mean EDI values across the experimental time points suggests sustained impairment of erythrocyte mechanical properties under diabetic conditions [3,6]. Crucially, because mature erythrocytes lack nuclei and organelles, they possess limited synthetic capacity for protein repair or de novo phospholipid synthesis [5,10]. Consequently, molecular damage inflicted upon the erythrocyte membrane and cytoskeletal scaffold during its lifespan accumulates, leading to progressive cell stiffening [8,11].

Biochemical Mechanisms Underlying Impaired Erythrocyte Deformability in Diabetes Mellitus

The biomechanical compliance of the erythrocyte depends on three primary factors: intracellular hemoglobin viscosity, the surface area-to-volume ratio and the viscoelastic properties of the lipid-protein membrane complex [3,6,9]. Hyperglycemia disrupts these physiological parameters through several interacting biochemical pathways. Because glucose transport into erythrocytes occurs independently of insulin [21], intracellular glucose concentrations mirror plasma levels [5,11]. Sustained hyperglycemia promotes

non-enzymatic glycation of hemoglobin and erythrocyte membrane-associated proteins, while the formation of advanced glycation end-products (AGEs) may further alter membrane-cytoskeleton interactions, potentially compromising erythrocyte flexibility and deformability [9,11,12]. In addition to glycation, oxidative stress and lipid peroxidation contribute to erythrocyte membrane dysfunction. Auto-oxidation of elevated intracellular glucose and hemoglobin generates reactive oxygen species (ROS) [8,13], which promote lipid peroxidation of polyunsaturated fatty acids within the erythrocyte membrane bilayer, reducing membrane fluidity [8,9]. Furthermore, oxidative modifications of erythrocyte cytoskeletal proteins, including spectrin, may impair membrane integrity and deformability [8,22]. Concurrently, increased glucose flux through the aldose reductase polyol pathway may increase NADPH consumption, potentially impairing glutathione regeneration and weakening the erythrocyte's antioxidant defenses [14]. This intracellular redox imbalance further increases erythrocyte susceptibility to oxidative stress [8,14].

Differential Impact of Preventive vs. Therapeutic Vitamin D Administration

In the preventive vitamin D group, supplementation initiated 14 days before STZ injection did not significantly attenuate the decline in erythrocyte deformability compared with untreated diabetic controls. On Day 21, the EDI value in the preventive group (2.00 ± 0.08%) was comparable to that in the untreated STZ control group (1.98 ± 0.10%), with no statistically significant difference ($p > 0.05$). These findings suggest that preventive vitamin D supplementation may be insufficient to counteract erythrocyte alterations associated with sustained hyperglycemia under the present experimental conditions. One possible explanation is that persistent hyperglycemia-induced glycation and oxidative stress may contribute to erythrocyte membrane damage despite vitamin D supplementation [8,17]. However, these mechanisms were not directly evaluated in the present study. In contrast, therapeutic vitamin D administration initiated on Day 3 after STZ injection, following confirmation of hyperglycemia, was associated with significantly higher erythrocyte deformability compared with untreated diabetic controls. This effect was evident on Day 14 (EDI: 2.28 ± 0.10%, $p < 0.05$ vs. STZ control) and remained significant on Day 21 (EDI: 2.30 ± 0.12%, $p < 0.05$ vs. STZ control). These findings suggest that the effects of vitamin D supplementation on erythrocyte mechanical properties may depend on the timing of administration, although direct statistical comparisons between the preventive and therapeutic groups are required to confirm this difference.

The observed effects of therapeutic vitamin D administration may involve genomic and non-genomic pathways associated with the pleiotropic actions of vitamin D [17,18]. Vitamin D may exert antioxidant and anti-inflammatory effects through the modulation of cellular signaling pathways and endogenous antioxidant defense mechanisms [17-19]. These properties may contribute to the observed improvement in erythrocyte deformability, although the underlying mechanisms were not directly investigated in the present study. Furthermore, vitamin D may influence systemic inflammatory responses and endothelial function, potentially contributing to changes in the vascular environment [2, 17,19].

Clinical Implications and Methodological Considerations

Reduced erythrocyte deformability compromises microcirculatory hemodynamics by limiting the ability of erythrocytes to traverse narrow capillaries, thereby increasing microvascular flow resistance and contributing to impaired tissue perfusion and microvascular ischemia [3,12,15]. Recent clinical evidence has highlighted reduced red blood cell deformability as a key contributor to diabetic microangiopathy, including retinopathy and nephropathy [12,15,16]. The observed improvement in erythrocyte deformability following therapeutic vitamin D administration suggests a potential role for vitamin D in modulating blood rheological properties under diabetic conditions. However, further experimental and clinical studies are required to determine the translational relevance of these findings.

Study Limitations

Certain limitations should be acknowledged. First, each temporal subgroup utilized n=6 animals; although statistically significant differences were established, expanded cohorts in future studies will further enhance statistical power. Second, biochemical markers of oxidative stress (e.g., malondialdehyde, reduced glutathione), serum 25-hydroxyvitamin D concentrations and advanced glycation end-products were not directly measured in this cohort. Third, microvascular perfusion was not assessed in vivo. Future mechanistic research directly measuring membrane lipid fluidity and cytoskeletal spectrin architecture is recommended to further elucidate these findings.

Conclusions

STZ-induced diabetes was associated with a progressive, time-dependent reduction in erythrocyte deformability, with the most pronounced impairment observed on Day 21. Preventive vitamin D administration did not significantly attenuate this decline, whereas therapeutic administration was associated with significantly improved erythrocyte deformability on Days 14 and 21 compared with untreated diabetic controls. These findings suggest that the effects of vitamin D on erythrocyte mechanical properties may depend on the timing of administration and warrant further mechanistic investigation.

Conflicts of interest. The authors have no conflict of interest to declare.

References

1. American Diabetes Association Professional Practice Committee for Diabetes. Diagnosis and classification of diabetes: Standards of Care in Diabetes—2026. Diabetes Care. 2026;49(Suppl 1):S27-S49. doi:10.2337/dc26-S002.
2. Yang DR, Wang MY, Zhang CL, Wang Y. Endothelial dysfunction in vascular complications of diabetes: a comprehensive review of mechanisms and implications. Front Endocrinol (Lausanne). 2024;15:1359255. doi:10.3389/fendo.2024.1359255.
3. Ebenuwa I, Violet PC, Tu H, Lee C, Munyan N, Wang Y, et al. Altered RBC deformability in diabetes: clinical characteristics and RBC pathophysiology. Cardiovasc Diabetol. 2024;23(1):370. doi:10.1186/s12933-024-02453-2.
4. Hassanein A, Akhtar S. Beyond oxygen transport: red blood cells as emerging players in mediating endothelial dysfunction in diabetes. Ann Med. 2026;58(1):2650021. doi:10.1080/07853890.2026.2650021.
5. Wang Y, Yang P, Yan Z, Liu Z, Ma Q, Zhang Z, et al. The relationship between erythrocytes and diabetes mellitus. J Diabetes Res. 2021;2021:6656062. doi:10.1155/2021/6656062.
6. Brun JF, Varlet-Marie E, Myzia J, Raynaud de Mauverger E, Pretorius E. Metabolic influences modulating erythrocyte deformability and eryptosis. Metabolites. 2022;12(1):4. doi:10.3390/metabo12010004.

7. Williams A, Bissinger R, Shamaa H, Patel S, Bourne L, Artunc F, et al. Pathophysiology of red blood cell dysfunction in diabetes and its complications. Pathophysiology. 2023;30(3):327-345. doi:10.3390/pathophysiology30030026.
8. Maruyama T, Hieda M, Mawatari S, Fujino T. Rheological abnormalities in human erythrocytes subjected to oxidative inflammation. Front Physiol. 2022;13:837926. doi:10.3389/fphys.2022.837926.
9. Pitocco D, Hatem D, Riente A, De Giulio MM, Rizzi A, Abeltino A, et al. Evaluating red blood cells' membrane fluidity in diabetes: insights, mechanisms, and future aspects. Diabetes Metab Res Rev. 2025;41(1):e70011. doi:10.1002/dmrr.70011.
10. Kosmachevskaya OV, Novikova NN, Topunov AF. Carbonyl stress in red blood cells and hemoglobin. Antioxidants (Basel). 2021;10(2):253. doi:10.3390/antiox10020253.
11. Turpin C, Catan A, Meilhac O, Bourdon E, Canonne-Hergaux F, Rondeau P. Erythrocytes: central actors in multiple scenes of atherosclerosis. Int J Mol Sci. 2021;22(11):5843. doi:10.3390/ijms22115843.
12. Garoufis M, Kostara C, Sakkou SF, Filippas-Ntekouan S, Bairaktari E, Tsimihodimos V. Hemorheological alterations as a driver of microangiopathy in diabetic kidney disease—the role of erythrocyte. Int J Mol Sci. 2026;27(8):3592. doi:10.3390/ijms27083592.
13. Inoue M, Udono Y, Kato Y, Fukui K, Watanabe N. Evaluation of erythrocyte membrane oxidation due to their exposure to shear flow generated by extracorporeal blood pump. Int J Artif Organs. 2024;47(3):155-161. doi:10.1177/03913988241230942.
14. Singh M, Kapoor A, Bhatnagar A. Physiological and pathological roles of aldose reductase. Metabolites. 2021;11(10):655. doi:10.3390/metabo11100655.
15. Han YE, Lim JS, Kim Y, Kim I, Moon JS, Lee J. Erythrocyte deformability correlates with microvascular ischemia and disease severity in diabetic retinopathy. J Diabetes Investig. 2026;17(3):483-491. doi:10.1111/jdi.70247.
16. Di Santo R, Niccolini B, Rizzi A, Bertini L, Marafon DP, Vaccaro M, et al. Sensing biomechanical alterations in red blood cells of type 1 diabetes patients: potential markers for microvascular complications. Biosensors (Basel). 2024;14(12):587. doi:10.3390/bios14120587.
17. Park CY, Shin S, Han SN. Multifaceted roles of vitamin D for diabetes: from immunomodulatory functions to metabolic regulations. Nutrients. 2024;16(18):3185. doi:10.3390/nu16183185.
18. Holick MF, Mazzei L, García Menéndez S, Martín Giménez VM, Al Anouti F, Manucha W. Genomic or non-genomic? A question about the pleiotropic roles of vitamin D in inflammatory-based diseas-

es. Nutrients. 2023;15(3):767. doi:10.3390/nu15030767.
19. Wu J, Atkins A, Downes M, Wei Z. Vitamin D in diabetes: uncovering the sunshine hormone's role in glucose metabolism and beyond. Nutrients. 2023;15(8):1997. doi:10.3390/nu15081997.
20. Sakhanberidze N, Namoradze M, Charkviani N, Mantskava M, Momtselidze N, Delibashvili D, Gamkrelidze N. Therapeutic potential of vitamin D in improving antioxidant defense and blood rheology in a rat model of experimental diabetes mellitus. Open Med (Wars). 2026;21(1):20261403. doi:10.1515/med-2026-1403.
21. Thomas N, Schröder NH, Nowak MK, et al. Sphingosine-1-phosphate suppresses GLUT activity through PP2A and counteracts hyperglycemia in diabetic red blood cells. Nat Commun. 2023;14:8329. doi:10.1038/s41467-023-44109-x.
22. Chatzinikolaou PN, Margaritelis NV, Paschalis V, Theodorou AA, Vrabas IS, Kyparos A, et al. Erythrocyte metabolism. Acta Physiol (Oxf). 2024;240(3). doi:10.1111/apha.14081.
23. Gupta JK. The role of aldose reductase in polyol pathway: an emerging pharmacological target in diabetic complications and associated morbidities. Curr Pharm Biotechnol. 2024;25(9):1073–1081. do i:10.2174/1389201025666230830125147.

Policy

Open Access statement

An open-access mandate is a policy adopted by a research institution, research funder, or government which requires or recommends researchers – usually university faculty or research staff and/or research grant recipients – to make their published, peer-reviewed journal articles and conference papers open access (1) by self-archiving their final, peer-reviewed drafts in a freely accessible institutional repository or disciplinary repository (″Green OA″) or (2) by publishing them in an open-access journal (″Gold OA″) or both.

We have a comprehensive outlook on open access policy

Open access refers to the practice of making peer-reviewed scholarly research and literature freely available online to science and researchers, specialist, students and another persons. This Open access publications are freely and permanently available online. Unrestricted use, distribution and reproduction in any medium is permitted, provided the author/editor/journal is properly attributed.

The articles is universally, freely accessible via the Internet, in an easily readable format. Our periodical (four time/year) are deposited immediately upon publication, without any technical, financial, gender limitations, in an agreed format – current preference is PDF and e-pub version of articles are available, which are the major forms of widely and internationally recognized open access repositories.

All articles are self archiving, with worldwide access through DOI number (Digital Object Identifier) – standardized by the International Organization for Standardization, provided for individual article published. Our journal follows Double Blind peer review process, which means that both the reviewer and author identities are concealed from the reviewers, and vice versa, throughout the review process. The benefits of open access publishing are next: a) Free availability of information; b) Authors retain copyright; c) High quality and rigorous peer review.

We are using the existence of politics of Registry of Open Access Mandatory Archiving Policies http://roarmap.eprints.org.

The quality control system

Our journal follows Double Blind peer review process, which means that both the reviewer and author identities are concealed from the reviewers, and vice versa, throughout the review process.

Plagiarism policy

Manuscripts containing original material are accepted for consideration if neither the article nor any part of its essential substance, tables, or figures has been or will be published or submitted elsewhere before appearing in our journal. Simultaneous submissions of the same article to multiple journals are prohibited. If an author violates this requirement or engages in similar misconduct, our Editorial Board may reject the manuscript.

Plagiarism is when an author passes off the work of someone else as his or her own. This can also include self-plagiarism, which happens when an author reuses portions of his or her previously published work without the proper references. Manuscripts containing plagiarized content will not be considered for publication in our journal. All authors need to take responsibility for their manuscripts. If your name is on a manuscript, make sure all of the material in the paper either is original or is properly cited and has proper permission to be reproduced. If you have a question about the originality of any part of a manuscript, verify it with your coauthors.

All articles are checked by the anti-plagiarism program.

Crossmark policy

Publication of any material in JOURNAL OF BIOMEDICAL AND MEDICAL SCIENCES denotes that all its authors have agreed to its content and have ensured that JOURNAL OF BIOMEDICAL AND MEDICAL SCIENCES's policies have been fully adhered to; adherence to sections 1-4 is compulsory for documents; sections 5 and 6 are strongly encouraged as they present good scientific practice and publishing standards.

We seek to ensure that the documents we publish and for which we provide a platform are responsible and have been selected and produced without bias.

We respect the intellectual property rights of our contributors and seek to avoid unethical publishing behaviors such as plagiarism, defamation and cultural misappropriation.

Our Publication Terms and Conditions set out the publishing standards by which we operate. We require that all work sets out to be fair and accurate, differentiates between fact and opinion, is obtained by straightforward and ethical means, and is promptly corrected where inaccurate or misleading. The acceptability of any document shall be decided by JOURNAL OF BIOMEDICAL AND MEDICAL SCIENCES at its discretion. JOURNAL OF BIOMEDICAL AND MEDICAL SCIENCES reserves the right, at its discretion, to not proceed with publication at any time or to remove the document following publication if there are legal or ethical concerns.

1. Originality

We are happy to publish documents those that are unpublished.

Authors of documents must ensure that they do not breach copyright with any content they post. Authors who wish to reproduce a figure or table from a previous copyrighted publication are responsible for obtaining the permission of copyright holders and for clearly referencing the original source. Figures that were previously published under a creative commons license may be reused under the condition of the specific license that applies to those figures.

2. Authorship on Documents

Any documents whose author's affiliation is a recognized research centre or clinical institution or organization clearly related to academic research can be posted. At least one author on document must meet this key criterion.

Documents always relate to specific gateways and usually only researchers who are directly affiliated with a gateway and have been invited by the gateway advisers will be able to publish documents.

3. Competing interests

Authors must include a 'Competing interests' statement. A competing interest will not preclude publication, but it provides full transparency for readers. If there are no competing interests to declare, the following standard statement is added: 'No competing interests were disclosed'.

A competing interest may be of non-financial or financial nature. Examples of competing interests include (but are not limited to):

- individuals receiving funding, salary or other forms of payment from an organization, or holding stocks or shares from a company, that might benefit (or lose) financially from the publication of the findings
- individuals or their funding organization or employer holding (or applying for)
- related patents
- official affiliations and memberships with interest groups relating to the con-
- tent of the publication
- political, religious, or ideological competing interests.

Authors from pharmaceutical companies, or other commercial organizations that sponsor clinical trials, should declare these as competing interests on submission. The relationship of each author to such an organization should be explained in the 'Competing interests' section. Publications in JOURNAL OF BIOMEDICAL AND MEDICAL SCIENCES must not contain content advertising any commercial products.

The International Society for Medical Publication Professionals provides good practice guidelines, which are aimed at ensuring that ″clinical trials sponsored by pharmaceutical companies are published in a responsible and ethical manner″.

If an undisclosed competing interest is brought to the attention of the editorial office after publication, JOURNAL OF BIOMEDICAL AND MEDICAL SCIENCES will follow the COPE guidelines (https://publicationethics.org/guidance/Guidelines).

4. Ethical Policies

JOURNAL OF BIOMEDICAL AND MEDICAL SCIENCES adheres to the COPE guidelines (https://publicationethics.org/guidance/Guidelines) relating to ethical oversight.

4.1 Research involving humans

4.1.1 Ethics approval

All studies involving humans (individuals, human data or material) must have been conducted according to the principles expressed in the Declaration of Helsinki. Approval must have been obtained for all protocols from the authors' institutional or other relevant ethics committee to ensure that they meet national and international guidelines. Details of this approval should be provided in the document, including the institution, review board name, and permit number(s).

Human studies categorized by race/ethnicity, age, disease/disabilities, religion, sex/ gender, sexual orientation, or other socially constructed groupings, should include a justification of the choice of definitions and categories, including whether any rules of human categorization were required by the relevant funding agencies. Appropriate non-stigmatizing language should be used when describing different groups.

Ethics approval must be obtained before the research is conducted; retrospective approval can usually not be obtained and it may not be possible to publish the study.

4.1.2 Patient privacy and informed consent for publication

As stated in the Recommendations of the International Committee of Medical Journal Editors: ″Patients have a right to privacy that should not be infringed without informed consent. Identifying information should not be published in written descriptions, photographs, and pedigrees unless the information is essential for scientific purposes and the patient (or parent or guardian) gives written in – formed consent for publication. Informed consent for this purpose requires that the patient be shown the manuscript to be published. When informed consent has been obtained it should be indicated in the published article.″

Consent to participate: For all studies involving human participants, informed written consent to take part in the research must have been obtained, and this should be stated in the document in a section entitled 'Consent'. If only oral consent was obtained (rather than written), the reasons need to be explained, confirmation of IRB approval that oral consent was adequate must be provided, and a statement of how it was documented included in the Consent section.

Consent for publication of identifiable data: For any documents that include information that could potentially identify an individual, please ensure that you have obtained written, informed consent from all patients or healthy participants

(or their legal guardians for minors, or next of kin if the participant is deceased), confirming that the results and any images can be published. This includes large clinical datasets with direct or indirect identifiers (see this article for information), specific details about individuals, images and so on.

If your document contains any identifiable images of individuals, you must include a statement confirming that you have permission to publish these images. If your document contains any clinical images or identifiable data then you must include an explicit consent statement under a separate heading of the 'Consent' section (we suggest: "We confirm we have permission to use [images/data] from the participants/patients/individuals included in this presentation [conditions under which the permission was obtained]").

Alternatively, if no consent for publication was required (e.g. the data has been anonymised), then this should be clearly stated and a note should be added confirming that such alterations have not distorted scientific meaning.

Signed consent forms should be made available to the JOURNAL OF BIOMEDICAL AND MEDICAL SCIENCES editorial office if requested.

4.2 Research involving animals

Authors describing studies involving animals must have consulted the 'Animal Research: Reporting in vivo Experiments' (ARRIVE) 2.0 guidelines, developed by the NC3Rs to improve standards of reporting, ensuring that the data from animal experiments can be fully scrutinized and utilized. Studies reporting in vivo experiments must adhere to the ARRIVE Essential 10 checklist as a minimum, and we encourage authors to use the full ARRIVE 2.0 checklist.

Experiments involving vertebrates or regulated invertebrates must be carried out within the ethical guidelines provided by the authors' institution and national or international regulations. Where applicable, a statement of ethics permission granted or animal licenses should be included. If animals were used but ethical approval was not required, a clear statement should be included stating why this approval was unnecessary.

In all cases, a statement should be made to confirm that all efforts were made to ameliorate any suffering of animals and details of how this was achieved should be provided.

Authors should comply with the Convention on Biological Diversity and the Convention on the Trade in Endangered Species of Wild Fauna and Flora.

4.3 Research involving plants

Studies on plants must be carried out within the guidelines provided by the authors' institution and national or international regulations. Where applicable, a statement of permissions granted or licenses should be included. Authors should comply with the Convention on Biological Diversity and the Convention on the Trade in Endangered Species of Wild Fauna and Flora.

5. Registration of trials and systematic reviews

5.1 Trial registration

JOURNAL OF BIOMEDICAL AND MEDICAL SCIENCES uses the WHO definition of a clinical trial to decide what constitutes a clinical trial:

"A clinical trial is any research study that prospectively assigns human participants or groups of humans to one or more health-related interventions to evaluate the effects on health outcomes. Interventions include (but are not restricted to) drugs, cells and other biological products, surgical procedures, radiologic procedures, devices, behavioral treatments, process-of-care changes, preventive care, etc".

Trials should be registered prospectively and the trial registration number and registration date must be included in the document.

Although prospective trial registration is preferable, several initiatives (such as the All Trials campaign) have recognized that retrospective trial registration will encourage publication of both positive and negative results.

5.2 Systematic reviews registration

We encourage authors to register their systematic reviews in PROSPERO or another registry for systematic reviews. The registration number should be included in the document.

6. Standards of reporting

For articles in the life sciences there are standards of reporting guidelines devised to help authors to ensure that they have provided a comprehensive description of their research, making it easier for others to assess and reproduce the work; for more detail and a comprehensive overview, see the FAIR Sharing initiative. Comprehensive lists of available reporting guidelines can be found on the EQUATOR network website for health research.

For example, reports of clinical trials should adhere to the CONSORT reporting guidelines. Any deviation from the original trial protocol should be explained.

7. Licenses

Most JOURNAL OF BIOMEDICAL AND MEDICAL SCIENCES documents are published under a CC BY license, which permits unrestricted use, distribution, and reproduction in any medium, provided the original work is properly cited, and leaves the copyright of the document with the current copyright holder (usually the author or his/her institution). However, in some cases other Creative Commons licenses may apply. The specific license is listed for each document and document.

8. Permanency of content

All documents published in JOURNAL OF BIOMEDICAL AND MEDICAL SCIENCES receive a DOI and are permanently published, so they cannot be withdrawn once a DOI has been issued.

In order to maintain the integrity and completeness of the scholarly record, we will apply the following policies when published content needs to be corrected; these policies take into account current best practice in the scholarly publishing and library communities:

8.1 Correction to Document

All documents may contain errors; authors and readers can point out such mistakes via the Comment system. In the rare instance that a document needs to

be formally corrected, for example, if a change needs to be made to the author list, a Correction statement will be added.

8.2 Retraction

This action is reserved for documents that are seriously flawed. They may be retracted for several reasons, including:

- honest errors reported by the authors (for example, errors due to the mixing up of samples or use of a scientific tool or equipment that is found subsequently to be faulty)
- research misconduct (data fabrication)
- duplicate or overlapping publication
- fraudulent use of data
- clear plagiarism
- unethical research.

For any retracted document, the reason for retraction and who is instigating the retraction will be clearly stated in the Retraction notice. A publication is usually only retracted at the authors' request or by the publisher because serious misconduct has been brought to our attention.

8.3 Removal

The removal of a document would only be undertaken where legal limitations have been placed upon the publisher, copyright holder or author(s), for example, if the documents clearly defamatory or infringes others' legal rights. The bibliographic information for a removed document will be retained on the site along with information regarding the circumstances that led to its removal.

9. Allegations of misconduct

JOURNAL OF BIOMEDICAL AND MEDICAL SCIENCES is a member of the Committee on Publication Ethics (COPE) and provides an ethical publishing framework in accordance with COPE's codes of conduct for editors and pubishers.

All documents are not peer-reviewed or checked before being posted in JOURNAL OF BIOMEDICAL AND MEDICAL SCIENCES; publication of such

shared content in JOURNAL OF BIOMEDICAL AND MEDICAL SCIENCES does not imply endorsement of its content, methods or ethical standards.

If a case of suspected research or publication misconduct is brought to our attention, we will follow guidelines. This may involve contacting the authors' research institution, an ethics committee or other third parties.

Research misconduct includes data fabrication or falsification, or cases where research involving animals or humans has not been carried out within an appropriate ethical framework. Publication misconduct includes duplicate publication of articles or plagiarism. Honest errors or differences of opinion are not considered 'misconduct'.

If you suspect potential misconduct in an article published on JOURNAL OF BIOMEDICAL AND MEDICAL SCIENCES, please contact the editorial office (editor-in-chief@eu.edu.ge).

10. Appeals and complaints

JOURNAL OF BIOMEDICAL AND MEDICAL SCIENCES follows the COPE guidelines (https://publicationethics.org/guidance/Guidelines) in relation tocomplaintsand appeals. If you wish to make an appeal or complaint you should contact the editorial office (editor-in-chief@eu.edu.ge). In the instance that your issue cannot be resolved by the editorial office, the Publishing Director should be contacted.

11. Policy for Comments on Documents

We encourage unsolicited open scientific discussion on all research outputs. Such contributions are published through our Comment system. To ensure that comments contribute to, and focus on, the scholarly debate, we usually only allow comments from readers who have a formal affiliation with a research institution, or other relevant organization. Alternatively, we may also allow comments from readers who have demonstrable expertise in a relevant area of research. Consistent with our commitment to full transparency, the reader's full name and affiliation appear on their public comment.

Comments should focus on the scholarly content presented in the documents with which they are associated.

Comments that appear to be advertising are potentially libelous or legally problematic (including comments revealing patient information) are not permitted. We will not accept Comments that are offensive, indecent or contain negative comments of a personal, racial, ethnic, sexual orientation, or religious character.

All Comments must be written in good English; a Comment may be rejected if it is deemed unintelligible.

Readers who wish to comment are asked to declare any competing interests. Competing interests can be of a financial nature (e.g. holding a patent or receiving fees from a company that may lose or gain financially from the publication of the Comment), or they can be personal, religious, political or other non-financial interests. When completing your declaration, please consider the issues summarized in the Declaration of Competing Interests.

While we welcome open scientific debate and discussion, we will not tolerate abusive behavior towards our authors and reviewers via our Comment system or via social media. In extreme cases we will consider contacting the affiliated institution to report the abusive behavior of individuals.


INTERNATIONAL
STANDARD
SERIAL
NUMBER
INTERNATIONAL CENTRE


doi


Crossref




Google
Scholar


E-LIBRARY








Scope Database
Journal indexing & Citation Analysis